

Characterizing Groundwater Flow in the Twin Cities Metropolitan Area, Minnesota
A Chemical and Hydrostratigraphic Approach

A DISSERTATION
SUBMITTED TO THE FACULTY OF THE GRADUATE SCHOOL
OF THE UNIVERSITY OF MINNESOTA
BY

Robert G. Tipping

IN PARTIAL FULFILLMENT OF THE REQUIREMENTS
FOR THE DEGREE OF
DOCTOR OF PHILOSOPHY

Dr. E. Calvin Alexander, Jr. Advisor

June 2012

© Robert G. Tipping 2012

Acknowledgements

This investigation is based largely on historical data that was collected by other people. I understand and appreciate the time and effort it takes to contact homeowners, business people or city staff; meet with them, take physical measurements on site, fill the bottles and tabulate results. Without those efforts, my thesis would not have been possible. In particular, I would like to thank Sandeep Burman and Richard Marsh, whose data from Scott County and Anoka County respectively filled large holes in growth areas where chemical data is most useful for establishing baseline conditions; Scott Alexander at the University of Minnesota, whose invisible hand is, in some way, part of the collection and analysis of nearly every dataset included in this investigation; the Minnesota Department of Health (MDH) staff, who, under the guidance of Bruce Olsen, have collected an extraordinary amount of tritium data (linked to a unique well number!) as part of source water protection efforts. Their work includes collection of general chemistry, stable isotope and contaminant data that are routinely used to understand groundwater flowpaths and residence times; Chris Elvrum, and Lanya Ross from the Metropolitan Council whose groundwater planning projects for the metropolitan area supported much of the work presented here; the staff at the Minnesota Geological Survey, Dale Setterholm and Tony Runkel in particular, who continue to encourage and expect good science with practical results; my committee members Randal Barnes, Martin Saar, Bruce Wilson, Tony and Advisor E. Calvin Alexander, Jr. who have graciously and patiently helped put these pieces together. That being said, I especially want to thank you, Calvin, for all your support and guidance.

Dedication

This work is dedicated to Dan, Sam, Michael, and Mary

Abstract

Historic chemical and isotopic data for groundwater within the 11 county Twin Cities Metropolitan Area, extended (TCMAx) were used to distinguish three regional groundwater types based on similar chemical and isotopic composition: 1.) recent waters, characterized by detectable tritium, elevated chloride and/or the presence of anthropogenic compounds; 2.) waters with elevated strontium to calcium plus magnesium ratios; and 3.) naturally elevated chloride—distinct from recent waters based on carbon-14 dating and low chloride to bromide ratios where sufficient data exists. The three-dimensional distribution of these hydrochemical facies were compared to permeability of unconsolidated sediments, the distribution of macropores within sedimentary (Paleozoic) bedrock, and the regional distribution of vertical hydraulic head gradient. Results of this investigation demonstrate that groundwaters within the TCMAx can be broadly categorized by chemical composition, and that their distribution is controlled both by regional differences in subsurface permeability and natural hydraulic head gradients, and by regional changes in hydraulic gradient due to high-capacity pumping. Chloride content and chloride to bromide ratios, in particular, can be used to identify the presence of recently recharged groundwater in bedrock aquifers and further characterize the movement of these recent waters through bedrock macropores.

Urban groundwater systems present unique challenges for resource management and scientific investigations due in large part to the transient nature of hydraulic head gradients and changing landuse. For urban planners charged with groundwater resource management, results in this thesis demonstrate the utility of having groundwater

hydrochemical types fully integrated with a hydrogeologic framework model in a three-dimensional geographic information system (GIS) environment, where age and chemical quality of groundwaters can be compared with other, more familiar factors, such as locations and pumping levels of high capacity wells. For groundwater modelers of urban aquifers, these same results can guide conceptual models of recharge to bedrock aquifers and constrain model calibration to produce flux estimates in agreement with flowpaths indicated by the distribution of recent waters.

Table of Contents

Acknowledgments.....	i
Dedication.....	ii
Abstract.....	iii
List of Tables	vii
List of Figures.....	viii
List of Acronyms	xi
INTRODUCTION AND SUMMARY.....	1
BACKGROUND AND THEORETICAL FRAMEWORK.....	12
Hydrogeologic setting.....	12
Previous chemical and isotopic investigations	16
Factors affecting groundwater flow and chemical composition in an urban area	18
Use of chemical and isotopic data to characterize groundwater flow systems.....	19
DATA AND METHODS	28
Sources of historic chemical and isotopic data	28
Regional hydrochemical facies and baseline conditions	34
Distribution of recent waters compared to bedrock hydrostratigraphy.....	35
Distribution of recent waters compared with vertical flux to upper bedrock aquifers.....	36
RESULTS AND DISCUSSION.....	40
Hydrochemical facies and baseline conditions	40

Distribution of recent waters compared to bedrock hydrostratigraphy.....	45
Distribution of recent waters compared with vertical flux to upper bedrock aquifers.....	50
Regional synthesis	52
CONCLUSIONS AND RECOMMENDATIONS	61
APPLICATIONS	68
REFERENCES CITED.....	143
APPENDICES (GIS data included in supplementary files).....	155
A. Methods for determining the distribution and hydraulic characteristics of subsurface unconsolidated materials	155
B. Point data geodatabase structure.....	165
C. Water chemistry database field names and descriptions.....	171
D. Regional summary geodatabase structure and field names and descriptions	178
E. Guide to database use.....	185

List of Tables

Table 1. Summary of horizontal and vertical hydraulic conductivity values by method (Tipping et al., 2010).....	14
Table 2. Summary of hydrochemical dataset sources and content.	31
Table 3. Hydraulic conductivity values for subsurface textures.	38

List of Figures

Figure 1 Study area extent	70
Figure 2. Location of major rivers and regional hydrologic gradients;	72
Figure 3. Groundwater-level changes in the Prairie du Chien-Jordan aquifer between March 2008 and August 2008, based on synoptic water level measurements (Sanocki et. al., 2009).	73
Figure 4. Regional distribution of unconsolidated materials and bedrock geologic map....	76
Figure 5. Distribution of bedrock valleys and major faults within the TCMAx.....	77
Figure 6. Schematic cross section through an urban setting showing examples of zones where water recharging bedrock aquifers could receive different chemical signatures	78
Figure 7. Schematic cross section through southern Washington County Minnesota, showing water well open hole intervals exposed to: zones of preferential flow (enhanced porosity and permeability bedrock valley conditions and bedrock surface conditions.	79
Figure 8. Schematic drawing showing the time of travel calculation.	80
Figure 9. 2D and 3D piper diagrams, showing regional differences in the chemical composition of groundwater in unconsolidated deposits of Scott, Hennepin, Anoka and Washington Counties, and in upper bedrock in Dakota County where unconsolidated deposits are largely thin or absent.....	82
Figure 10. Scatterplot of calcium plus magnesium compared to bicarbonate concentration in millimoles per liter for all water well samples with charge balance errors less than 5 percent.....	84
Figure 11. Scatterplot of strontium compared to calcium plus magnesium concentrations in millimoles per liter for all water well samples with charge balance errors less than 5 percent.....	85
Figure 12. Regional map showing distribution of Sr/(Ca+Mg) molar ratios.....	88
Figure 13. Scatterplot and summary statistics for chloride concentrations in wells with and without detectable tritium.	90
Figure 14. Regional maps showing the distribution of recent waters.....	92
Figure 15. Regional maps showing naturally elevated chloride concentrations.	93
Figure 16. Scatterplot and summary statistics for chloride concentrations compared to distance from casing bottom to the bedrock surface, domestic wells only.....	96
Figure 17. Scatterplot and summary statistics for chloride concentrations compared to distance from a bedrock valley, domestic wells only, threshold distance of 400 meters. .	98
Figure 18. Scatterplot and summary statistics for chloride concentrations compared to distance from a bedrock valley, domestic wells only, threshold distance of 2000	

meters.	100
Figure 19. Scatterplot and summary statistics for PFBA concentrations greater than 1 microgram per liter, compared to distance from a bedrock valley, threshold distance of 1000 meters.	102
Figure 20. Lithostratigraphic column showing distribution of residence time by open hole interval.	104
Figure 21. Boxplots of chloride concentrations in Prairie du Chien and Jordan samples, grouped by western, central and eastern regions of the TCMAx.	106
Figure 22. Series of stacked columns, showing the number of detect verses non-detects of PFBA for both the Prairie du Chien and Jordan wells, in regularly spaced sectors across southern Washington County.	108
Figure 23. Estimated composite vertical hydraulic conductivity in feet per day from the land surface to the bedrock surface.	110
Figure 24. Regional maps showing adjusted vertical change in hydraulic head for March and August 2008.	111
Figure 25. Calculated vertical travel time from regional water table the bedrock surface (saturated conditions).	114
Figure 26. Oblique views of the TCMAx from the southeast, showing the three dimensional distribution of regional hydrochemical facies in bedrock and surfical deposits. Selected bedrock units included for vertical reference.	116
Figure 27. Cross section key for Figures 28 through 35.	122
Figure 28 and 29. Left and right sides of regional cross section A-A', Sherburne County to Mississippi River.	126
Figure 30. Regional cross section B-B', St. Francis, Anoka County to Mississippi River.	130
Figure 31. Regional cross section C-C', Big Marine Lake, Washington County to Mississippi River near downtown St. Paul.	132
Figure 32. Regional cross section D-D', western Dakota County to Mississippi River near Hastings.	134
Figure 33. Regional cross section E-E', southeastern Scott County to Minnesota River near Shakopee.	136
Figure 34A. Local cross section F-F' Edina area. Age inversion within the open hole of a single well is shown.	138
Figure 34B. Local cross section G-G' Eastern Hennepin County.	138
Figure 35A. Local cross section H-H', south central Washington County to Mississippi River.	140

Figure 35B. Local cross section I-I', southeastern Washington County to St. Croix River.....	140
Figure 36. Histogram comparing chloride concentrations to top-of-open-hole elevation in sampled wells.....	141
Figure 37. Temporal variability of chloride concentrations compared with depth. Greater variability in chloride concentrations are found at depths less than 150 feet below the land surface.	142
Figure 38. Eleven county extended TCMAx showing areas where subsurface Quaternary stratigraphy has been mapped. (Meyer and Tipping, 1998; Lusardi and Tipping, 2006; Meyer and Tipping, 2007; Lusardi and Tipping, 2009; Meyer, 2010).	163
Figure 39. Schematic drawing of Quaternary points model.	164

List of Acronyms

CFC	Chlorofluorocarbon
CWI	County Well Index
DEET	N,N-Diethyl-meta-toluamide
GWMAP	Ground Water Monitoring and Assessment Program, Minnesota Pollution Control Agency
MDA	Minnesota Department of Agriculture
MDH	Minnesota Department of Health
MGS	Minnesota Geological Survey
MPCA	Minnesota Pollution Control Agency
PFBA	perfluorobutanoic acid
PFC	peroflourochemicals
SF ₆	sulfur hexafluoride
TCMA	7 county Twin Cities Metropolitan Area
TCMAx	extended 11 county Twin Cities Metropolitan Area
TDS	Total Dissolved Solids
THCM	Traditional hydrogeologic conceptual model
USGS	United States Geological Survey

INTRODUCTION AND SUMMARY

The seven central counties within the eleven county Twin Cities Metropolitan Area, extended (TCMAx) (Figure 1) have, at present, over 2.8 million residents (Metropolitan Council, 2010). With the exceptions of Minneapolis and, in part, St. Paul, groundwater is the primary drinking and industrial water source, with the majority of that supply coming from Paleozoic bedrock aquifers. In addition, an abundance of surface water bodies in the TCMAx, including lakes, streams, and wetlands constitute a surface water-groundwater system providing essential ecosystem functions that support not just a diversity of biological life but are also the foundation of Minnesota's recreation and tourism industries.

Within this context of multiple and often conflicting use, decision makers are faced with choices regarding utilization of groundwater resources. Common questions include: "What is the quality of water in my area? Is it getting worse or better? If we increase our use of groundwater, what are the consequences?" Furthermore, the nature of groundwater resources are largely in the realm of "out of sight, out of mind" and traditionally, decision makers have been inclined not to act until there is a tangible problem such as a contaminated public supply well, drought, or conflicts due to multiple uses.

Difficulties arise because the spatial and temporal variability in groundwater composition and flow is often poorly characterized. These problems are compounded in an urban area, where the effects of groundwater pumping and variable groundwater

recharge amounts and compositions complicate matters further. In the past, numerical groundwater flow models have been the primary tool used to make decisions about land and water use. Shortcomings of groundwater flow models in current use as decision-making tools are most apparent when applied to problems of contaminant transport. The TCMAx aquifers are typically characterized as dual-porosity aquifer systems under transient hydraulic conditions. In the TCMAx, most applied models are steady-state and do not address transient conditions such as peak pumping periods during summer droughts. The result is that decision makers are ill-equipped to respond to questions about groundwater quality, particularly when contaminants unexpectedly appear in wells. The shortcomings of these models are typically not due to limitations in modeling technology. Many applied groundwater models currently in use in the Twin Cities area were developed using a conceptual model of groundwater flow that defines aquifer and confining units by stratigraphic boundaries and assumes that each behave hydraulically as isotropic and homogeneous porous media. These assumptions, referred to herein as the traditional hydrogeologic conceptual model (THCM), result in flow models that provide reasonable estimates of groundwater yield, but do not accurately describe rates or pathways of groundwater movement.

The use of hydrochemical and isotopic data as environmental tracers addresses spatial and temporal variability of groundwater flow in a different way. The most direct and intuitive example of this is the introduction of an artificial tracer at one place and its detection somewhere else. The detection of the tracer indicates that there is a hydraulic connection between the two points, regardless of what a model predicts (Kendall, 2005).

When hydrochemical facies are mapped in three dimensions, their spatial distribution can be compared to other subsurface data, including location and depth of high-capacity wells, elevations of major rivers, and the presence and absence of confining units. For decision makers not trained in hydrogeology, this type of tool is useful because it shows differences in groundwater chemical types and the hydrogeologic and anthropogenic factors that control their distribution.

The overall objective of this project is to provide decision makers with a tool to assess changing groundwater quality conditions in an urban area. Specific research objectives are to 1.) Classify and map the three-dimensional distribution of groundwater types based on interpreted age and chemical composition. 2.) Evaluate that distribution in the context of a three-dimensional geologic framework model of the TCMAx, showing how groundwater types are related to subsurface permeability and hydraulic head gradient. The research objectives are accomplished by evaluating the following hypotheses:

1. Broad similarities in the natural (pre-anthropogenic) chemical composition of groundwater in metropolitan bedrock aquifers allow recently recharged groundwater to be easily identified by the presence of anthropogenic tracers.
2. Groundwater develops a distinct chemical signature as it moves through the ground that can be used to identify its recharge area.
3. The distribution of elevated chloride or other conservative anthropogenic tracers in bedrock aquifers can be explained, in part, by the geologic conditions that enhance development of secondary porosity and permeability.

These features include buried bedrock valleys, proximity to the bedrock surface, faults, and zones of preferential groundwater flow.

Based on the analysis of chemical and isotopic data presented in this thesis, several conclusions can be drawn about the chemical composition and nature of groundwater flow in the TCMAx:

- Three regional groundwater types can be distinguished within the TCMAx based on similar chemical and isotopic composition: 1.) recent waters, characterized by detectable tritium, elevated chloride and/or the presence of anthropogenic compounds; 2.) waters with elevated strontium to calcium plus magnesium ($\text{Sr}/(\text{Ca}+\text{Mg})$) ratios; and 3.) naturally elevated chloride—distinct from recent waters based on carbon-14 dating and low chloride to bromide ratios where sufficient data exists.
- Recent waters are associated with an upper ‘active’ zone of groundwater flow characterized by shorter residence times, higher concentrations of anthropogenic compounds and greater variability in chemical composition. The presence of recent water at depth in the central TCMAx, below the elevation of the regional discharge to the Mississippi, Minnesota and St. Croix Rivers, shows that changes in groundwater flowpaths have occurred since the advent of high-capacity groundwater pumping. More water moves in the vertical direction in these areas than did before 100 years of groundwater pumping began. Extending out from the central TCMAx, this active zone is found most often within 60 to 100 feet of

the land surface. This active zone includes tills, where the upper 60 feet has markedly higher permeability than the same textures at greater depths.

- Elevated Sr/(Ca+Mg) groundwaters are found in the western TCMAx and at depth, and are associated with recharge through Des Moines Lobe till and/or longer residence times. The distribution of this hydrochemical facies appears to have changed with time as hydraulic conditions changed. Elevated Sr/(Ca+Mg) ratios in the western TCMAx may have, at one time, extended further east toward regional discharge in the Mississippi River under natural hydrologic conditions. In eastern Hennepin County, these waters are thought to have been replaced by recent waters due to an increased vertical head gradient resulting from high capacity pumping, combined with a lack of overlying till.
- In bedrock aquifers, differences in chemical and isotopic composition subdivide traditional hydrogeologic conceptual model (THCM) aquifers into subunits of similar porosity and permeability. Specifically, within the THCM Prairie du Chien-Jordan aquifer, chloride content is significantly higher in the Shakopee Formation than it is in the Jordan Sandstone. Similarly, where there is adequate data from both the Shakopee and the Jordan in proximity to one another, PFC's are detected more often in the Shakopee Formation.
- Although there are considerably less data for comparison, similar results are found in the THCM Franconia-Ironton/Galesville (Tunnel City Group-Wonewoc) aquifer, with recent waters found in the upper Franconia (Tunnel City Group), a lack of well completions in the lower Tunnel City Group where permeability is

low, and an absence of recent waters in the Ironton/Galesville (Wonewoc Formation).

- Below the Eau Claire Formation, chemical and isotopic data show that flow in the Mt. Simon is isolated from flow in the units above it. Residence times in the Mt. Simon are considerably longer (centuries to millennia), strontium concentrations are higher, and naturally elevated chloride is present in its lower sections and near major fault zones. This aquifer currently has residence times far longer than the less than 50 years seen in the upper bedrock aquifers.
- There is an apparent trend toward higher chloride, and by inference, greater flux of groundwater in proximity to the bedrock surface and near bedrock valleys. Although the trend is not statistically significant, it is expected that these areas are capable of producing more water to pumped wells compared to wells in dissimilar settings. As with wells finished in other areas of the enhanced macropore development, it is also expected that these wells will show a greater temporal variability in chemical composition.

In the context of the groundwater flowpaths outlined above, a number of steps can be taken to apply this information toward groundwater management in the TCMAx:

- In 2012, revisions are underway on the current Metro Area Groundwater Model, referred to as Metro Model II (Metropolitan Council, 2012). The regional distribution of chemical types should be used in this modeling effort to constrain possible groundwater flowpaths from the land surface to bedrock. Because the

distribution of chemical types, in particular, the distribution of recent waters matches the estimated vertical hydraulic head gradient distribution across the TCMAx, flux estimates on a cell by cell basis from the regional groundwater model should be compared to the distribution of recent waters to test recharge/pumping scenarios for the central TCMAx outlined above. Flux estimates should also be compared for other portions of the metro area where bedrock aquifers are hydraulically isolated from the land surface, such as portions of western Hennepin, Carver and Scott Counties, and in areas where hydraulic conditions are expected to change due to population growth, such as Anoka County.

- Evaluating groundwater flowpaths from the land surface to bedrock aquifers depends largely on boundary conditions used. Several separate numeric solutions should be considered, including, at a minimum, no-flow boundaries for bedrock layers on the western edge of the model where subcrop edges of bedrock units are overlain by a thick sequence of glacial tills. No-flow boundaries would eliminate a constant lateral source of water for these layers. Chemical and isotopic data show that bedrock aquifers in portions of western Hennepin County have no recent water. Calculated vertical travel times reflect the low vertical gradient/low permeability of unconsolidated material in this area; model results should reflect that recharge applied to the upper cells in this area are not in steady state with bedrock layers over the time scales of less than one hundred years.

- Pre-development data on strontium concentrations in eastern Hennepin County do not exist. Therefore, source water conditions should be tested in the proximity of the Sr/Ca+Mg—recent water border shown on cross section A-A' (Figure 28) by sampling municipal wells in that area. Waters with Sr/Ca+Mg molar ratios greater than 0.001 are likely drawing water laterally from western areas that receive limited vertical recharge.
- From a water management perspective, the question arises as to whether the pattern of recharge and use indicated by recent waters at depth within the central TCMAx is sustainable. Water volume calculations should be conducted to see whether the volume of water pumped within this zone matches the amount of water available via recharge from above it. Using the 750 foot contour on Figure 14.C to approximate the boundary of recent waters at depth, if the recharge volume over this area is considerably less than the pumping volume within it, then it is expected that water levels in the Prairie du Chien Group and Jordan Sandstone will drop with time, and are not sustainable under current pumping and recharge conditions.
- Hydrostratigraphic units should be incorporated into bedrock model layers by modifying hydraulic conductivity values and reducing aquifer thicknesses. In both the Shakopee Formation and upper Tunnel City Group, the occurrence of recent waters combined with documented higher permeability due to enhanced macropore development, suggests greater flux through these units relative to the Oneota Dolomite and its basal Coon Valley member (lower Prairie du Chien

Group), and lower Tunnel City Group, with greater temporal variability in chemical composition. Higher K ranges for Shakopee and upper Tunnel City Group should be incorporated into the model, with thicknesses of these layers reduced to reflect the permeable thicknesses of these subunits. Thicknesses of the Prairie du Chien and Tunnel City Groups vary across the TCMAx, but the lower permeability portions of both these units (approximately 40 feet in the Prairie du Chien and 60-80 feet in the Tunnel City Group) can be subtracted from the bottom of each to leave a remainder of permeable bedrock.

- Chemical and isotopic data show a trend toward higher bedrock permeability near the bedrock surface and bedrock valleys, regardless of bedrock lithology, presumably because of a higher density of vertical, through-going fractures. In GIS, this hydrostratigraphic zone of higher bedrock permeability is most easily defined creating a separate raster equal to the bedrock surface minus 50 feet. The resulting raster can be used to modify K values within bedrock groundwater model layers.
- Buried bedrock valleys provide “windows” to lower bedrock aquifers. From a groundwater resource management perspective, these windows are important in areas where a vertical hydraulic gradient is present, or could be present in the future as the distribution of high-capacity pumping changes with time. The presence of the Platteville and Glenwood Formation in the central TCMAx, combined with a large vertical gradient in this area highlights the hydrologic importance of these bedrock valley windows where the Platteville/Glenwood

confining units are absent. The Quaternary subsurface regional texture dataset included in this thesis, provides an up-to-date distribution of textures in these bedrock valleys, both in areas where subsurface mapping as occurred, and in areas modeled by interpolation from the Minnesota state water well database, CWI. These data are in GIS format, and should be used to guide hydraulic conductivity estimates for buried bedrock valleys in regional and local groundwater models.

- There are significant gaps in chemical, isotopic, subsurface, and hydraulic head data that should be addressed in future data collection. Stable isotopes of oxygen and hydrogen—useful for both identification of surface water/ground water interaction and recharge from glacial melt water—are largely absent from this dataset. This dataset also has a limited number of bromide analyses that are extremely useful for identifying sources of chloride. In the subsurface, Quaternary subsurface mapping is missing for important recharge areas of the central TCMAx, including southern and eastern Hennepin County, Ramsey, and Dakota Counties. Finally, real time hydraulic head data, both from pumping and observation wells, are necessary to evaluate transient conditions within and between aquifers. These data, along with chemical and isotopic data, should be collected and archived in a georeferenced database so that trends can be identified as groundwater quality and flowpaths change with time.

The work presented in this thesis has applicability to the broader, non-provincial hydrogeologic community. For planners, it demonstrates, for the first time, the utility of having mapped, three-dimensional hydrochemical facies in a GIS format, combined with a hydrogeologic framework model over a regional urban area. Groundwater managers can compare the age and chemical quality of groundwater with other, more familiar factors in an urban setting, such as the location and pumping levels of high capacity wells. Furthermore, it demonstrates the need for continued archival of georeferenced chemical data. This type of data collection is critical in an urban setting, where hydraulic conditions change with time over regional scales. For the technical hydrogeologic community, this work investigates the distribution of hydrochemical facies at regional and local scales, interpreted in the context of a revised hydrogeologic conceptual model, where water-bearing characteristics of sedimentary aquifers and aquitards are more closely aligned with regional compilations of borehole geophysical measurements, temperature profiling, short-interval packer testing, multi-level hydraulic head measurement, and dye tracing results. Specifically, it documents the presence of recent waters in areas of known macropore development, both parallel to bedding along previously identified stratigraphic horizons, and perpendicular to bedding in proximity to the bedrock surface and/or buried bedrock valleys. For both planners and the technical hydrologic community, this work raises fundamental questions about the pathways for groundwater to move vertically in urban settings, where high capacity pumping creates conditions to move contaminants at depths, either along vertical fractures or multiple

aquifer wells, at rates that greatly exceed modeled porous media transport through aquitards.

BACKGROUND AND THEORETICAL FRAMEWORK

Hydrogeologic setting

The TCMAx is trisected by the Minnesota and Mississippi Rivers, and bordered to the east by the St. Croix River (Figure 2). At elevations ranging from 700 to 800 feet above mean sea level, these major rivers are discharge zones for regional groundwater flow from topographic highs in Scott and Dakota Counties to the south, Carver, Western Hennepin and Wright Counties to the west, and northern Washington, Chisago and Isanti Counties to the northeast.

These regional flow directions are seen in potentiometric surfaces for both the regional water table (Barr, 2010) and the combined potentiometric surfaces of the Prairie du Chien and Jordan aquifers (Sanocki et al., 2009) (Figure 2). The Prairie du Chien Group along with the underlying Jordan Sandstone provide the majority of groundwater used in the TCMAx. Higher summer groundwater pumpage lowers the combined Prairie du Chien and Jordan potentiometric surface seasonally (Sanocki et al., 2009) (Figure 3). The spatial distribution of this seasonal change matches the distribution of municipal groundwater use (Minnesota Department of Natural Resources, 2011), with largest decreases in water levels occurring in west central Hennepin, Ramsey and eastern Washington Counties.

Covering the bedrock surface are glacial deposits ranging from northwest

provenance loam to clay loam, carbonate-rich tills and associated fluvial sands and gravels, to northeast provenance sandy loam and associated fluvial sands and gravels containing abundant silicate minerals. The TCMAx has experienced many glacial advances and retreats. Depositional environments include a continuum of subglacial, proglacial fluvial, ice contact, stagnation moraine and lacustrine deposits—a complex distribution of textures and hydraulic properties that range in thickness from a few to greater than several hundred feet. At the land surface, unconsolidated sediments consist of primarily loam to clay loam materials to the west, sand and gravel to the east and southeast and in terrace deposits along major rivers, and sand, fine sand, and peat to the north (Figure 4.A) (Meyer, 2007).

Below the glacial sediments, Paleozoic bedrock within the TCMAx consists of nearly flat-lying sandstone, carbonate and shales of Middle Cambrian to Upper Ordovician age, greater than 1000 feet in thickness, dissected by numerous bedrock valleys (Figure 4.B) (Mossler, 2000). These rocks, extending southwards over much of the midcontinent, are preserved locally within the Twin Cities Basin, which was formed by adjustments of basement Proterozoic rock associated with the Mid-Continent Rift (Mossler, 2008). The edges of the basin are bound by faults that extend into the Paleozoic rocks with local offsets of 100 feet or more. The dissecting bedrock valleys range in width from less than 1000 to over 10,000 feet and reach depths of over 400 feet (Figure 5).

Porosity and permeability of glacial sediments in the TCMAx can vary over five orders of magnitude, based on measurements over a range of scales, from laboratory to

field studies (Table 1) (Tipping et al., 2010). Layering of sediments, seen in well records and scientific borings and outcrop, can be extremely complex. Nonetheless, some regional differences, at least for uppermost sediments, are discernible. Northwest provenance tills (Des Moines Lobe) to the west are, on average an order of magnitude less permeable than northeast provenance tills to the east (Superior Lobe). Superior Lobe

Table 1. Summary of horizontal and vertical hydraulic conductivity values by method (Tipping et al., 2010)

Hydraulic Conductivity - horizontal (ft/day)						
<i>method/hydro_class</i>		n	mean	min	max	geomean
Grain size						
1	loam to clay loam	1155	2.37E-01	2.83E-05	5.45E+00	9.64E-02
2	loam to sandy loam	325	1.26E+00	2.78E-03	1.42E+01	5.70E-01
3	loam, silt rich; silt and clay	79	3.45E-01	8.57E-03	3.35E+00	1.39E-01
4	loam to sandy clay loam	37	1.35E+00	8.85E-02	3.42E+00	1.02E+00
5	sand and gravel	168	5.47E+01	2.83E-02	3.09E+02	1.92E+01
6	fine sand	32	4.81E+00	5.84E-05	3.69E+01	1.61E-01
7	sandy silt	38	5.65E-01	1.42E-04	1.13E+01	2.42E-02
Lab Permeameter						
5	sand and gravel	3	2.34E+00	4.30E-01	4.50E+00	1.60E+00
Aquifer test						
5	sand and gravel	118	1.17E+02	4.82E-01	4.15E+02	6.53E+01
Slug test						
1	loam to clay loam	17	3.87E-01	5.67E-04	3.83E+00	2.80E-02
2	loam to sandy loam	34	2.27E+00	2.83E-03	4.30E+01	2.00E-01
3	loam, silt rich; silt and clay	7	1.43E-02	7.65E-05	9.35E-02	7.74E-04
5	sand and gravel	215	3.98E+01	5.00E-03	5.40E+02	8.07E+00
6	fine sand	14	3.91E+00	1.42E-03	2.61E+01	5.11E-01
7	sandy silt	18	2.49E+01	1.40E-01	1.50E+02	5.54E+00
Specific Capacity - excluding CWI						
5	sand and gravel	17	40.7294	1.5	152	2.66E+01
Lab Permeameter - constant head						
1	loam to clay loam	17	1.68E-01	6.24E-05	2.83E+00	7.26E-04
5	sand and gravel	51	7.79E+00	4.82E-05	1.11E+02	1.69E+00
6	fine sand	2	1.70E+00	1.50E+00	1.90E+00	1.69E+00
7	sandy silt	9	8.55E-01	8.50E-04	5.67E+00	8.88E-02
Lab Permeameter - falling head						
1	loam to clay loam	37	7.14E-02	2.83E-06	1.98E+00	2.19E-04
2	loam to sandy loam	14	2.45E-01	1.98E-05	3.40E+00	9.81E-04
3	loam, silt rich; silt and clay	4	1.94E-04	6.80E-05	3.97E-04	1.55E-04

Table 1. (continued)

<i>method/hydro_class</i>	n	mean	min	max	geomean
5 sand and gravel	4	4.27E-01	6.80E-03	1.13E+00	1.22E-01
6 fine sand	1	2.35E-01	2.35E-01	2.35E-01	2.35E-01
7 sandy silt	31	1.07E-01	9.35E-06	1.64E+00	1.73E-03
Aquifer test	3				
5 sand and gravel	3	6.76E+01	7.00E-01	1.01E+02	1.93E+01

sediments are less uniform, with a greater abundance of sand bodies within what drillers typically describe as “sandy clay,” “clay and sand,” “clay and gravel” or “gravelly clay.” Based on literature review and a limited number of measurements within the TCMAx, it is expected that the hydraulic conductivity of fine grained sediments for both northwest and northeast provenance tills decrease one to two orders of magnitude at depths greater than 60 feet (20 meters) (Tipping et.al., 2010).

In southeastern Minnesota, porosity and permeability of the Paleozoic bedrock have traditionally been linked in a conceptual way to stratigraphic boundaries. Aquifers and aquitards have been assigned bulk hydraulic conductivities over entire or multiple formations, under an assumption of isotropic, porous media. Examples include the Prairie du Chien-Jordan and Franconia-Ironton-Galesville aquifers in Minnesota, and the Cambro-Ordovician aquifer in Wisconsin and Illinois (e.g. Delin and Woodward, 1984; Woodward, 1986). Significant efforts have been made over the past decade to define water-bearing characteristics of aquifers and aquitards in the Paleozoic rocks of the Midwest that are more closely aligned with regional compilations of borehole flowmeter

logging, optical and acoustical borehole imaging, temperature profiling, short-interval packer testing, multi-level hydraulic head measurement, and dye tracing results (Bradbury and Runkel, 2011). These investigations are developing a revised hydrostratigraphic framework showing that measurements and observations of macropore development at borehole scales can be correlated regionally. From a hydraulic perspective, such zones of preferential macropore development are revealed under natural vertical gradients, such as regional discharge areas, or under conditions of induced stress from groundwater pumping (Runkel et al., 2003). The observations have led to revised conceptual models of groundwater flow, reinterpretation of apparently contradictory hydraulic head data (e.g., Wenck and Associates, Inc., 1997) and application to groundwater flow models (e.g Barr, 2005; 2010). An important component of this investigation is to evaluate the distribution of recently recharged groundwaters in the context of this revised hydrostratigraphic framework.

Previous chemical and isotopic investigations

In the TCMAx, there is a large amount of high-quality historic chemical and isotopic data that was collected for a variety of purposes, often solely for monitoring groundwater quality. Interpretations of these data applied to groundwater flow systems have been based on the THCM (i.e., Andrews et al., 1998; Fong et al., 1998) as hydrochemical systems that operate independently of geologic constraints (Nemetz, 1993; Smith and Nemetz, 1996), or that the geology of the study area is too complex to

be used for analysis (MPCA, 2000b). Many of these studies have focused only on surficial aquifers (e.g., Andrews et al., 1999) while others combine hydrochemical and hydraulic data over several aquifer units (Woodward, 1986; Smith and Nemetz, 1996; Andrews et al., 1998). Types of high-quality data collected include physical parameters (temperature, electrical conductivity, and oxidation/reduction potential), major cations and anions, nutrients, dissolved organic carbon, trace metals, radon, tritium, pesticides, and volatile organic compounds. Additional high-quality hydrochemical data have been collected as part of local groundwater concerns, including well-head protection (Walsh, 1992); groundwater management areas (MDH, 2004); individual sewage treatment studies (MPCA, 2000a); and nitrate studies (MPCA, 2000b; MPCA 2002). Several investigations involving surface water and shallow groundwater have been analyte-specific, including chlorides (Novotny et al., 2007; Fallon and Chaplin, 2001) and peroflourochemicals (PFCs) (MDH, 2008).

Several reports have taken a systematic look at regional hydrochemical conditions either specifically designed as a hydrochemcial investigation (Maderak, 1963; Sabel, 1985; Kanivetsky, 1986; Lively et al., 1992; MPCA, 1998a,b) or as part of a more general hydrogeologic study (Hall, 1911), but, as with previous investigations, interpretations of chemical data in these studies are largely based on a traditional hydrogeologic framework that links hydraulic characteristics to traditional stratigraphic boundaries at the formation scale.

Factors affecting groundwater flow and chemical composition in an urban area

Urban hydrogeologic settings differ from non-urban settings in a number of distinct ways. High-capacity pumping influences vertical and horizontal hydraulic head gradients in a significant and transient manner. Multi-aquifer wells interconnect aquifer units. In the TCMAx, the number and distribution of these wells is largely undocumented. In urban areas, increased vertical hydraulic head gradients due to high-capacity pumping can move water rapidly through aquifers and aquitards via multi-aquifer wells. Flow log and borehole video data provide evidence for rapid downward and upward flow in multi-aquifer test wells located near municipal well fields. Less well documented, but likely just as important is downward and upward flow through vertical fractures (Hart, 2006). In both cases, increased vertical hydraulic head gradients caused by high-capacity pumping create conditions for rapid migration of water in the vertical direction.

From a chemical perspective, land surface activities in urban areas often provide the means to link groundwaters to particular recharge areas (Figure 6; Lerner, 2002). Conditions unique to urban settings include recharge due to leaky infrastructure. The distribution of marker species, such as boron used as a detergent additive, has been used to assess sewer-groundwater interaction (Wolf, et al., 2006). Other urban marker species include iodinated x-ray contrast material, caffeine, and pharmaceuticals. Organic materials as waste water indicators often do not persist, as they are not chemically conservative. Moran (2006) found that the occurrence of wastewater compounds in ambient groundwater is rare and that these compounds are substantially removed during recharge to groundwater. In contrast, other anthropogenic compounds are more

conservative and ubiquitous in surface water and shallow groundwaters. N,N-Diethyl-meta-toluamide (DEET) is among the compounds most often detected in recent and ongoing investigations by the United States Geological Survey (USGS) (Stark et.al., 2001; Lee et.al., 2008).

Chemical loading in urban settings occurs as continuous, one-time, and seasonal events, and is variable over time with changes in land use and subsurface infrastructure (Lerner, 2002). The nature of the tracer application is important and in part determines the manner in which subsurface concentrations are interpreted (Scanlon, 2010). Aging sewers, for example, are often self-sealing, and open up again after large rain events (Held et al., 2007). Depending on the timing of discovery and their composition, one time “pulses” such as a chemical spills may not be traceable back to the land surface. (Lerner, 2002). Chlorides from road salt applications have increased in the TCMAx as population has increased (Sander et al., 2007) and have been found to be accumulating in metro area lakes (Novotny et al., 2007). Depending on the geologic setting and hydraulic head gradient, seasonal loading of chlorides due to road salt application may form a continuous plume that is traceable back to the land surface (Howard and Maier, 2007).

Use of chemical and isotopic data to characterize groundwater flow systems

The use of hydrochemical data to characterize groundwater flow is based on the concept of hydrochemical facies (Back, 1960, 1966) where geochemical observations are made in the context of groundwater flow through aquifers of relatively homogeneous

hydrologic and mineralogic properties (Glynn and Plummer, 2005). The development of a regional water chemistry database and subsequent analysis requires that baseline conditions are established (Edmunds and Shand, 2008). In an urban area, it is particularly important to establish whether anthropogenic or strictly natural processes are involved (Camp and Walreavens, 2008). Specific to this investigation, chemical composition of groundwaters that are different from natural background conditions have been used to determine the depth of recent recharge in urban settings (Taylor et al., 2006) and flow near public well fields (Mendizabal et al., 2011). A major goal of data collection, analysis, and archiving is to establish background data to compare with recent data reflecting changing conditions.

Statistics are often used to establish baseline conditions although methods and design vary depending on study goals. Statistical approaches typically are designed to distinguish differences between populations, such as regional or vertical differences between hydrostratigraphic units, anomalous “hot spots,” or changes in chemical composition with time. Specific statistical methods include traditional descriptive statistics, focusing on distinguishing central measures (mean or median) and variability of populations, and methods designed to identify populations themselves. The latter, broadly defined as multivariate statistical approaches, include principle component analysis, factor analysis, correspondence analysis, and K-measure cluster analysis (e.g. Agrawala, 2007; Woocay, 2008). Applied to groundwater chemistry, these methods focus on reducing the number of variables describing a system and identifying relationships between major ions. Advocates of multivariate methods argue the methods

can objectively reveal patterns in the data that would be otherwise indistinguishable, or perhaps more importantly, unexpected (e.g. Dragon and Gorski, 2009). Advocates of more traditional approaches argue that expert knowledge must guide statistical design, and that a “black box” approach to chemical data ignores insights into chemical processes of physical setting in developing and testing conceptual models (Plummer, et al., 2004; Camp and Walraevens, 2008).

Additional hydrochemical facies can be defined by anthropogenic components (Suk and Lee, 1999; Swanson, et al., 2001) and have been particularly useful for characterizing recharge in urban areas (Appleyard, 1995; Barrett, et al., 1999; Lerner, 2002; Morris, et al., 2005). Anthropogenic components used as tracers are typically conservative anions such as chloride, although other anions, such as nitrate and sulfate have proven useful as anthropogenic tracers in conditions where they are present above natural background levels. Other compounds found in urban groundwater that have been used to identify recent recharge include pesticides, herbicides and their breakdown products, and a host of other man-made compounds including caffeine, pharmaceuticals, and bug repellants (e.g. Vazquez-Sune and others, 2005).

Chloride as a proxy to characterize the distribution of recently recharged groundwater has several advantages: 1.) Chloride is a conservative tracer; as such, it is expected to move relatively freely through aquifer materials. 2.) Chloride analyses are readily available and are included in routine chemical analyses; 3.) Chloride concentrations used to distinguish between natural background levels and anthropogenic inputs are above historical detection limits. Therefore, a large temporal range of

hydrochemical data can be used. In the TCMAx, a study in Dakota County found that chloride trends were increasing in time within the Jordan aquifer between 1999 to 2003, based on repeated sampling of the same wells (Dakota County, 2006). Similar trends have been identified in the Chicago area where long-term increases of chloride concentrations in groundwater have been documented, again based on repeated sampling in the same wells over the period of decades (Kelly, 2008)

Chloride, because of its conservative chemical properties, works well for establishing baseline conditions both in absolute concentration and in comparison to other anions. Chloride has also been used in mass balance calculations to estimate recharge rates in a number of different hydrogeologic settings, including arid to semi-arid alluvial areas (Subyani, 2004; Edmunds et al., 2002) and in areas of changing agricultural land use (Huang and Pang, 2011). Extensive literature exists on using chloride as an indicator of anthropogenic source-waters (e.g., Panno, 2006). In this study, chloride concentrations are compared to tritium concentrations to show correlation between elevated chloride levels and its occurrence in groundwater that, at least in part, recharged within the last 60 years. Chloride to bromide ratios are also useful to distinguish elevated chloride due to anthropogenic sources (Mullaney et al., 2009; Eckman and Alexander, 2005) and the presence of older, more saline waters (Davis et al., 1998; Alexander, 2005; Freeman, 2007). Older waters with elevated chloride typically have higher bromide concentrations compared to recently recharged waters. As analytical detection limits for bromide have lowered, ratios are an increasingly effective tool for identifying a broad range of source waters (Alexander, 2005).

In addition to chloride, other marker species or environmental tracers in groundwater can help identify groundwater flowpaths. The term ‘environmental tracer’ can encompass a wide range of chemical compounds. In reference to atmospheric sources, it is defined as constituents and dissolved gases (e.g., chlorofluorocarbons, isotopes of hydrogen, helium and other noble gases, carbon, and oxygen) that are entrained in precipitation and recharged to groundwater (Shapiro, 2011). Tracers can be natural/environmental, inadvertent (as in the case of groundwater contamination), and intentionally applied (Scanlon et al., 2002).

Environmental tracers are also useful for characterizing groundwaters by their residence times. Where age determinations are based on a known rate of isotopic decay (i.e. carbon 14, tritium/helium) or on a known atmospheric concentration or loading rate such as chlorofluorocarbons (CFC) or sulfur hexafluoride (SF₆), a piston flow assumption is often used to calculate time of travel. When the piston flow assumption is not used, calculating a groundwater age from a tracer requires some type of interpretation relating measured concentrations to an age distribution in groundwater discharge and a mean residence time of water in the aquifer (Glynn and Plummer, 2005). Flow lines of different lengths and travel times contribute water to a single sampling site, and mixing of groundwater ages in a single water sample makes the piston flow assumption tenuous (Zuber et al, 2005).

In a study that combined CFC measurements, multiple geostatistical realizations of permeability distributions and a numerical groundwater flow and contaminant transport model, Weissmann et al., (2004) showed that groundwater reaching a well in a

heterogeneous aquifer (stream dominated alluvial fan) typically consists of a wide distribution of groundwater ages, even over screened intervals less than 1.5 meters long. They concluded that the significant dispersion of groundwater ages “implies that ultimate, maximum effects of nonpoint source, anthropogenic contamination of groundwater may not be reached until after many decades or centuries of gradual decline in groundwater quality” (Weissmann et al., 2004).

Differential advection of anthropogenic tracers has also been used to interpret groundwater flowpaths. Zhang et al., 2001, concluded that microorganisms, whose size limits their passage through small aquifer pores, sample a subset of total pathways that favor higher groundwater velocities. In contrast, conservative solutes are less limited by pathway geometries and reflect bulk (mean) groundwater flow velocities. In fractured porous media, such as fractured clayey or silty aquitards or fractured sedimentary rocks, diffusion into the low-conductivity matrix prevents the use of methods such as tritium/helium -3 dating to obtain more precise groundwater ages (Bradbury et al., 2006). Difficulties in interpreting residence time from environmental concentrations in fracture rocks settings arise because of abrupt spatial changes in hydraulic properties; macropores with a wide range of dimensions and connectivities result in velocities that can vary over orders of magnitude (Shapiro, 2011).

In contrast to their use for calculating absolute ages, both chemical and isotopic data have been used in the TCMAx and elsewhere in southeastern Minnesota to assign residence time classifications to water samples. A widely used model that has shown to be useful is the three-component model of Alexander and Alexander (1989). In this

model, a “vintage” age is assigned to waters with no detectible tritium and chloride concentrations at natural background levels. These waters are thought to be dominated by waters having entered the ground prior to 1953. “Recent” waters are identified by having tritium concentrations greater than 10 tritium units and have chloride levels well above natural background levels. These waters are thought to be dominated by waters that entered the ground since 1953. Finally, “mixed” waters are considered mixtures of these two end members, with detectible tritium < 10 tritium units and intermediate chloride concentrations. It should be noted that all groundwaters are mixtures to some degree.

Recognizing that all groundwaters are mixtures, the presence of an atmospheric tracer such as tritium, CFC, or SF₆ indicates a hydraulic connection between the land surface and an aquifer, and a groundwater age for at least a portion of the water sampled can be assigned that is less than or equal to its first known ubiquitous atmospheric occurrence. Furthermore, the premise applied in this study is that groundwater with a detectible anthropogenic tracer has traveled wholly or in part along relatively rapid pathways, and groundwater without these components traveled along less rapid pathways (Bradbury et al., 2006).

Chemical and isotopic data have been used to identify zones of preferential flow due to secondary porosity and permeability in sedimentary rocks. There is extensive literature on the use of artificial tracers to characterize groundwater flow in karst aquifers (see Benishcki et al., (2007) for a summary of methods and references). More relevant to this study is the use of changes in water chemistry, isotopes or physical parameters such

as temperature or conductivity to identify zones of preferential flow at a regional scale. The persistence of distinct chemical signatures over larger regions has been attributed to groundwater flow along discrete zones that limit the amount of dispersive mixing (Scheiber et al., 1999). Swanson et al., (2006) found that abrupt changes in fluid temperature, fluid resistivity from borehole geophysical logs corresponded to changes in flow rate within specific portions of the Tunnel City Group in Wisconsin, and that these zones could be correlated over tens of kilometers. Novakowski and Lepcevic (1988), found evidence for rapid flow in the upper portion of a bedrock aquifer based on chemical composition and electrical conductivity that matched detailed hydraulic measurements using multiple packer tests. In terms of groundwater flow, similar findings of both regional correlation and changes in near-surface and deep bedrock conditions have been documented in Minnesota for the Tunnel City Group (Runkel et al., 2006) and the Prairie du Chien Group (Tipping et al., 2006).

Finally, hydrochemical and isotopic information can complement groundwater flow modeling efforts in several ways, including interpretation of groundwater recharge mode and origin, model calibration, and refinement of conceptual flow models (Lerner, 2002; Mazar, 2004; Glynn and Plummer, 2005). Chemical and isotopic data are useful for identification of recharge areas, geochemical evolution along flowpaths, mixing of different chemical types, and identifying hydraulic connections (flowpaths) between aquifers (Matter et al., 2005). Isotope studies greatly benefit from the addition of hydrochemical analyses by providing insights in to groundwater pathways (Matter et al., 2005; Kendall, 2005). Different recharge areas and moisture sources can be proposed

based on environmental isotope data and tested for their consistency with the overall geochemical evolution of the groundwaters (e.g. Matter et al., 2005). When used in conjunction with groundwater flow models, chemical and isotopic data can help refine conceptual models of groundwater flow based on hydraulic head data alone.

Several recent studies have attempted to fully integrate groundwater flow modeling with hydrochemical and isotopic data, involving an iterative procedure of flow model refinement and hydrochemical facies reinterpretation, ultimately resulting in a more accurate depiction of aquifer systems than by either approach on its own (Mattle et al., 2001; Plummer et al., 2004; Sanford et al., 2004). Tracers can reveal the complexity of subsurface systems not predicted by numeric modeling based solely on hydraulic head (e.g. Clark et al., 2004). Information on residence time and pathway from chemical and isotopic data can help guide calibration of regional groundwater flow models. Inverse modeling of hydraulic properties based on calibration on hydraulic heads does not necessarily always provide a unique solution; the use of chemical and isotopic data as tracers help constrain conceptual models of groundwater flow, leading to hydraulic conductivity distributions that are more consistent with physical measurements and depositional settings. In urban areas, the difficulty in quantifying flux, points to the utility of using chemical markers to indicate zones of preferential recharge (Lerner, 2002).

DATA AND METHODS

One of the goals of this project is to collect data that could be analyzed spatially in both the horizontal and vertical sense. To that end, data was not included unless the location and subsequent elevation at the land surface of the well that the water sample came from could be determined with some degree of certainty (either field-located for more recent data or plotted on a map in the case of older data). Furthermore, data were linked to a Minnesota unique well number wherever possible, allowing the water sample to be interpreted in the context of available well construction information. All wells contained in this dataset, with a six digit unique well number, can be found in the Minnesota state water well database, County Well Index (CWI) (MDH and MGS, 2012). Chemical and isotopic data used in this investigation are stored in a geographic information systems “geodatabase” structure (ESRI, 2012), included as an electronic appendix to this thesis. Database structure and field definitions are included in Appendices B and C.

As discussed, in more recent TCMAx studies, sample populations based on traditional hydrogeologic framework have assumed hydrogeologic unit boundaries correspond to stratigraphic unit boundaries. By focusing instead on the open-hole interval of a sampled well and where it falls with a formation, historical water chemistry data was used in this investigation to re-evaluate conclusions reached in previous studies.

Sources of historic chemical and isotopic data

Sources of historic water chemistry data used in this investigation are: the U.S. Geological Survey National Water Inventory System (U.S. Geological Survey, 2010); the Minnesota Department of Health; the Minnesota Pollution Control Agency GWMAP program—both ambient groundwater monitoring and land-use studies (Minnesota Pollution Control Agency, 2010); University of Minnesota graduate studies (Tipping, 1992; Nemetz, 1993; Burman, 1995); Dakota County Environmental Management (2006); Anoka County Community Health and Environmental Services (Marsh, 1996, 2001); and samples from 27 wells in northwestern Hennepin County, where there were limited existing data. Additional data include earlier historic data from both regional (Hall et al., 1911; Maderak, 1963; Lively et al., 1992) and local studies (Alexander and Ross, 2003; Andrews et al., 2005), along with tritium and strontium isotope analyses from northwestern Hennepin County (Tipping et al., 2010).

Types of data, summarized in Table 2 include major cations and anions; field parameters, including temperature, electrical conductivity, pH, dissolved oxygen, and Eh; stable isotopes of oxygen and hydrogen, radioactive isotopes of carbon and tritium used to estimate residence times; and specific groundwater contaminants targeted by public health investigations (nitrate and peroflourochemicals).

Combining a large number of data collected over time by different organizations and analyzed by different labs compounds uncertainty in summarizing data values. Where documented, field samples were collected by sampling raw water (not having passed through a treatment system), typically from an outside faucet for domestic wells, or from the well house for municipal wells. Water was run until field parameters of

temperature, conductivity, and pH stabilized. Cation samples were acidified, and alkalinity titrations were generally performed within 24 hours of the time the sample was taken. The analyses included in this investigation were performed by labs adhering to standard quality assurance and quality control protocol, and collected according to similar standards. Calculations involving cation ratios used a subset of the data where a charge balance error of less than 5% could be determined. To reduce uncertainty where only a limited number of analyses were available (charge balance could not be calculated), only threshold values higher than the highest recorded detection limit plus estimated uncertainty for that analyte were used.

Table 2 Summary of chemical and isotopic data used in this investigation						
dataset	reference	no. of sample events	major cations and anions	trace metals	temperature	conductivity
SCA_1	Alexander, 2010a	23	x, includes Sr and Ba		x	x
SCA_2	Alexander, 2010b	5	x, includes Sr and Ba; Br		x	x
SCA_3	Alexander, 2010c	20	x			
QWDATA	USGS, 2010; includes Andrews et al., 2005;	644	x, includes Sr, Ba; Br		x	x
SBUR_MS	Burman, 1995	107	x, includes Sr, Ba; Br		x	x
C19 - EM	Dakota County, 2006	146				
CMTS	DNR, 2001 (American Linen - one analysis)	1				x
EOR	EOR, 2003; Alexander, S.C. and Ross, M., 2003?	70	x, includes Sr, Ba; Br		x	x
Hall_etal	Hall et al., 1911	37	x			
CMTS_RA	Lively et al., 1992	51	x, includes Sr and Ba		x	x
Maderak	Maderak, 1963	130	x		x	x
ACHES	Marsh, 1996; Marsh, 2001	134	x, includes Sr and Ba; Br		x	x
GWM_04-08	MPCA, 2010a; MPCA, 2010b	207	x includes some Br		x	x
GWM_92-96	MPCA, 1998	107	x, includes Sr and Ba; Br		x	x
LCMROPDC	MGS, 2001	5	x, includes Sr and Ba; Br		x	x
PFC	MDH, 2010a	3273				
PWS	MDH, 2010b; MDH, 2010c	1236	x, manganese, chloride, sulfate, nitrate			
RTIP_MS	Tipping, 1992	22	x, includes Sr and Ba; Br		x	x
DNEM_MS	Nemetz, 1993	94	x		x	x
CGA-RHA	MGS, 2010a	59	x, includes Sr and Ba; Br		x	x
ES	METC (single well, MW ED3); Braun, 2009	7	x, includes Sr and Ba; Br		x	
METC_NW1	MGS, 2007	27	x, includes Sr and Ba; Br		x	x

Table 2 Summary of chemical and isotopic data used in 1										
dataset	reference	pH	dissolved oxygen	Eh	O18	H2	tritium	carbon-14	nitrate	PFC's
SCA_1	Alexander, 2010a	x					x	x		
SCA_2	Alexander, 2010b	x								
SCA_3	Alexander, 2010c	x								
QWDATA	USGS, 2010; includes Andrews et al., 2005;	x	x	x						
SBUR_MS	Burman, 1995	x	x	x			x			
C19 - EM	Dakota County, 2006								x	
CMTS	DNR, 2001 (American Linen - one analysis)						x			
EOR	EOR, 2003; Alexander, S.C. and Ross, M., 2003?	x			x	x	x			
Hall_etal	Hall et al., 1911									
CMTS_RA	Lively et al., 1992	x						x		
Maderak	Maderak, 1963	x								
ACHES	Marsh, 1996; Marsh, 2001	x	x	x			x			
GWM_04-08	MPCA, 2010a; MPCA, 2010b	x	x	x						
GWM_92-96	MPCA, 1998	x	x	x						
LCMROPDC	MGS, 2001	x	x	x			x			
PFC	MDH, 2010a									x
PWS	MDH, 2010b; MDH, 2010c						x			
RTIP_MS	Tipping, 1992	x	x				x	x		
DNEM_MS	Nemetz, 1993	x	x	x			x			
CGA-RHA	MGS, 2010a	x	x		x	x	x			
ES	METC (single well, MW ED3); Braun, 2009	x								
METC_NW1	MGS, 2007	x					x			

dataset	reference	other
SCA_1	Alexander, 2010a	
SCA_2	Alexander, 2010b	
SCA_3	Alexander, 2010c	
QWDATA	USGS, 2010; includes Andrews et al., 2005;	
SBUR_MS	Burman, 1995	
C19 - EM	Dakota County, 2006	
CMTS	DNR, 2001 (American Linen - one analysis)	
EOR	EOR, 2003; Alexander, S.C. and Ross, M., 2003?	
Hall_etal	Hall et al., 1911	
CMTS_RA	Lively et al., 1992	gross alpha, Po, Rn, Ra226, Ra228, U, U234/U238
Maderak	Maderak, 1963	
ACHES	Marsh, 1996; Marsh, 2001	
GWM_04-08	MPCA, 2010a; MPCA, 2010b	
GWM_92-96	MPCA, 1998	
LCMIROPDC	MGS, 2001	
PFC	MDH, 2010a	
PWS	MDH, 2010b; MDH, 2010c	
RTIP_MS	Tipping, 1992	
DNEM_MS	Nemetz, 1993	
CGA-RHA	MGS, 2010a	
ES	METC (single well, MW ED3); Braun, 2009	
METC_NW1	MGS, 2007	Sr87/Sr86

Regional hydrochemical facies and baseline conditions

Regional hydrochemical facies were established by using a subset of the dataset whose calculated charge balance error was less than 5 percent. Piper diagrams were used to characterize general chemical composition by regions. Cation ratios from this same subset were used to further distinguish water types. Residence time data was then combined with chemical composition to differentiate between waters that have been impacted by activities at the land surface from those that have not.

The three-dimensional distribution of water types was mapped by contouring the top of open-hole elevations for each hydrochemical facies. Maximum and minimum elevations for each water type were determined either by their occurrence in water samples or by inference based on the presence or absence of confining units or proximity to underlying Proterozoic bedrock. Facies types were not extended into areas of insufficient data with the exception of naturally elevated chloride facies, where it is assumed that the source of these waters is from underlying Proterozoic bedrock.

To represent the three-dimensional distribution of water types in GIS, upper and lower boundary elevations for each hydrochemical facies were used to assign attributes to a matrix of points spaced 500 meters apart in the horizontal and 20 feet apart in the vertical direction. Points, as opposed to boundary rasters, were chosen based on three-dimensional viewing considerations when combining with other subsurface data. Point density was chosen based on reasonable memory limitations of current desktop computers.

Distribution of recent waters compared to bedrock hydrostratigraphy

The hypothesis that recent waters are found in macropores within the Paleozoic sedimentary bedrock of the TCMAx was tested by comparing open-hole elevation intervals of wells with measured chloride concentrations to elevations of known macropore development. These zones include an area within 50 feet of the bedrock surface, proximity to bedrock valleys, and enhanced macropore development within stratigraphic units (Figure 7). Specific stratigraphic targets were the Shakopee Formation and Shakopee-Oneota contact of the Prairie du Chien Group, and the upper Tunnel City Group (Franconia Formation).

In order to test enhanced permeability near the bedrock surface, a subset of the data was chosen where depth to bedrock was greater than or equal to 100 feet. This cutoff was chosen to reduce the likelihood that elevated chloride in a water sample was the result of proximity to the land surface. Open-hole intervals for bedrock wells with chloride data were classified by distance from the top of casing to the bedrock surface, and median chloride concentrations compared for wells with distances less than or equal to 10 feet to wells with distances greater than 10 feet.

In order to test enhanced permeability near bedrock valleys, two separate subsets of the data were chosen: bedrock wells with chloride data and bedrock wells analyzed for PFCs. Occurrence of chloride concentrations above background levels and detectable PFCs were compared with horizontal distances from the well's open-hole interval to a

bedrock valley. Edges of bedrock valleys were defined by mapped bedrock topographic contours between 400 and 800 feet above mean sea level.

Wilcoxon rank-sum statistics with the normal approximation for large sample sets were used to compare populations based on water well open-hole intervals (Wilcoxon, 1945; Helsel and Hirsch, 2002). Non-parametric methods were used because chloride concentrations in the sample data are not normally distributed. Test and descriptive statistics, combined with box plots and maps of well locations were used to summarize the range of data values and spatial distribution of each sample set.

Distribution of recent waters compared with vertical flux to upper bedrock aquifers

In order to evaluate the regional distribution of recent waters based on contoured well casing elevations, this distribution was compared with estimated flux through glacial deposits by calculating vertical travel times from the regional water table surface to upper bedrock aquifers. Focus on the downward flux of groundwater as a means of assessing groundwater recharge through glacial deposits is not a new approach. Larson-Higdem et al. (1975) applied similar methods to investigate downward groundwater leakage to the Prairie du Chien–Jordan aquifer system in the Twin Cities metropolitan area; their work was incorporated into a more recent evaluation of recharge to Twin Cities unconfined bedrock aquifers (Ruhl et al., 2002). In a more general application, vertical flux of groundwater is the fundamental part of groundwater sensitivity mapping (Minnesota Department of Natural Resources, 1991). In all cases, the complex pathways of

groundwater movement through unconsolidated materials are simplified by considering the vertical component of groundwater flow only.

While the vertical movement of groundwater is conceptually clear, its calculation is dependent on estimates of vertical hydraulic conductivity that are highly variable and difficult to measure. Most aquifer tests are designed to estimate horizontal hydraulic conductivity, based on the premise that groundwater flow to a pumping well is primarily horizontal. Direct measurements of vertical hydraulic conductivity are largely limited to laboratory experiments; field based values are typically based on leakage estimates derived from deviations from typical water level response curves to pumping.

Notwithstanding scale effects that account for increases in hydraulic conductivity due to scale of measurement—lab to field to regional—it is assumed that a reasonable regional scale estimate of vertical hydraulic conductivity falls within the broad range of measured horizontal hydraulic conductivities for a given geologic material. For this investigation, mean horizontal hydraulic conductivity values from an earlier investigation for the Metropolitan Council (Tipping et al., 2010) were used as estimates of vertical hydraulic conductivity (Table 3). Methods used to calculate mean vertical hydraulic conductivity in the TCMAx are provided in Appendix A. The regional texture database is included in the electronic data appendix.

Table 3 hydraulic conductivity values for subsurface textures

Corresponds to field “K_composite” in gridpoint. code specifies range of expected hydraulic conductivity in feet/day. Reference to “deep” in codes 8-11 are for point depths greater than 60 feet from land surface, estimated to be 2 orders of magnitude lower hydraulic conductivity than equivalent textures in shallow settings:

<i>code</i>	<i>Texture Description</i>	<i>Kmax (ft/day)</i>	<i>Kmin (ft/day)</i>
1	loam to clay loam	3.0E-3	1.0E-3
2	loam to sandy loam	2.0E+1	1.0E-1
3	loam, silt rich; silt and clay	2.0E-2	3.0E-4
4	loam to sandy clay loam	2.0E+1	1.0E-1
5	sand and gravel	5000	100
6	fine sand	30	0.3
7	sandy silt	3	0.1
8	loam to clay loam - deep	3.0E-5	1.0E-5
9	loam to sandy loam - deep	2.0E-1	1.0E-3
10	loam, silt rich; silt and clay - deep	2.0E-4	3.0E-6
11	loam to sandy clay loam - deep	2.0E-1	1.0E-3

The most complete data on the distribution of subsurface materials comes from areas where Quaternary stratigraphic mapping has taken place (see Appendix A, Figure 38). In the TCMAx, Quaternary subsurface mapping occurred first in Washington County as part of a county project (Meyer and Tipping, 1998), was included as part of a hydrogeologic investigation of the northwestern metropolitan area (Meyer and Tipping, 2007), and has been part of more recent county atlases in Scott, Carver, and Chisago Counties (Lusardi and Tipping, 2006; Lusardi and Tipping, 2009; Meyer, 2010). In areas not covered by subsurface mapping, subsurface texture distributions were estimated from data in the Minnesota state water well database County Well Index (CWI), as described in Appendix A.

Data on vertical hydraulic head gradients come from two sources. Water table elevations were taken from a regional investigation on groundwater/surface-water interaction (Barr, 2010). Bedrock potentiometric surfaces are based primarily on synoptic measurements of the Prairie du Chien and Jordan aquifers (Sanocki et al., 2009), augmented with data from CWI where these rocks are absent. Based on bedrock hydrostratigraphy, elevation of bedrock units and elevation of regional discharge (Mississippi, St. Croix and Minnesota Rivers), horizontal groundwater flux is assumed to be greatest within Prairie du Chien Group and Jordan Sandstone. It is expected that this flux drops off significantly below the St. Lawrence Formation. By combining synoptic measurements from the Prairie du Chien and Jordan aquifers, with CWI data for uppermost bedrock units beyond the extent of the Prairie du Chien and Jordan, the resultant bedrock potentiometric surface is meant to provide generalized base hydraulic head data for flow systems most directly connected to activities at the land surface.

Vertical travel times were calculated as follows:

$$T = L / ((K_v * 365_{\text{days}} * (\Delta h / L)) / n)$$

$$= L^2 n / (365_{\text{days}} * K_v * \Delta h)$$

T = vertical time of travel in years

L = distance from regional water table to bedrock surface, in feet

K_v = bulk vertical hydraulic conductivity in feet/day

for saturated conditions: mean value of gridpoints from water table to bedrock surface

Δh = difference in elevation between regional water table and bedrock potentiometric surfaces in feet. (vertical hydraulic head gradient = $\Delta h / L$)

n = effective porosity, set equal to 0.20

The hydraulic head gradient between the regional water table and bedrock aquifers was determined by dividing the difference in hydraulic head, Δh , by the vertical distance, L , from the water table to the bedrock surface (Figure 8). Perched conditions in the central metropolitan area are present within and above the Platteville Formation; in places, the upper St. Peter Sandstone is unsaturated below it. These conditions invalidate the use of a Darcy flux-based calculation to estimate travel time from the water table to the Prairie du Chien Group and Jordan Sandstones. Although unsaturated conditions within glacial sediments are known to occur under the regional water table surface, the unconsolidated deposits below the regional water table were considered to be fully saturated for the travel-time calculation.

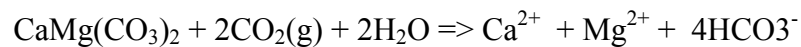
RESULTS AND DISCUSSION

Hydrochemical facies and baseline conditions

The chemical composition of groundwater in the TCMAx is broadly similar between aquifers. Regional Piper diagrams (Figure 9) of Quaternary (Scott, Hennepin, Anoka, and Washington Counties) and bedrock (Dakota County) show predominantly calcium-magnesium-bicarbonate waters. An exception is in Anoka County and to a lesser degree in Scott and Hennepin Counties, where a portion of samples have more sodium relative to calcium and magnesium. Higher sodium relative to calcium plus magnesium is also found in Carver County (not shown). Residence time classification based on tritium concentrations are represented by color. Three-dimensional representations of these points are also included, where stick height is relative to total

dissolved solids (TDS) content (Alexander et al., 2005)

Recent waters, shown in red, typically have a greater concentration of chloride and/or sulfate relative to older samples. The substitution of chloride and sulfate for bicarbonate in waters dominated by recent recharge can also be seen by comparing calcium and magnesium concentrations to bicarbonate (Figure 10). In a system where chemical composition of groundwater is controlled solely by the dissolution of dolomite, bicarbonate molar concentrations would be expected to be twice the molar concentration of calcium plus magnesium:



This ratio is shown as a straight line in Figure 10. Waters with no detectable tritium, shown in blue, generally plot close to the line, whereas recent waters, shown in red, plot above it. Outliers plotting close to the x axis are likely vintage sodium-bicarbonate waters in Anoka County and a mixed-age sodium-bicarbonate-sulfate sample from Scott County that have gone through water softeners prior to sampling.

A comparison of major cations with residence times provides the first clear distinction in water types. Vintage waters are, for the most part, calcium-magnesium-bicarbonate waters, whose chemistry is controlled by dissolution of calcite and dolomite. Noticeable exceptions to this trend are vintage waters with elevated sodium; recent waters typically have elevated chloride and/or sulfate. Vintage waters with elevated sodium could be indicative of ion exchange or contact with end member naturally elevated chloride waters discussed later in this section.

Further distinction between water types can be made by comparing molar ratios of

strontium to calcium and magnesium (Figure 11). Wells below the Eau Claire Formation have markedly higher concentrations of strontium relative to calcium plus magnesium. Wells above the Eau Claire Formation show a much smaller, non-linear increase in strontium concentrations as calcium plus magnesium concentrations increase. Regionally, Sr/(Ca+Mg) ratios in wells above the Eau Claire are most evident in the western and southwestern TCMAx (Figure 12.A.) Based on available data, their distribution with depth varies, with higher ratios in the Quaternary limited to the west, (Figure 12.B), higher ratios in the Jordan limited to its western extent (Figure 12.C) and higher ratios extending throughout the basin in the Mt Simon (Figure 12.D). Results are hand contoured; correlation lengths based on variograms for wells exceeding threshold ratio of 0.0009 range from 6600 meters (Mt. Simon) to 80,000 meters (Jordan).

Elevated Sr/(Ca+Mg) ratios in Quaternary groundwater samples are interpreted to be the result of aragonite dissolution and re-precipitation of pure calcite. Primary aragonite, expected to be present in Des Moines lobe diamicton, contains relatively higher strontium substituting for calcium in its crystal structure. As aragonite dissolves, strontium is released into solution, but does not preferentially re-precipitate as calcite (Appelo and Postma, 1994). These strontium-enriched waters are present in bedrock wells above the Eau Claire Formation in the western TCMAx. Below the Eau Claire Formation (Mt. Simon Aquifer), still higher ratios exist and may not be attributable to the aragonite dissolution/calcite precipitation model (Figure 11). Because of their regional extent, elevated Sr/(Ca+Mg) waters are used to distinguish water from west to east and at depth, as a subset of calcium-magnesium-bicarbonate waters.

Recent waters, characterized by elevated chloride and/or sulfate relative to bicarbonate are the second regional hydrochemical facies addressed in this investigation. The abundance of groundwater samples with both tritium and chloride data allows the determination of chloride concentrations in waters that have not been impacted by recent recharge. Tritium to chloride concentrations are compared both as a scatterplot and by comparing the range of chloride values in wells with detectable tritium versus wells without detectable tritium (Figure 13). These data support conclusions reached from earlier regional work that natural, or background chloride levels in the Paleozoic aquifers of southeastern Minnesota are less than 5 milligrams per liter (Tipping, 1994), and are similar to a value of 10 milligrams per liter for bedrock aquifers reported by Mullaney et al. (2009). This threshold value makes chloride a useful surrogate for indicating the presence of recent waters where tritium data are not available.

The distribution of chloride concentrations compared to tritium concentrations across the TCMAx is broadly similar (Figure 14A and B). Contouring the elevation of the open-hole tops of bedrock wells with detectable tritium shows the uneven distribution of tritium with depth across the TCMAx (Figure 14 C and D). Results are hand-contoured; correlation lengths based on variograms for wells with detectable tritium range from 50 meters (average open-hole elevations less than 500 feet) to 5000 meters (average open-hole elevations greater than 750 feet). Other open-hole intervals with anthropogenic compounds such as PFCs fall within (above) these contours. Combining these elevations of recent waters where data is not available (Tipping et al., 2010) allows for construction of a region-wide digital elevation model that marks the base elevation of

recent waters within the TCMAx.

Not all chloride concentrations above 5 milligrams per liter are indicative of recent waters. Furthermore, as mentioned earlier, several wells in Anoka County have vintage waters with sodium concentrations that are distinctly different than elsewhere within the TCMAx. The third hydrochemical facies addressed in this investigation are wells with naturally elevated chloride. These waters have high chloride concentrations that are not attributable to man-made sources.

Low chloride to bromide ratios in waters with elevated chloride are indicative of bedrock sources, often associated with deeper water and longer residence times, where longer rock-water interaction has increased the amount of bromide relative to chloride in the groundwater. In this dataset, many of the samples from lower aquifers that do have elevated chloride do not have accompanying bromide analyses for comparison. They do, however, have estimated groundwater ages based on carbon 14 samples. The distribution of these samples, along with major fault locations in the TCMAx, is shown in Figure 15. The spatial association of naturally elevated chloride and faults is also seen in earlier bedrock well data from Hall et al., (1911), and in unconsolidated deposits within a bedrock valley near the Belle Plaine Fault system in western Scott County (Figure 15.A). Source waters for naturally elevated chloride at these locations are thought to be Proterozoic bedrock, where fractures associated with faults provide pathways for these deeper, more saline waters to mix with the more dilute waters in Paleozoic bedrock.

These Proterozoic waters may also be the source for elevated sodium relative to calcium and magnesium seen in several Anoka County wells discussed earlier. Mean

concentrations for water samples with carbon-14 derived ages of greater than or equal to 1200 years have a mean sodium concentration of 77 mg/l (n = 40), whereas remaining vintage waters with measured sodium concentrations have a mean value of 16 mg/l (n=267). The location of these older waters are included in Figure 15.A and were used along with other points to define the upper extent of this hydrochemical facies.

High chloride to bromide ratios, where available in the rest of the dataset, are useful for distinguishing chloride that is not from bedrock sources. Their locations fall within (above) the base elevation contours for recent waters discussed earlier (Figure 15.B).

Distribution of recent waters compared to bedrock hydrostratigraphy

Comparison of recent waters to the distribution of bedrock macropores

The second goal of this investigation was to test whether recent waters are preferentially found in areas of enhanced macropore development. One zone of enhanced macropore development is near the bedrock surface. Chloride concentrations were compared to the distance from this surface to a well's casing bottom. To remove the influence of high-capacity pumping on the results, only domestic wells were used. The subset of data was chosen by the additional constraint that depth to bedrock had to be greater than or equal to 100 feet to reduce the influence of shallow to bedrock conditions.

A scatterplot of the data shows a trend of decreasing chloride concentrations with increasing distance from the casing bottom to the bedrock surface (Figure 16). However, median concentrations for datasets with distances greater than or less than 10 feet are not significantly different from one another at $\alpha = 0.05$. The spread of chloride values

from samples with a distance less than or equal to 10 feet is greater and reflected in a higher mean value for this data group (Figure 16).

A second zone of enhanced macropore development is near bedrock valleys, where a greater density of vertical fractures is expected. Chloride concentrations are compared to distance from the sampled well to a buried bedrock valley (Figure 17). As with the bedrock surface comparison, a subset of domestic wells was used to lessen the possible impact of high-capacity pumping on the results. A scatterplot of the data shows a trend of decreasing chloride with increasing distance from the bedrock valley. As with the bedrock surface comparison, median values for data grouped by a threshold distance are not significantly different from one another at the alpha level of 0.05. Similarly, the range of values for distances less than 400 meters is greater, and reflected in a higher mean value for this data group. The test was repeated for all wells over a greater distance with similar results (Figure 18). Although a trend of lower chloride concentrations with greater distance from the bedrock valley is evident in the scatterplot, median values between groups separated by a threshold distance of 2000 meters are not significantly different at $\alpha = 0.05$.

A final chemical test for enhanced macropore development near bedrock valleys, perfluorobutanoic acid (PFBA) concentrations were substituted for chloride and a comparison of concentration to bedrock valley distance was repeated. A subset of the PFC (PFBA) data was chosen, using only samples whose concentration was greater than 0.1 micrograms per liter. This cutoff was used because it is the higher detection limit from earlier PFC sampling, uniformly limiting the data to only wells where PFBA was

detected.

As with the chloride data, the scatter plot shows a trend of decreasing PFBA concentration with increasing distance from a buried bedrock valley (Figure 19). In this case, median values for a sample set less than 1000 meters are significantly higher than sample set greater than 1000 meters at the $\alpha = 0.05$ level ($p < 0.001$; one sided test).

Enhanced macropore development within stratigraphic horizons

To test whether recent waters are preferentially found in stratigraphic intervals of known macropore development, open-hole intervals were compared with stratigraphic position. Specific stratigraphic targets were the Shakopee Formation and Shakopee-Oneota contact within the Prairie du Chien Group, and the upper Tunnel City Group (Franconia Formation).

An initial assumption was that there would be enough of a spread of open-hole intervals across a stratigraphic unit that separate sample sets could be established. In actuality, wells are typically completed within stratigraphic horizons of enhanced macropore development and not elsewhere.

The stratigraphic distribution of waters by age class shows recent waters are found most often above the St. Lawrence Formation (Figure 20). Within the Prairie du Chien Group, the majority of wells sampled are classified as recent waters. Furthermore, the few wells completed in the lower Prairie du Chien Group highlight by their absence the relatively low permeability in this portion of the stratigraphic unit.

In the Tunnel City Group, there are similar patterns in both the distribution of

recent waters and stratigraphic position of well completions (Figure 20). Recent and mixed waters are found in the upper Tunnel City Group, where the presence of macropores has been documented regionally (Runkel, 2006, Swanson, 2006, 2007). As with the Prairie du Chien Group, there is a lack of well completions in the lower Tunnel City Group, indicating relatively low porosity and permeability at this stratigraphic position.

The presence or absence of recent waters and the stratigraphic position of open-hole intervals broadly supports the revised hydrostratigraphic framework for these rocks. Although the resolution of the chemical combined with open-hole interval data does not discriminate flow systems to the degree seen in borehole measurements, it does support separation of traditionally lumped stratigraphic intervals (i.e., the Prairie du Chien-Jordan, and Franconia-Ironton/Galesville aquifers) into separate hydrostratigraphic units. Comparison of chemical data between wells finished in the Prairie du Chien Group and the Jordan Sandstone warrant further discussion due to the number and distribution of wells sampled.

Together, the Prairie du Chien Group and Jordan Sandstone provide the majority of groundwater for municipal and industrial use in the TCMAx. Traditional lumping of the these two rock units into a single aquifer has largely been based on hydraulic head differences of tens of feet or less, which on a regional scale, were considered insignificant.

A comparison of chloride content by aquifer shows distinct regional differences between Prairie du Chien Group and Jordan samples (Figure 21). In the west region,

concentrations are low in both Prairie du Chien and Jordan samples, with a greater spread and higher median value in the Prairie du Chien. Median chloride values for the Prairie du Chien samples are not significantly different than Jordan samples at $\alpha = 0.05$ ($p = 0.192$, one sided test). Greater spread and higher median values in the Prairie du Chien are also found in the east region, with overall median values for both Prairie du Chien and Jordan sets greater than respective units in the other two regions. Median Prairie du Chien values are significantly different than Jordan values at $\alpha = 0.05$ ($p = < 0.001$, one sided test). In the central region, there are lower median values but a greater spread in the Jordan compared to the Prairie du Chien. Median Prairie du Chien values are not significantly different than Jordan values at $\alpha = 0.05$ ($p = 0.149$, one sided test). The greater spread in Jordan values from the central TCMAx is attributed to increased vertical mixing of recent waters at depth due to high capacity pumping in that region.

PFC contamination in Washington County combined with the number and distribution of wells sampled provides an independent means to evaluate the hydraulic connection between these rock units on a regional scale. Figure 22 contains a series of stacked columns, depicting the number of detect verses non-detects of PFBA for both the Prairie du Chien and Jordan wells, in regularly spaced sectors across southern Washington County. In a few sectors, shown by asterisk, there are enough samples from each rock unit to show stratification of detections, with markedly greater amount of detections in the Prairie du Chien group than in the Jordan. Cross section H-H' refers to Figure 35.A, discussed in the later section under regional synthesis.

Distribution of recent waters compared with vertical flux to upper bedrock aquifers

The regional distribution of recent waters was compared to calculated vertical flux to upper bedrock aquifers, as a means to evaluate the distribution based on elevation contour mapping alone. The TCMAx (Figure 23) was divided into 250 x 250 meter cells. Estimated vertical hydraulic conductivity of unconsolidated deposits in the TCMAx ranges from 2×10^{-5} to 2550 feet per day (Figure 23). A harmonic mean for each cell was chosen in order to give greater weight to low-conductivity sediments. Details on the subsurface texture database construction used in this calculation are provided in Appendix A. The calculated hydraulic head differential between the regional water table and March and August 2008 bedrock potentiometric surfaces shows a seasonal increase in the downward vertical hydraulic head gradient in the central TCMAx (Figure 24). These changes reflect increased drawdown in the bedrock potentiometric surface due to higher summer pumping rates from the Prairie Du Chien Group and Jordan Sandstone. Together, bulk vertical hydraulic conductivity and vertical hydraulic head gradient were used to estimate groundwater flux from the regional water table to the bedrock surface.

Estimated travel times from the water table to upper bedrock aquifers are shown in Figure 25. The distribution of recent waters in upper bedrock aquifers broadly supports estimated vertical travel times, with recent water found at depth in areas with large vertical hydraulic head gradients and coarse material over bedrock. It should be noted that these estimates are based on one of many possible combinations (realizations) for composite vertical hydraulic conductivity; each change in subsurface texture is represented by a single value of hydraulic conductivity that falls within a range of values

considered reasonable for that texture. In this way, the resulting estimates of vertical travel times show relative differences in vertical flux across the TCMAx, rather than differences in absolute values.

The regions with the shortest calculated vertical travel times are in Dakota and Washington Counties, where there are both shallow-to-bedrock conditions and areas of thick sand deposits—both on bedrock plateaus and filling bedrock valleys. Shorter travel times are also found in southeastern Hennepin and central Ramsey Counties, where there is a greater vertical hydraulic head gradient than elsewhere in the TCMAx. Shorter travel times are also found in central and western Sherburne County where geologic conditions are predominantly sand-over-bedrock. Sherburne County is beyond the extent of Paleozoic bedrock aquifers, and surficial deposits are the primary groundwater source.

Areas with longer calculated vertical travel times are found in Scott, Carver, and western Hennepin Counties, where thick northwest provenance tills are found in combination with a small vertical hydraulic head gradient. Longer calculated travel times are also found in Anoka County. The Anoka Sandplain has traditionally been considered a recharge area for Paleozoic aquifers. Subsurface mapping of glacial deposits reveal a more complex stratigraphy below the surficial sand (Meyer, 2007). These conditions, combined with a low vertical hydraulic head gradient, result in a longer calculated vertical travel time.

Regional synthesis

Combining estimated vertical travel times with the distribution of hydrochemical facies provides a general picture of regional groundwater flow patterns in the TCMAx. A series of oblique images combining hydrochemical facies and key bedrock units are shown in Figure 26. Figure 26.A depicts the Pre-Cambrian surface, considered the bottom of the TCMAx bedrock aquifer/aquitard system. Major river elevations are shown for comparison. Naturally elevated chloride waters are largely limited to the lower Mt. Simon aquifer, near the Pre-Cambrian surface (Figure 26.B), with the exception of areas near major faults, where it appears above the Eau Claire confining unit in parts of Anoka, and northwestern Dakota/southeastern Washington Counties, and where the Eau Claire is absent in a bedrock valley near Belle Plaine in western Scott County (Figure 26.C).

Elevated Sr/(Ca+Mg) waters are found in the western TCMAx, in both glacial deposits and in the Jordan Sandstone and Prairie du Chien Group (Figure 26, D, E and F). Elevated Sr/(Ca+Mg) waters are also found in the Mt. Simon aquifer as discussed earlier. Not shown on Figure 26, these Mt Simon strontium-enriched waters may have a different strontium source than waters above the Eau Claire Formation.

Recent waters are found below the elevation of the major rivers in the central TCMAx, near the intersection of the Mississippi and Minnesota Rivers (Figure 26.G.), expanding to higher elevations in the broader TCMAx (Figure 25.H), to present everywhere within 50 feet of the land surface (Figure 26.I). For the most part, recent

waters are found above the elevation of the major rivers, with the exception of areas where increased vertical gradient due to high capacity pumping draws water below river discharge elevations. In a stratigraphic sense, most of these recent waters are found above the St. Lawrence Formation (Figure 20).

These regional water types combined with subsurface geologic conditions and vertical hydraulic gradient are summarized regionally by cross sections A-A' through E-E' (Figures 28 to 33; cross section locations are shown on Figure 25; a key for cross section symbols is included in Figure 27). From Sherburne County to Mississippi River (cross section A-A', Figures 28 and 29), recent waters are interpreted as present in the upper 50 feet of unconsolidated deposits, increasing with depth in the central part of the basin. The lowest elevation of recent waters occurs in the Jordan Sandstone. Carbon 14 dates for Mt. Simon are shown, indicating a sharp contrast in recharge rates for the upper and lower aquifer systems.

From St. Francis, in Anoka County to Mississippi River (cross section B-B', Figure 30), recent waters are interpreted as present in the upper 50 feet of unconsolidated deposits, increasing with depth in the central part of the basin. The lowest elevation of recent waters occurs in the Jordan Sandstone. Complexity of unconsolidated deposits over bedrock, below surficial sands is shown.

From Big Marine Lake, Washington County to Mississippi River near downtown St. Paul (cross section C-C', Figure 31), recent waters are shown between Big Marine and White Bear Lake in the Prairie du Chien Group, largely based on tritium measurements from samples west and east of the cross section line interpreted as mixed

waters (TU between 1 and 10). Recent water is found at depth toward downtown St. Paul, coincident with a larger downward gradient and coarse unconsolidated deposits over bedrock. A slight upward gradient is present at White Bear Lake. A downward gradient near Big Marine possibly marks a groundwater divide, with regional discharge west toward the St. Croix River. Vintage waters on this cross section are found in the Mt. Simon aquifer, based on carbon 14 measurements.

From western Dakota County to Mississippi River near Hastings (cross section D-D', Figure 32), limited data show that the presence of clay, based on the interpolated model, restrict the downward movement of water west of the South Branch of the Vermillion River. The remainder of the cross section is largely sand and gravel over Prairie du Chien Group. A large buried valley filled with sand and gravel is present west of Hastings. Recent waters are present within this valley based on sampled wells within and on the edges of the valley to the southeast.

From southeastern Scott County to Minnesota River near Shakopee (cross section E-E', Figure 33), recent waters are absent below cover of alternating NW and NE provenance tills. Elevated Sr/(Ca+Mg) ratios are limited to a bedrock valley in upper aquifers and to the Mt. Simon in the lower aquifer. Naturally elevated chloride is present in the Mt. Simon at the northeast end of the cross section. The presence of recent water in the Jordan in this area based on sampled wells to the east and west of the cross section line. A strong upward hydraulic gradient from the Jordan is present near the Minnesota River.

Examples of local hydraulic conditions and the effect of strata-bound secondary porosity and permeability on groundwater movement are shown by cross section in Figures 34 and 35 (cross section locations shown on Figure 25). In the Edina area (cross section F-F', Figure 34.A), an age inversion within the open-hole of a single well is shown. Grab samples from the lower portion of the open-hole had detectible tritium, while the uppermost sample, located within the Shakopee Formation–Prairie du Chien Group, did not (MDH, 2010). Flow logging from a nearby test well (MN unique well no. 748656) showed strong downflow from the lower Shakopee to the Jordan Sandstone, corresponding to stratigraphic position of detectible tritium in this well. A stagnation zone of older water shown on the figure is interpreted as present underneath the central portion of the Platteville/Glenwood cap in this area.

In eastern Hennepin County (cross section G-G', Figure 34.B), recent water occurs at depth only east of till cover present in the western portion of the cross section. Flow logging east of Highway 169 showed strong upflow from fractures in the upper Jordan Sandstone to the upper Oneota Formation–Prairie du Chien Group (MN unique well no. 676445). Vintage water is interpreted as moving out of the Jordan Sandstone at this site, into a zone of lower hydraulic gradient within the Prairie du Chien Group within this portion of the cross section.

In south central Washington County to Mississippi River (cross section H-H', Figure 35.A), stratification of perflourochemical (PFC) detections between Shakopee (upper Prairie du Chien Group) and Jordan samples is shown. Results infer separate flow

systems, with possibly greater flux through the Shakopee Formation compared to the Jordan Sandstone.

From southeastern Washington County to St. Croix River (cross section I-I', Figure 35.B), a downward gradient is present over a north-south trending bedrock valley in the center of the cross section, west of Manning Avenue. The valley, filled with primarily coarse-grained material, shows cluster of PFC detections. Occurrence of PFCs near the St. Croix River indicates movement of groundwater through fractures and fault blocks, crossing stratigraphic units with wide ranging permeability.

Regional and local conditions provide the context for refining conceptual models of groundwater flow within the TCMAx. In southern Washington and central to east central Dakota County, coarse sediments overlie the Prairie du Chien Group. Much of this area is less than 50 feet to bedrock and the water table is largely below the bedrock surface. A large bedrock valley west of Hastings is also filled with coarse sediments. In areas where sufficient data exists, calculated vertical travel times are generally less than a year. Vertical gradients are controlled largely by regional discharge, although high capacity pumping for public water supply, commercial use and irrigation enhance vertical gradients locally.

In central and northern Washington County, relatively recent recharge occurs in areas of sandy NE provenance till over bedrock. Calculated vertical travel times are generally less than one to greater than 50 years depending on the presence of fine-grained sediment in the subsurface. A groundwater divide runs north-south through this portion

of the county as water moves either east toward the St. Croix River or southwest toward the Mississippi River. Vertical gradients are controlled largely by regional discharge.

Recent waters are found at elevations below regional discharge in east central and southeastern Washington County, where high capacity pumping increases vertical gradients locally.

Northeastern Washington, western Chisago and eastern Anoka and Northern Ramsey Counties have calculated vertical travel times generally greater than 500 years, largely due to the presence of fine-grained NW provenance tills and lacustrine sediment in the subsurface combined with a low vertical gradient. In western Anoka County, calculated vertical travel times are less, where the subsurface is composed of a greater percentage of coarse-grained sediments. Further west into Sherburne County, predominantly coarse grained sediments over bedrock result in calculated vertical travel times of less than a year. Recent waters are generally found only at shallower depths. Elevated Sr/(Ca+Mg) waters are limited to deeper aquifers in the central metro area, indicating diminished NW provenance till signature in recharge waters within these counties.

Where sufficient data exists, western Hennepin, Wright, Carver and Scott Counties generally have calculated vertical travel times of greater than 500 years. In these areas, a thick succession of NW and NE provenance tills and minimal vertical gradient restrict the downward movement of groundwater to bedrock. Water samples from bedrock wells below these tills have no detectible tritium, low chloride, and elevated Sr/(Ca+Mg) ratios, all indicative of older water receiving minimal recharge from

the land surface. In northeastern Hennepin County, water chemistry changes to more recent waters at depth, concomitant with a thinning and replacement of NW provenance till by coarse-grained terrace deposits along the Mississippi River. Calculated vertical travel times in the area are generally less than 50 years.

Eastern Hennepin and southern Ramsey County generally have calculated vertical travel times of less than a year, with the exception of areas where fine-grained material is present in the subsurface. Recent waters are found at elevations below regional discharge where high capacity pumping increases vertical gradients locally. These areas have the largest downward vertical gradients in the metropolitan area, in large part due to the presence of the Platteville and Glenwood Formations, along with remnants of Decorah Shale above them. Recognizing that much of the water table is perched within and above these formations, seasonal changes in the bedrock potentiometric surface based on synoptic measurements in March and August clearly demonstrate the influence of high capacity pumping on vertical gradient in these areas (Figure 24).

In eastern Hennepin and southern Ramsey County and elsewhere, recent waters are found at depth in areas with large vertical gradients and coarse material over bedrock. These areas are commonly located in bedrock valleys which provide important “windows” to lower aquifers where upper bedrock aquitards are absent. Data provided in this investigation show that not all bedrock valleys are filled with coarse material. Texture-based hydraulic conductivity estimates stored in a regular three dimensional grid format should help with groundwater modeling across these bedrock valleys.

Overall, calculated vertical travel times from the water table to upper bedrock aquifers range from less than a year to well over 500 years. Results show differences in near surface and deeper subsurface hydraulic conditions. Anoka County, for example, has short travel times to the regional water table through coarse-grained deposits at the land surface, and long vertical travel times to bedrock, through complex subsurface layering of NE and NW provenance till and sand (Figure 30, cross section B-B'). Areas in the central metropolitan area with travel times that are faster in saturated conditions than unsaturated result from texture differences between shallow and deeper sediments, and distance differences from the land surface to the water table and water table to bedrock, and areas near the Plateville subcrop edges where the saturated vertical gradient is greater than 1.

Chemical results show recent waters in uppermost bedrock aquifers at elevations generally above 750 feet (Figure 36). A limited number of wells in this dataset were sampled more than once, allowing variability in chloride concentrations to be compared with open-hole depth (Figure 37). More variability in chloride concentrations is found at shallower depths; recent waters detected at lower elevations are most often found in high capacity wells and in wells near areas of high capacity pumping. Bedrock aquifers containing highest percentage of recent waters are stratigraphically above the St. Lawrence Formation (Figure 20). Furthermore, chemical results support the premise that waters most impacted by activities at the landsurface—"manageable waters"—occur at elevations controlled by regional discharge to the major rivers, and high capacity

pumping from the Prairie du Chien and Jordan aquifers or other uppermost bedrock aquifers where these rocks are not present.

In the Twin Cities metropolitan area, groundwater ages range from less than a year to over 30,000 years. Stratification of groundwater ages, with younger water found in local and intermediate flow systems over older waters is common to most hydrologic settings. In urban settings, the influence of high capacity groundwater pumping on vertical hydraulic head gradients can change groundwater flowpaths, resulting in a greater contribution of vertical flow to municipal well fields. In the absence of detailed hydraulic head data, these flowpath changes in an urban setting are only recognizable over time by monitoring changes in groundwater chemical and isotopic composition.

For groundwater resource managers and groundwater modelers working in urban settings, changes in groundwater flowpaths over time have implications for both long-term water supply and water quality. In terms of water supply, limited recharge in areas of increased vertical flow can result in conditions that are not sustainable. Conversely, recharge may be adequate, but source water may change, resulting in a change in water quality. Source waters in urban include leaky infrastructure, enhanced infiltration from stormwater management, or surface water bodies.

With the exception of changes in land use and land cover, the rates and pathways of urban source-waters into the subsurface will depend on hydraulic head gradient. In an urban setting, these gradients are transient over hourly to seasonal to decadal time scales. As with hydrochemical data, collecting and archiving hydraulic head data in urban settings is best accomplished using GIS, where relational database capability combined

with spatial information allows for storage and analysis of large volume real-time data. These data are critical for understanding groundwater pathways, and the response of hydrologic systems to change in recharge and discharge.

CONCLUSIONS AND RECOMENDATIONS

Based on the analysis of chemical and isotopic data presented in this thesis, several conclusions can be drawn about the chemical composition and nature of groundwater flow in the TCMAx:

1. Three regional groundwater types can be distinguished within the TCMAx based on similar chemical and isotopic composition: a.) recent waters, characterized by detectable tritium, elevated chloride and/or the presence of anthropogenic compounds; b.) waters with elevated strontium to calcium plus magnesium ratios; and; c.) naturally elevated chloride—distinct from recent waters based on carbon-14 dating and low chloride to bromide ratios where sufficient data exists.
2. Recent waters are associated with an upper ‘active’ zone of groundwater flow characterized by shorter residence times, higher concentrations of anthropogenic compounds and greater variability in chemical composition. The presence of recent water at depth in the central TCMAx (Figures 14.D and 26.G), below the elevation of regional discharge, show that changes in groundwater flowpaths have occurred since the advent of high-capacity groundwater pumping. More water moves in the vertical direction in these areas than did before 100 years of groundwater pumping began. Extending out from the central TCMAx, this active

zone is found most often within 60 to 100 feet of the land surface. This active zone includes tills, where the upper 60 feet has markedly higher permeability than the same textures at greater depths

3. Elevated Sr/(Ca+Mg) groundwaters are found in the western TCMAx and at depth (Figures 12.B-D and 26.D-F) and are associated with recharge through Des Moines Lobe till and/or longer residence times. The distribution of this hydrochemical facies appears to have changed with time as hydraulic conditions changed. Elevated Sr/(Ca+Mg) ratios in the western TCMAx may have, at one time, extended further east toward regional discharge in the Mississippi River under natural hydrologic conditions. In eastern Hennepin County, these waters are thought to have been replaced by recent waters due to an increased vertical head gradient resulting from high capacity pumping, combined with a lack of overlying till.
4. In bedrock aquifers, differences in chemical and isotopic composition subdivide traditional hydrogeologic conceptual model (THCM) aquifers into subunits of similar porosity and permeability. Specifically, within the THCM Prairie du Chien-Jordan aquifer, chloride content is significantly higher in the Shakopee Formation than it is in the Jordan Sandstone. Similarly, where there is adequate data from both the Shakopee and the Jordan in proximity to one another, PFC's are detected more often in the Shakopee Formation.
5. Although there are considerably less data for comparison, similar results are found in the THCM Franconia-Ironton/Galesville (Tunnel City Group-Wonewoc)

aquifer, with recent waters found in the upper Franconia (Tunnel City Group), a lack of well completions in the lower Tunnel City Group where permeability is low, and an absence of recent waters in the Ironton/Galesville (Wonewoc Formation).

6. Below the Eau Claire Formation, chemical and isotopic data show that flow in the Mt. Simon is isolated from flow in the units above it. Residence times in the Mt. Simon are considerably longer (centuries to millennia), strontium concentrations are higher, and naturally elevated chloride is present in its lower sections and near major fault zones. This aquifer currently has residence times far longer than the less than 50 years seen in the upper bedrock aquifers.
7. There is an apparent trend toward higher chloride, and by inference, greater flux of groundwater in proximity to the bedrock surface and near bedrock valleys. Although the trend is not statistically significant, it is expected that these areas are capable of producing more water to pumped wells compared to wells in dissimilar settings. As with wells finished in other areas of the enhanced macropore development, it is also expected that these wells will show a greater temporal variability in chemical composition.

In the context of the groundwater flowpaths outlined above, a number of steps can be taken to apply this information toward groundwater management in the TCMAx:

1. In 2012, revisions are underway on the current Metro Area Groundwater Model, referred to as Metro Model II (Metropolitan Council, 2012). The regional

distribution of chemical types should be used in this modeling effort to constrain possible groundwater flowpaths from the land surface to bedrock. Because the distribution of chemical types, in particular, the distribution of recent waters matches the estimated vertical hydraulic head gradient distribution across the TCMAx, flux estimates on a cell by cell basis from the regional groundwater model should be compared to the distribution of recent waters to test recharge/pumping scenarios for the central TCMAx outlined above. Flux estimates should also be compared for other portions of the metro area where bedrock aquifers are hydraulically isolated from the land surface, such as portions of western Hennepin, Carver and Scott Counties, and in areas where hydraulic conditions are expected to change due to population growth, such as Anoka County.

2. Evaluating groundwater flowpaths from the land surface to bedrock aquifers depends largely on boundary conditions used. Several separate numeric solutions should be considered, including, at a minimum, no-flow boundaries for bedrock layers on the western edge of the model where the subcrop edges of bedrock units are overlain by a thick sequence of glacial tills. No-flow boundaries would eliminate a constant lateral source of water for these layers. Chemical and isotopic data show that bedrock aquifers in portions of western Hennepin County have no recent water. Calculated vertical travel times reflect the low vertical gradient/low permeability of unconsolidated material in this area; model results

should reflect that recharge applied to the upper cells in this area are not in steady state with bedrock layers over the time scales of less than one hundred years.

3. Pre-development data on strontium concentrations in eastern Hennepin County do not exist. Therefore, source water conditions should be tested in the proximity of the Sr/Ca+Mg – recent water border shown on cross section A-A' (Figure 28) by sampling municipal wells in that area. Waters with Sr/Ca+Mg molar ratios greater than 0.001 are likely drawing water laterally from western areas that receive limited vertical recharge.
4. From a water management perspective, the question arises as to whether the pattern of recharge and use indicated by recent waters at depth within the central TCMAx is sustainable. Water volume calculations should be conducted to see whether the volume of water pumped within this zone matches the amount of water available via recharge from above it. Using the 750 foot contour on Figure 14.C to approximate the boundary of recent waters at depth, if the recharge volume over this area is considerably less than the pumping volume within it, then it is expected that water levels in the Prairie du Chien Group and Jordan Sandstone will drop with time, and are not sustainable under current pumping and recharge conditions.
5. Hydrostratigraphic units should be incorporated into bedrock model layers by modifying hydraulic conductivity values and reducing aquifer thicknesses. In both the Shakopee Formation and upper Tunnel City Group, the occurrence of recent waters combined with documented higher permeability due to enhanced

macropore development, suggests greater flux through these units relative to the Oneota Dolomite and its basal Coon Valley member (lower Prairie du Chien Group), and lower Tunnel City Group, with greater temporal variability in chemical composition. Higher K ranges for Shakopee and upper Tunnel City Group should be incorporated into the model, with thicknesses of these layers reduced to reflect the permeable thicknesses of these subunits. Thicknesses of the Prairie du Chien and Tunnel City Groups vary across the TCMAx, but the lower permeability portions of both these units (approximately 40 feet in the Prairie du Chien and 60-80 feet in the Tunnel City Group) can be subtracted from the bottom of each to leave a remainder of permeable bedrock.

6. Chemical and isotopic data show a trend toward higher bedrock permeability near the bedrock surface and bedrock valleys, regardless of bedrock lithology, presumably because of a higher density of vertical, through-going fractures. In GIS, this hydrostratigraphic zone of higher bedrock permeability is most easily defined creating a separate raster equal to the bedrock surface minus 50 feet. The resulting raster can be used to modify K values within bedrock groundwater model layers.
7. Buried bedrock valleys provide “windows” to lower bedrock aquifers. From a groundwater resource management perspective, these windows are important in areas where a vertical hydraulic gradient is present, or could be present in the future as the distribution of high-capacity pumping changes with time. The presence of the Platteville and Glenwood Formation in the central TCMAx,

combined with a large vertical gradient in this area highlights the hydrologic importance of these bedrock valley windows where the Platteville/Glenwood confining units are absent. The Quaternary subsurface regional texture dataset included in this thesis, provides an up-to-date distribution of textures in these bedrock valleys, both in areas where subsurface mapping as occurred, and in areas modeled by interpolation from the Minnesota state water well database, CWI. These data are in GIS format, and should be used to guide hydraulic conductivity estimates for buried bedrock valleys in regional and local groundwater models.

8. There are significant gaps in chemical, isotopic, subsurface, and hydraulic head data that should be addressed in future data collection. Stable isotopes of oxygen and hydrogen—useful for both identification of surface water/ground water interaction and recharge from glacial melt water—are largely absent from this dataset. This dataset also has a limited number of bromide analyses that are extremely useful for identifying sources of chloride. In the subsurface, Quaternary subsurface mapping is missing for important recharge areas of the central TCMAx, including southern and eastern Hennepin County, Ramsey, and Dakota Counties. Finally, real time hydraulic head data, both from pumping and observation wells, are necessary to evaluate transient conditions within and between aquifers. These data, along with chemical and isotopic data, should be collected and archived in a georeferenced database so that trends can be identified as groundwater quality and flowpaths change with time.

APPLICATIONS

The work presented in this thesis has applicability to the broader, non-provincial hydrogeologic community. For planners, it demonstrates, for the first time, the utility of having mapped, three-dimensional hydrochemical facies in a GIS format, combined with a hydrogeologic framework model over a regional urban area. Groundwater managers can compare the age and chemical quality of groundwater with other, more familiar factors in an urban setting, such as the location and pumping levels of high capacity wells. Furthermore, it demonstrates the need for continued archival of georeferenced chemical data. This type of data collection is critical in an urban setting, where hydraulic conditions change over regional scales and human time scales. For the technical hydrogeologic community, this work investigates the distribution of hydrochemical facies at regional and local scales, interpreted in the context of a revised hydrogeologic conceptual model, where water-bearing characteristics of sedimentary aquifers and aquitards are more closely aligned with regional compilations of borehole geophysical measurements, temperature profiling, short-interval packer testing, multi-level hydraulic head measurement, and dye tracing results. Specifically, it documents the presence of recent waters in areas of known macropore development, both parallel to bedding along previously identified stratigraphic horizons, and perpendicular to bedding in proximity to the bedrock surface and/or buried bedrock valleys. For both planners and the technical hydrologic community, this work raises fundamental questions about the pathways for groundwater to move vertically in urban settings, where high capacity pumping creates conditions to move contaminants at depths, either along vertical fractures or multiple

aquifer wells, at rates that greatly exceed modeled porous media transport through aquitards.

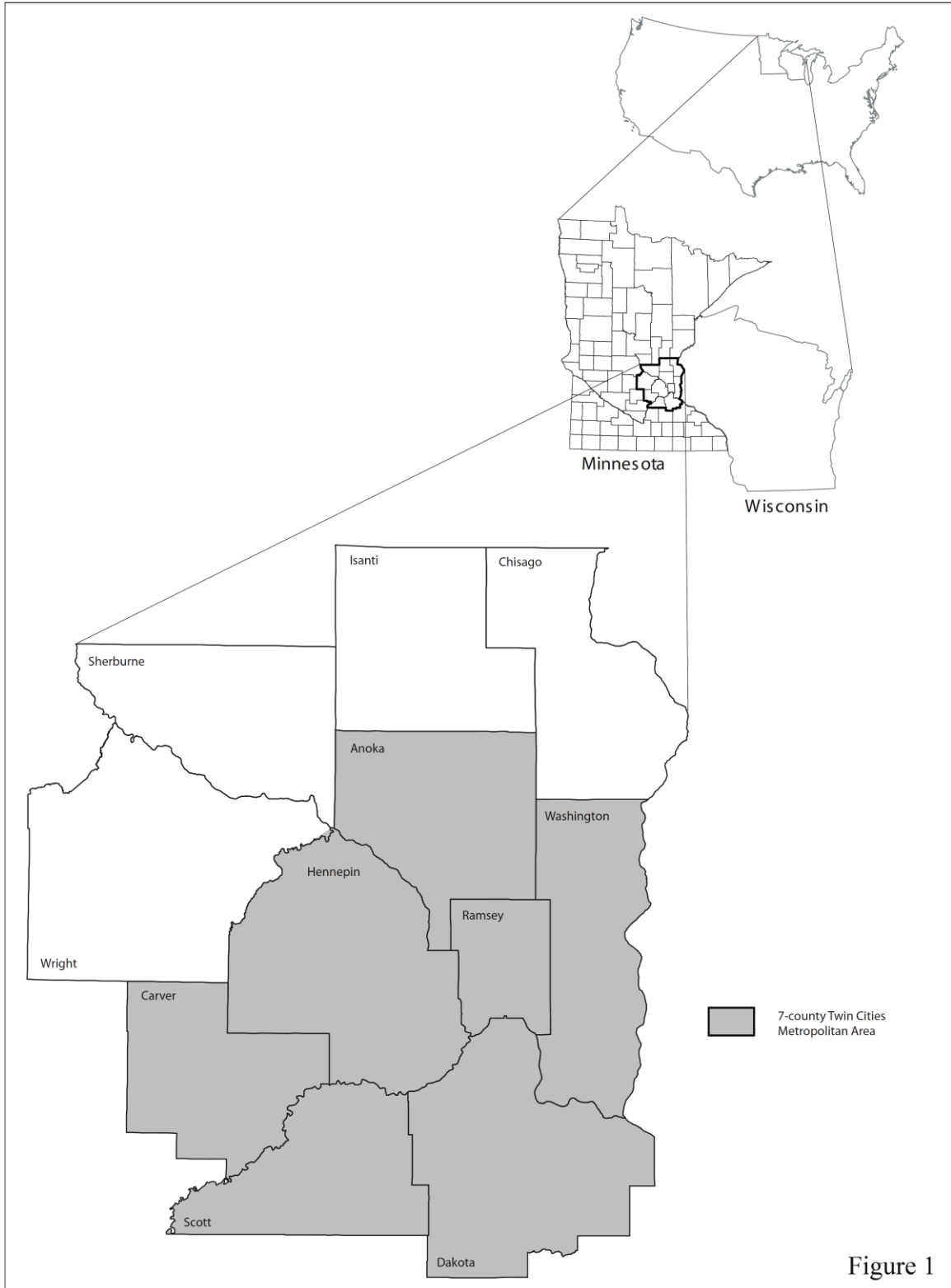


Figure 1. Investigation covers the extended 11 county Twin Cities metropolitan area (TCMAx), Minnesota. 7 county metropolitan area (TCMA) shown in grey.

Figure 2. Location of major rivers and regional hydrologic gradients. **A.** March 2008 Prairie du Chien-Jordan potentiometric surface (Sanocki et al., 2009); **B.** Regional water table surface (Barr, 2010). Arrows show directions of groundwater flow. Regional discharge for both unconsolidated deposits and uppermost bedrock aquifers is toward the Mississippi, Minnesota, and St. Croix Rivers.

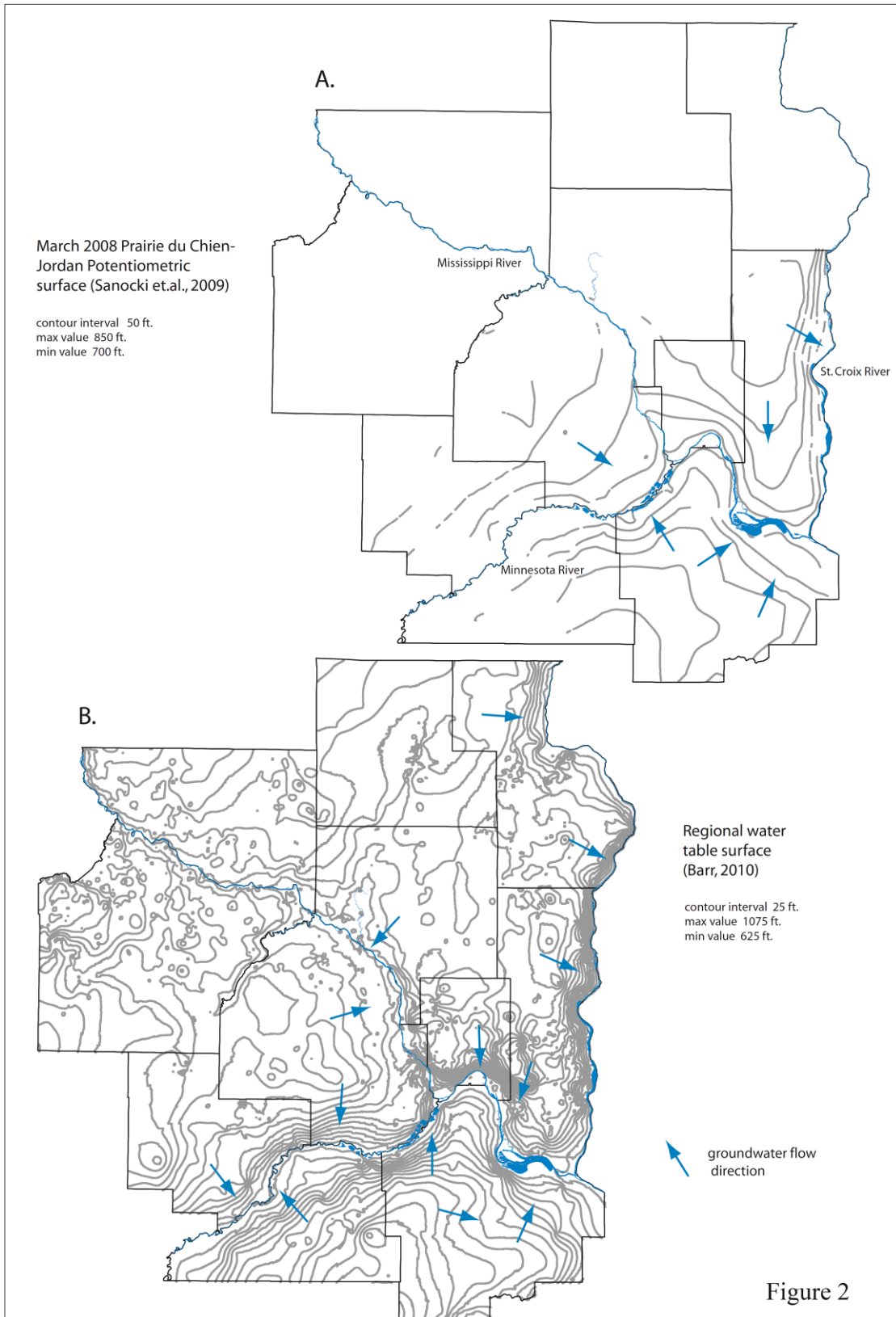


Figure 2

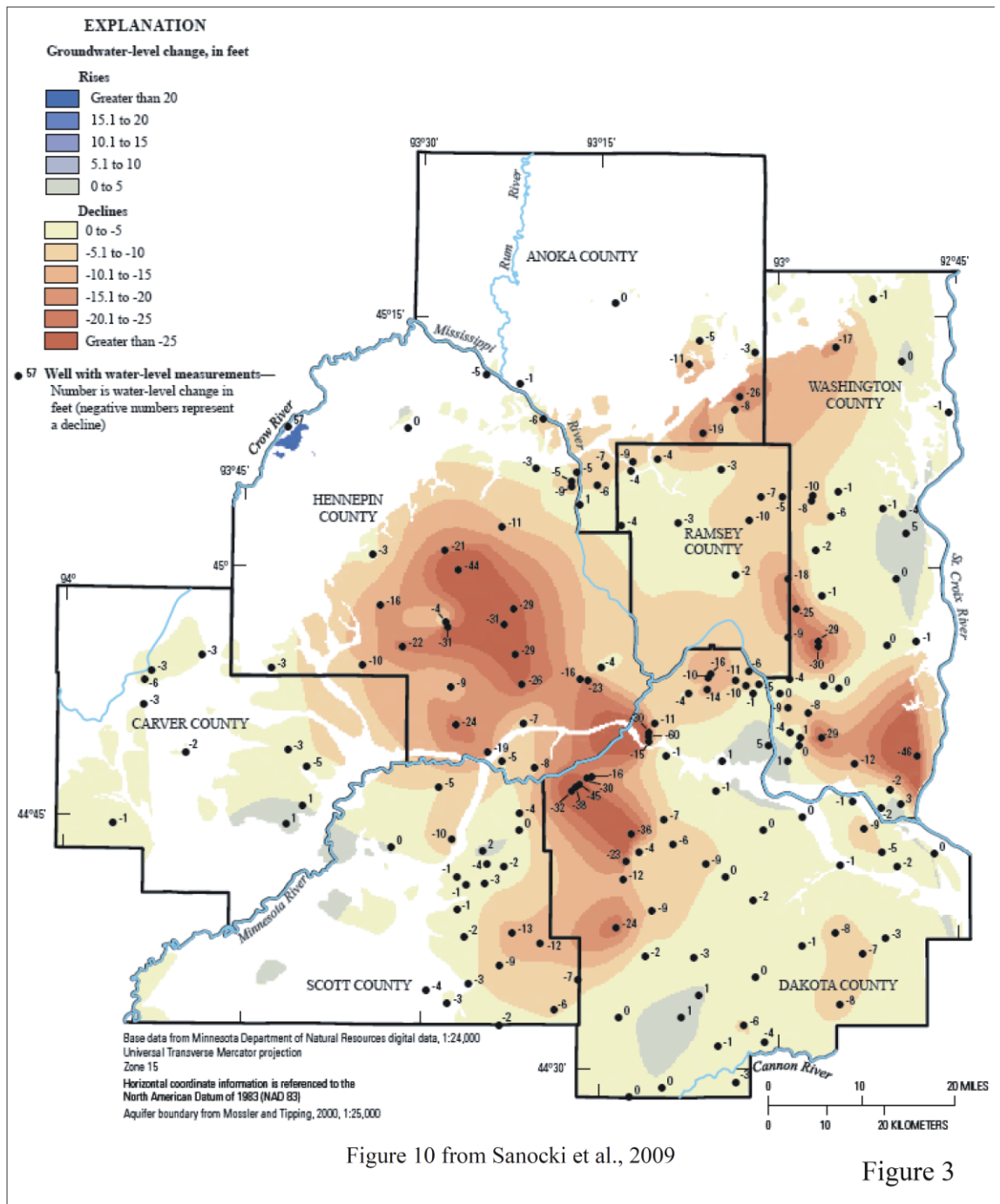


Figure 10 from Sanocki et al., 2009

Figure 3

Figure 3. Groundwater-level changes in the Prairie du Chien-Jordan aquifer between March 2008 and August 2008, based on synoptic water level measurements. (Figure 10 from Sanocki et al., 2009).

This page is blank

Figure 4. Regional distribution of unconsolidated materials and bedrock geologic map.
A. Generalized lithology of parent materials at the land surface (sub soil), modified from Meyer, 2007. **B.** Bedrock map modified from Mossler and Tipping, 2000

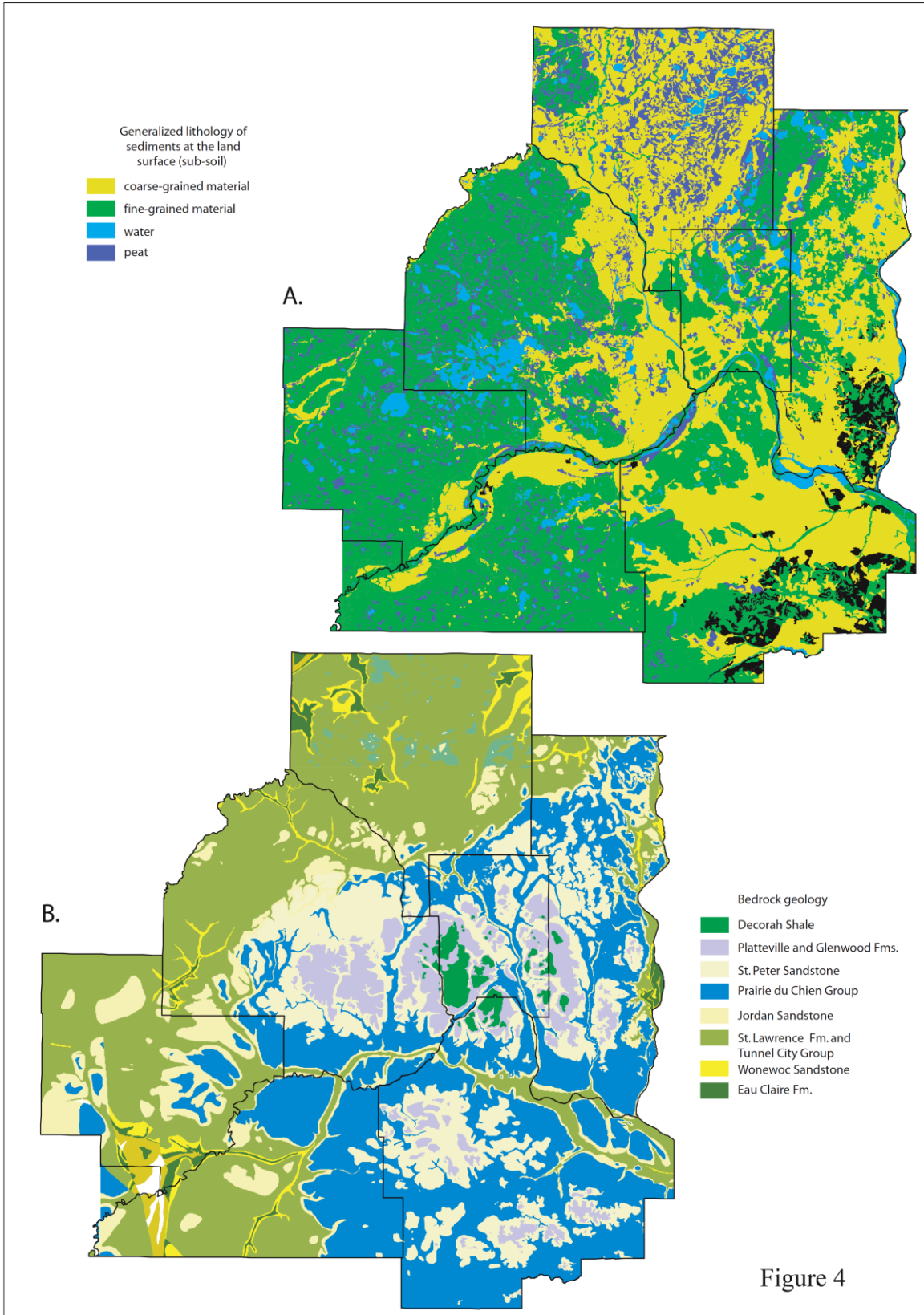


Figure 4

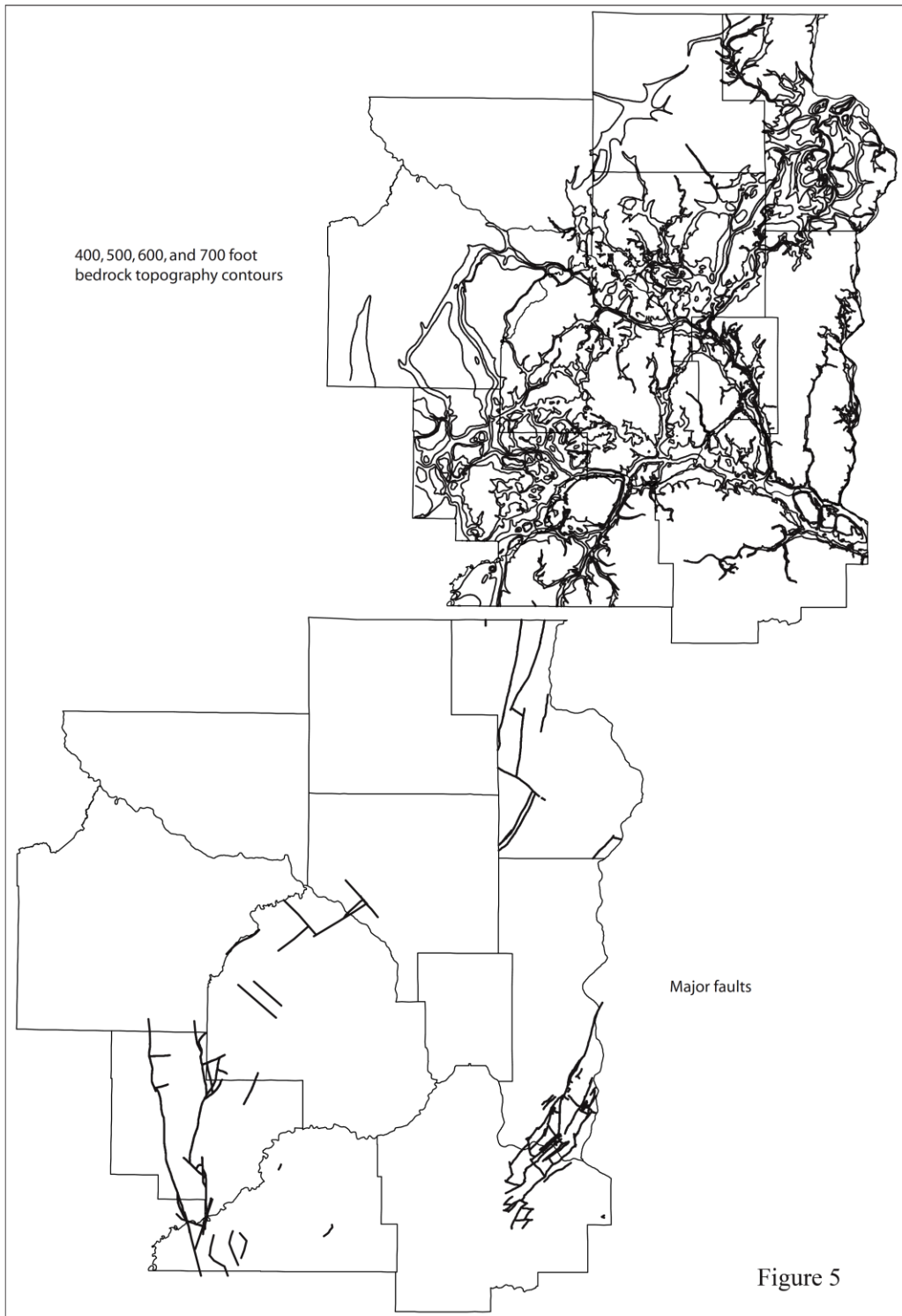


Figure 5. Distribution of bedrock valleys and major faults within the TCMAX. Bedrock valleys from Mossler and Tipping, 2000. Faults modified from Jirsa et al., 2011.

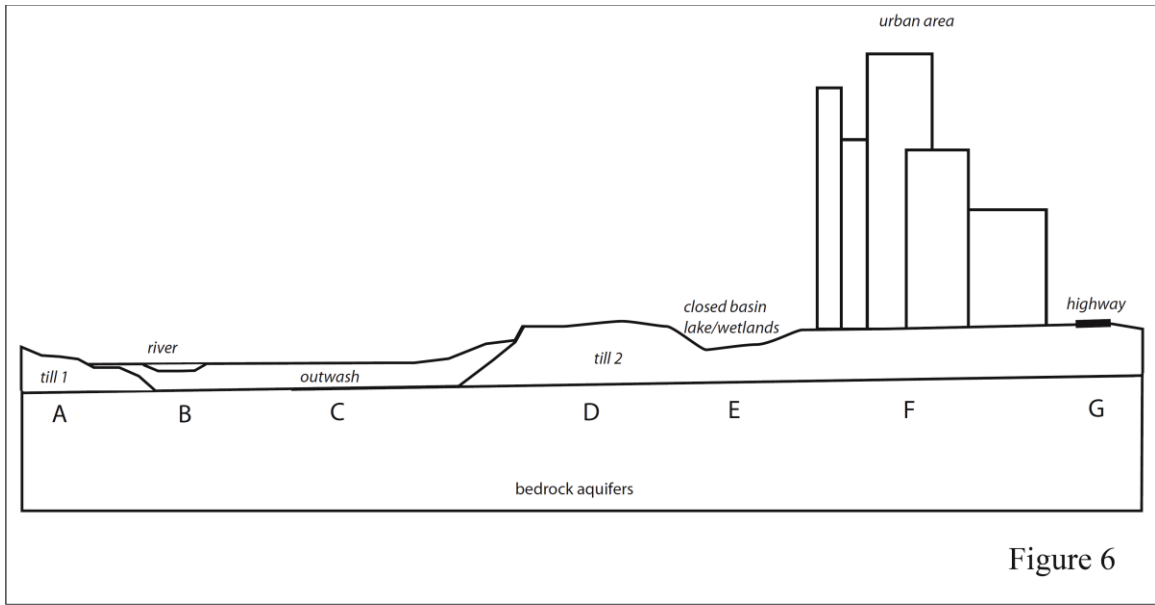


Figure 6. Schematic cross section through an urban setting showing examples of zones where water recharging bedrock aquifers could receive different chemical signatures: tills with different compositions (zones A and D); river seepage (zone B); rapid recharge through outwash (zone C); evaporative setting – closed basin lake or wetlands (zone E); urban infrastructure recharge such as water mains and sewers (zone F); and highways (zone G).

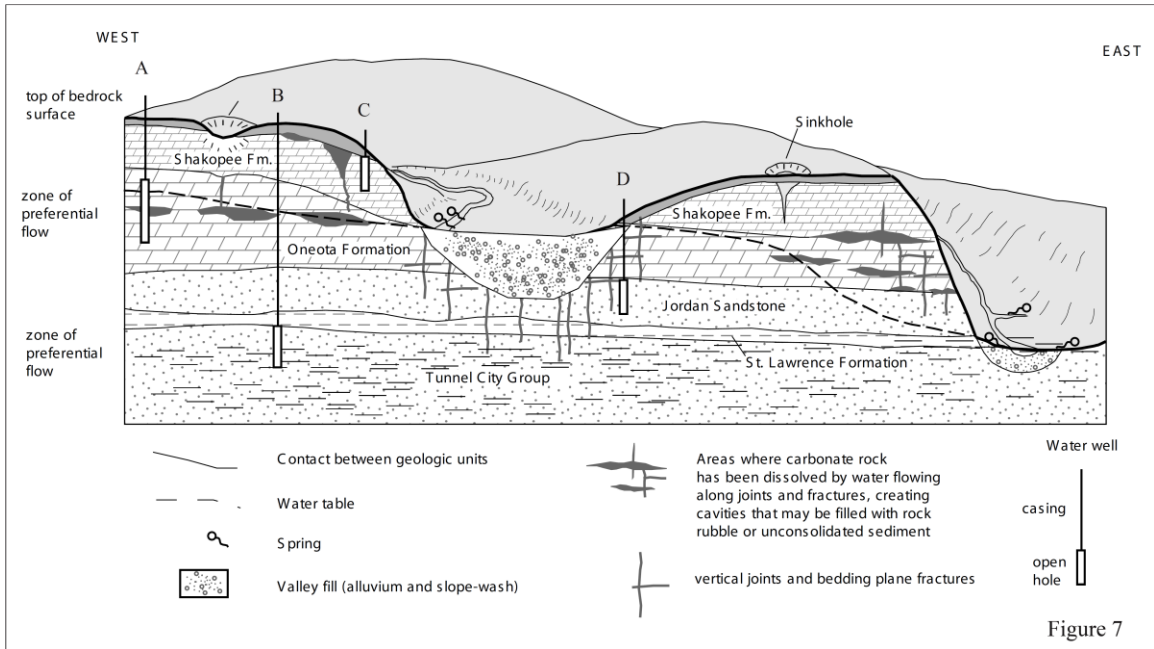


Figure 7. Schematic cross section through southern Washington County Minnesota, showing water well open hole intervals exposed to: zones of preferential flow (enhanced porosity and permeability – wells A and B), bedrock valley conditions (well C), and bedrock surface conditions (well D).

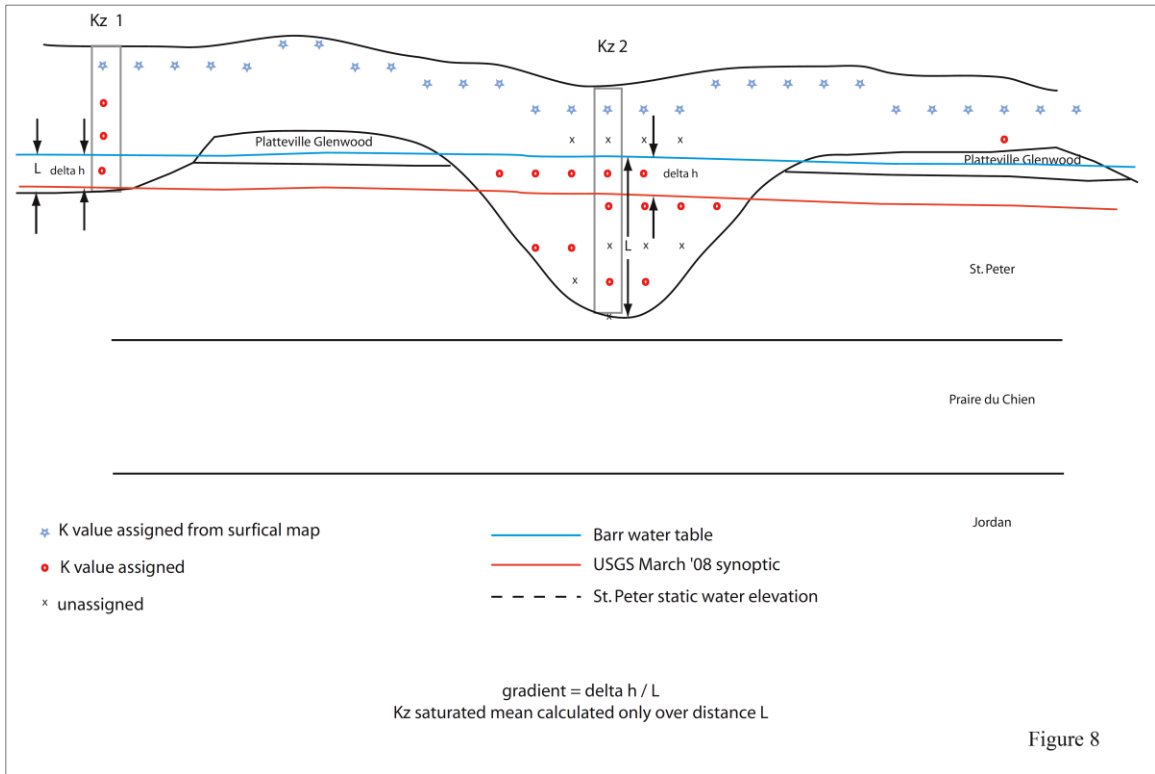


Figure 8. Schematic drawing showing the time of travel calculation. Mean hydraulic conductivity is calculated for points that fall between the water table and the bedrock surface. Hydraulic gradient is calculated over this same distance. The presence of Decorah/Platteville/Glenwood Formations and the possibility of unsaturated St. Peter Sandstone below precludes the use of Darcy calculation for time of travel where these units area present.

Figure 9. 2D and 3D piper diagrams, showing regional differences in the chemical composition of groundwater in unconsolidated deposits of Scott, Hennepin, Anoka and Washington Counties, and in upper bedrock in Dakota County where unconsolidated deposits are largely thin or absent. Colors indicate age class based on tritium content (TU): Red are recent waters, $TU \geq 10$; Green are mixed waters, $TU > 1$ and < 10 ; Blue are vintage waters, $TU < 1$.

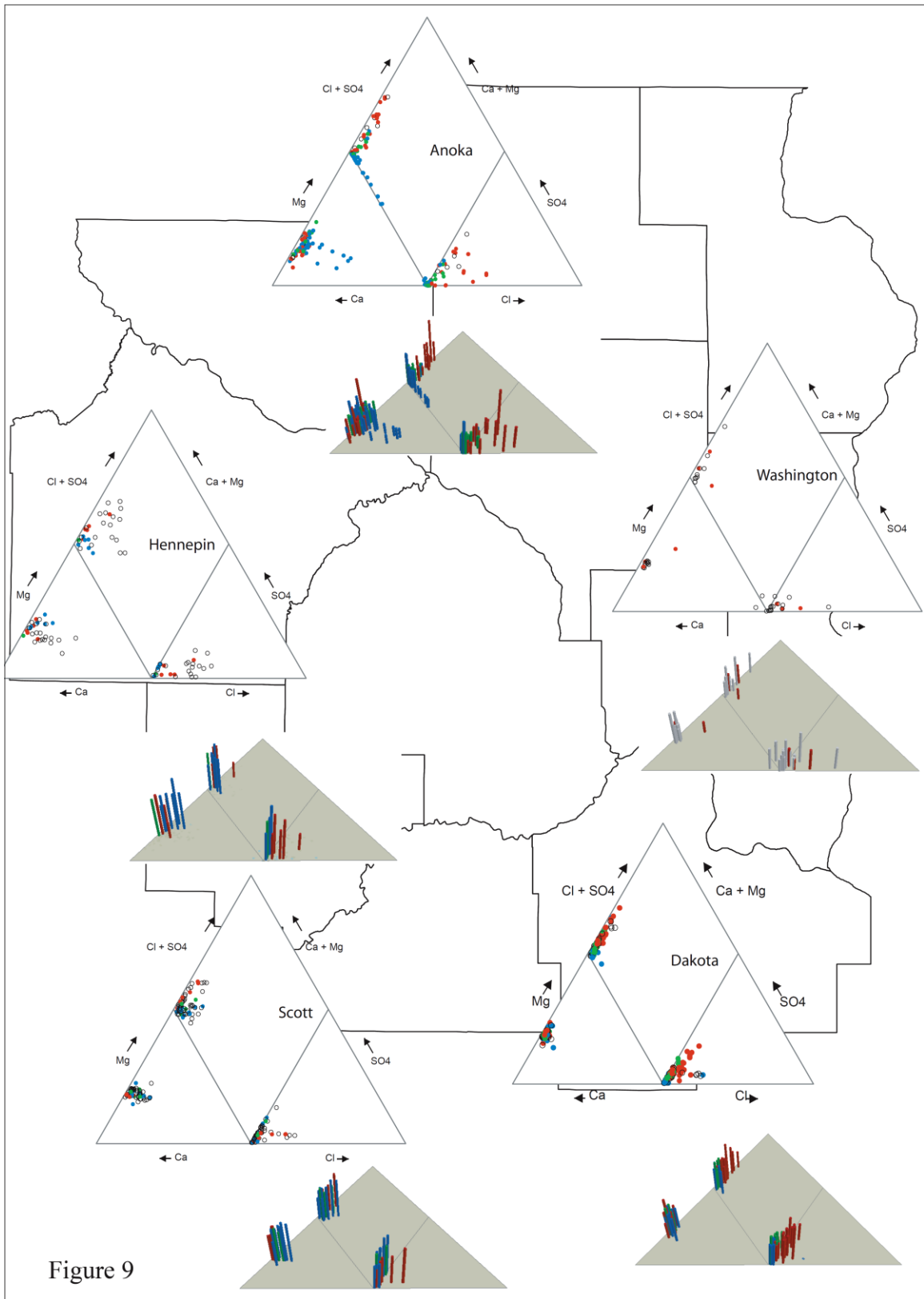
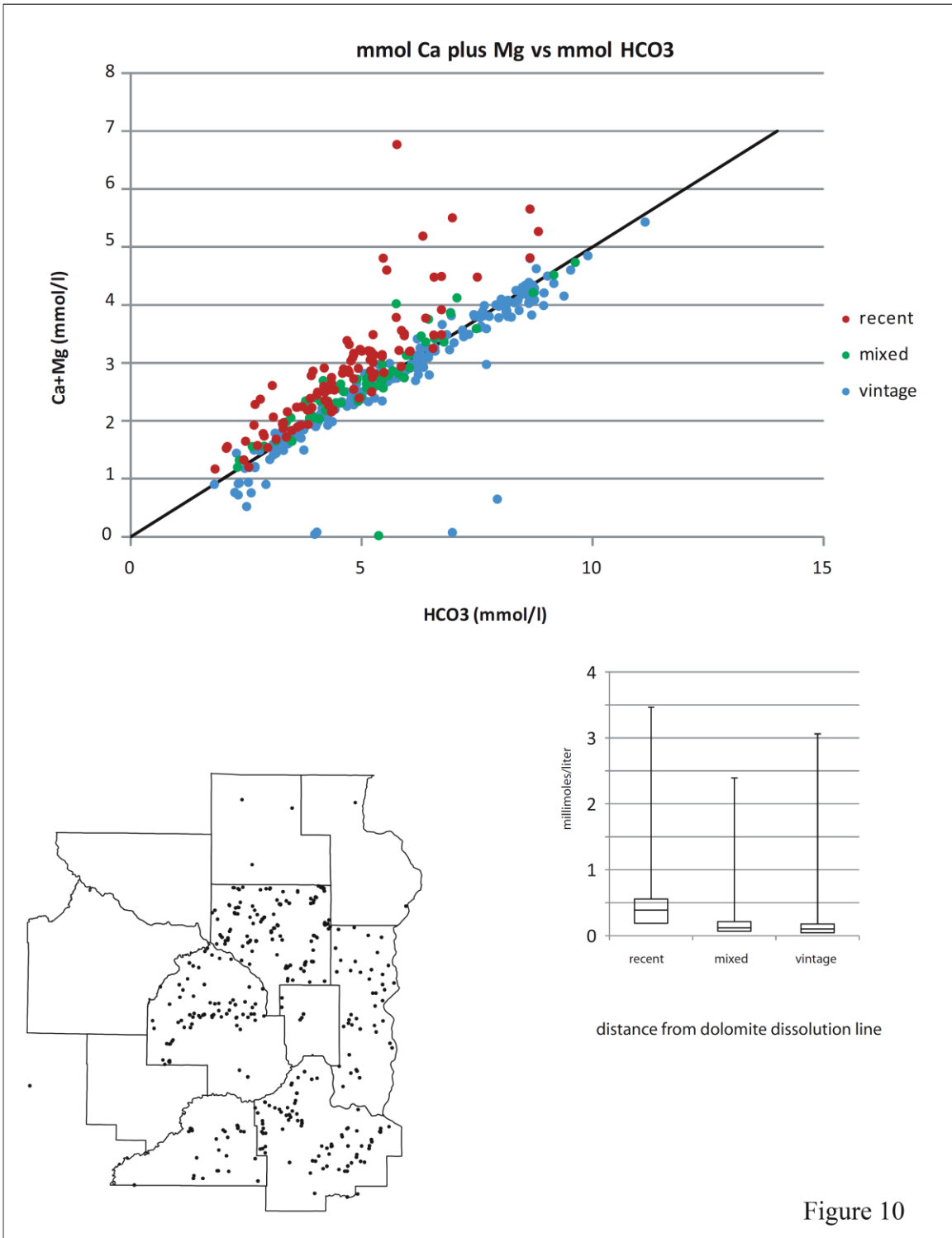


Figure 9

Figure 10. Scatterplot of calcium plus magnesium compared to bicarbonate concentration in millimoles per liter for all water well samples with charge balance errors less than 5 percent. Age classification based on the presence of detectible tritium. Location map shows distribution of points. Box plots show median, upper and lower quartile and outlier values for distance from point to the dolomite dissolution line for recent, mixed and vintage waters.



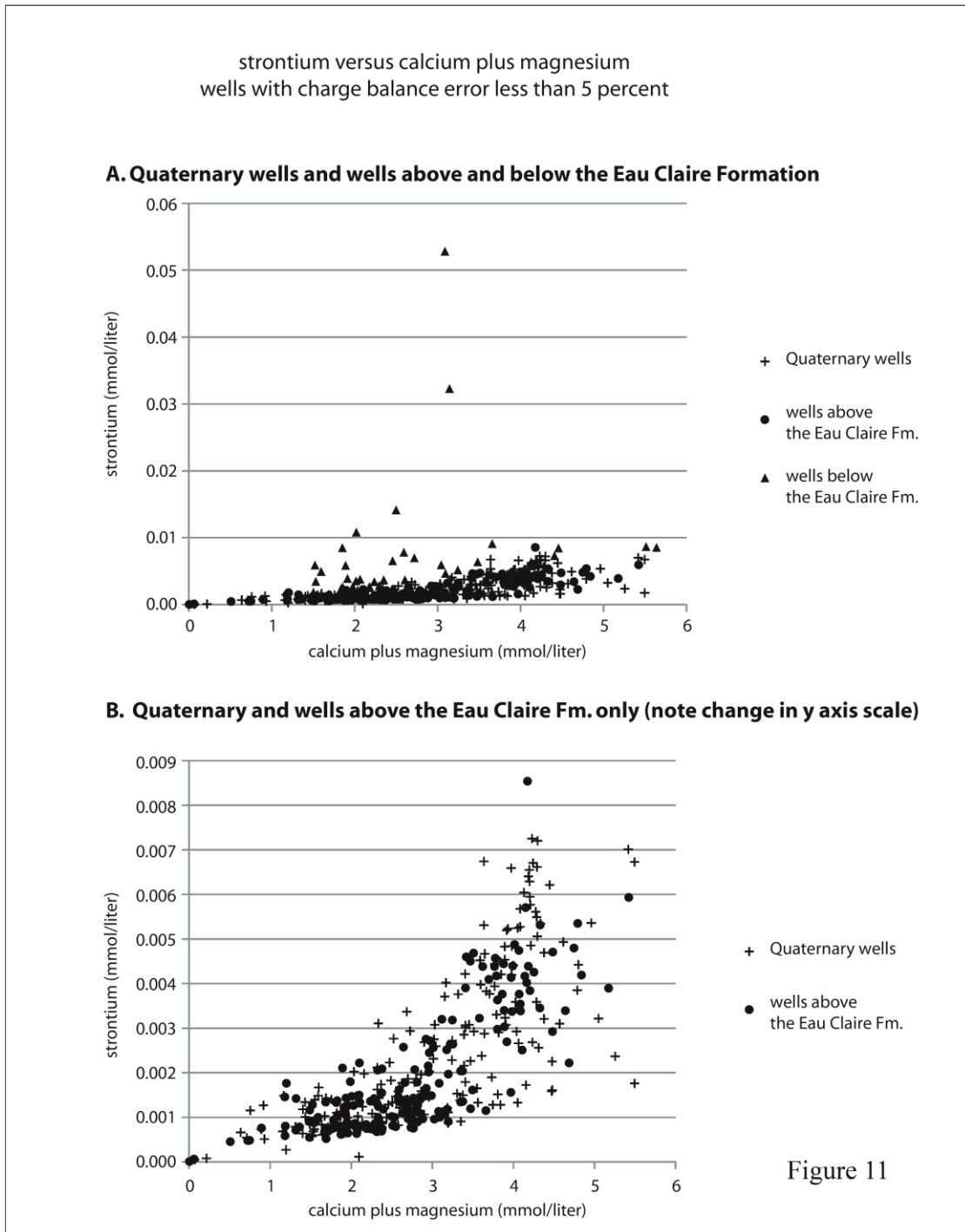


Figure 11. Scatterplot of strontium compared to calcium plus magnesium concentrations in millimoles per liter for all water well samples with charge balance errors less than 5 percent. **A.** Wells below the Eau Claire formation have markedly higher concentrations of strontium relative to calcium plus magnesium. **B.** wells above the Eau Claire Formation show a smaller, non-linear increase in strontium as calcium plus magnesium concentrations increase.

This page is blank

Figure 12. Regional map showing distribution of Sr/(Ca+Mg) ratios. **A** Sr/(Ca+Mg) molar ratios for all wells with acceptable charge balance. Elevated ratios to the west and southwest. **B.**) Contours of open hole top (casing bottom) elevation for Quaternary wells with Sr/(Ca+Mg) ratios greater than 0.001. Variogram above shows correlation length of approximately 8000 meters **C.**) Contours of open hole top (casing bottom) elevation for Jordan wells with Sr/(Ca+Mg) ratios greater than or equal to 0.001. Variogram above shows correlation length of approximately 80000 meters **D.**) Contours of open hole top (casing bottom) elevation for Mount Simon wells Sr/(Ca+Mg) ratios greater than 0.001. Variogram above shows correlation length of approximately 6600 meters. Elevated ratios may be associated with recharge through NW provenance tills and/or longer residence time.

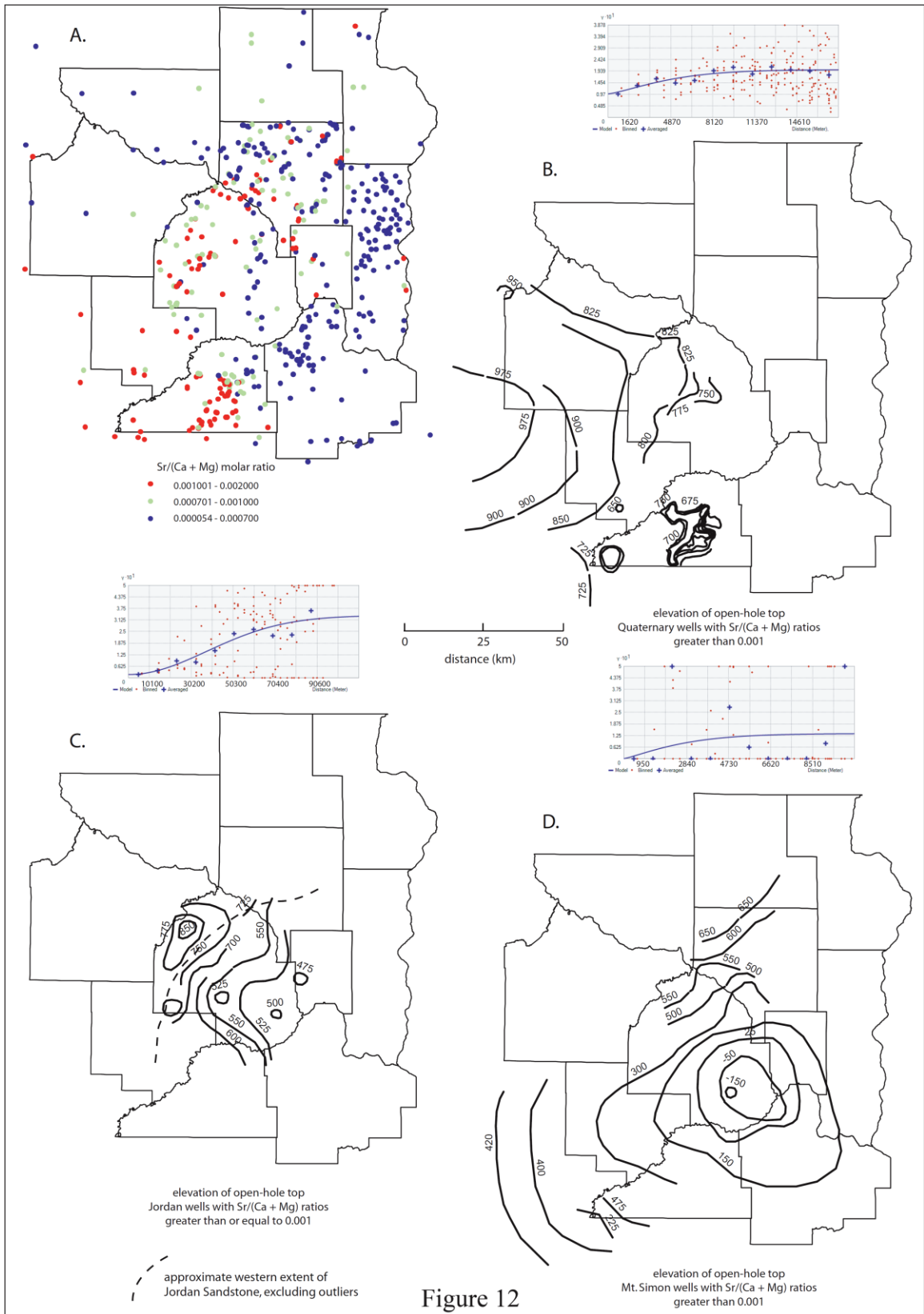
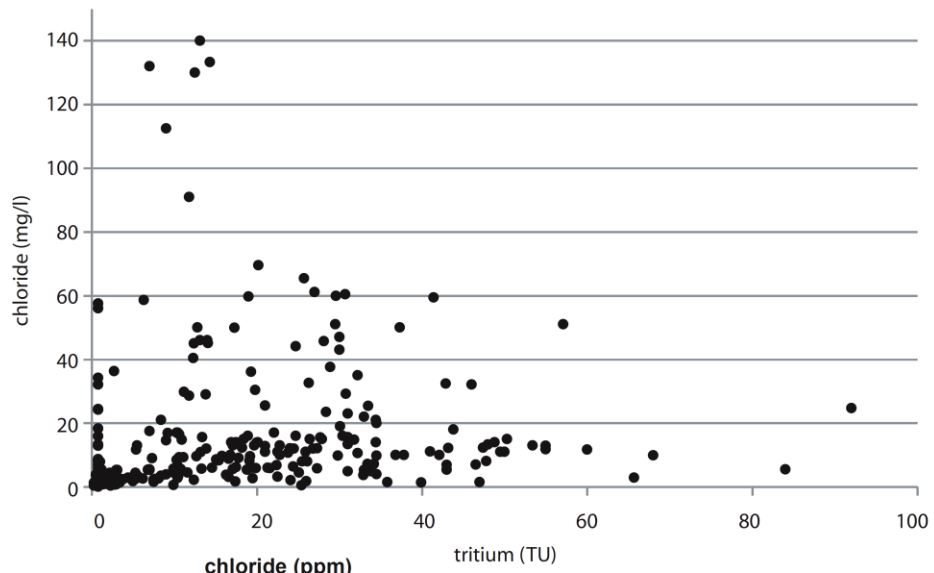


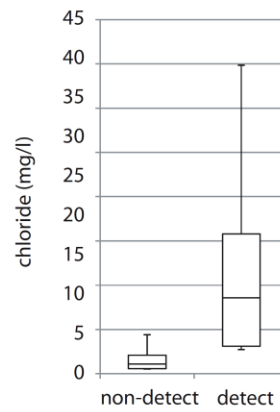
Figure 12

Figure 13. Scatterplot and summary statistics for chloride concentrations in wells with and without detectable tritium. Location map shows distribution of points. Box plots show median, upper and lower quartile and outlier values for chloride concentrations versus tritium detection. Median chloride concentrations for samples with detectable tritium are significantly higher than from samples without detectable tritium at $\alpha = 0.05$. The spread of chloride values from samples with detectable tritium is greater and reflected in a higher mean value for this data group.



	tritium non-detect	tritium detect
min	0.04	0.4
max	57.5	370.0
median	1.1	8.6
mean	2.7	17.6
upper quartile	2.1	15.8
lower quartile	0.6	3.1
std dev	6.6	32.9
n = 229		n = 251

median values different at 0.05 significance level ($p < 0.00001$ two sided test)



(maximum values not shown)

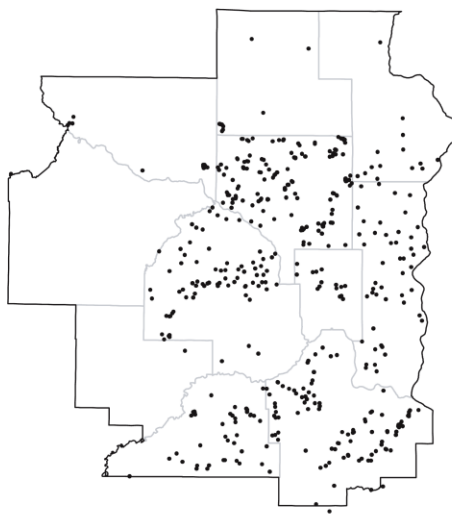


Figure 13

Figure 14. Regional maps showing the distribution of recent waters. **A.)** Chloride concentrations from water wells. Concentrations greater than 5 mg/l considered to be indicator of recent recharge. **B.)** Tritium results from water wells. Well with tritium concentrations greater than 10 tritium units (TU) considered to be dominated by waters having entered the ground since 1960; wells with less than 1 TU considered to be dominated by waters having entered the ground prior to 1960; intermediate values from 1 to 10 TU considered a mixture of older and recent waters. Distribution of elevated chloride and tritium is broadly similar. **C.)** Contours of open hole top (casing bottom) elevation for wells with detectable tritium. **D.)** raster surface marking the base elevation for recent waters, constructed in part using the contours shown in C.

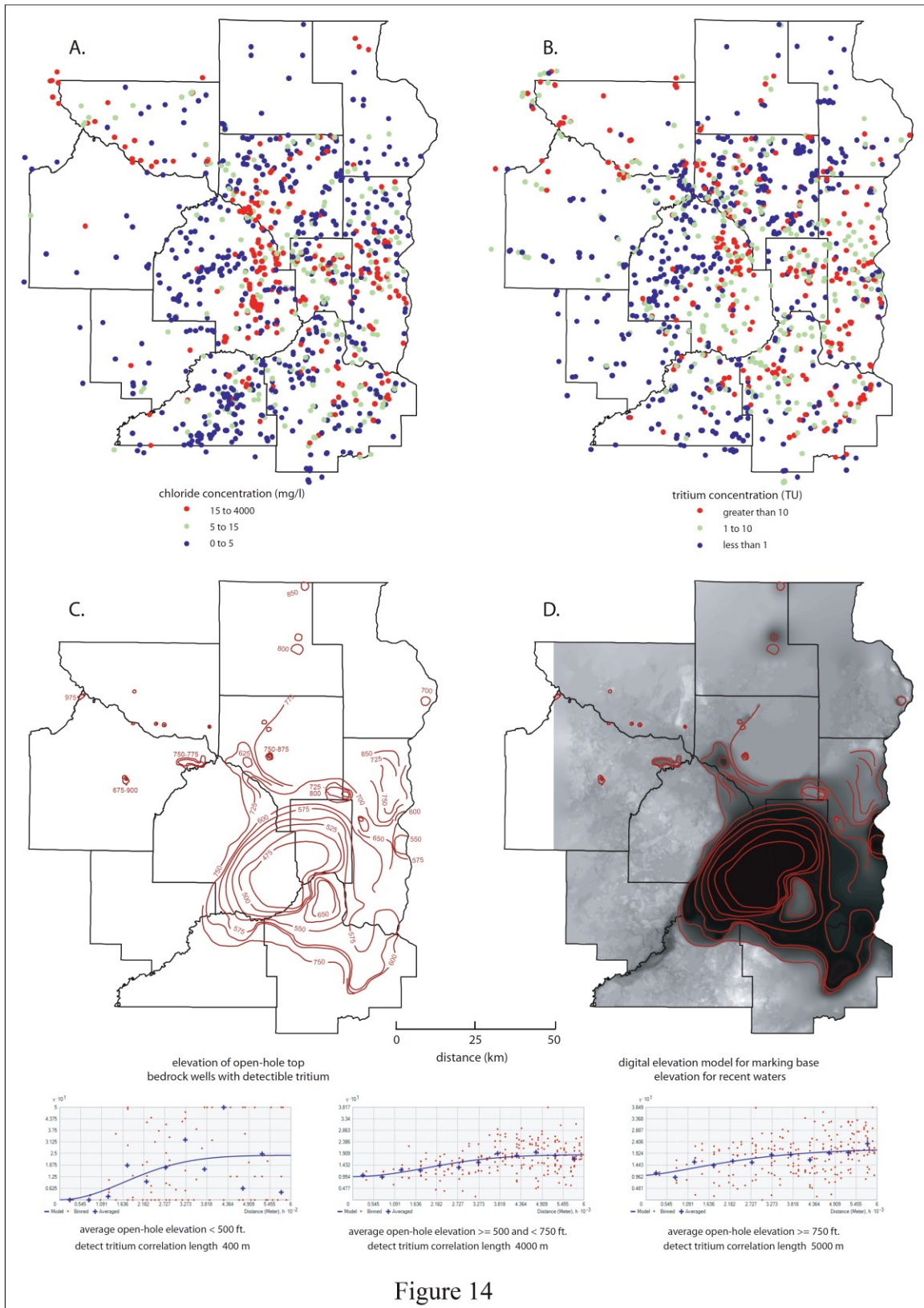


Figure 14

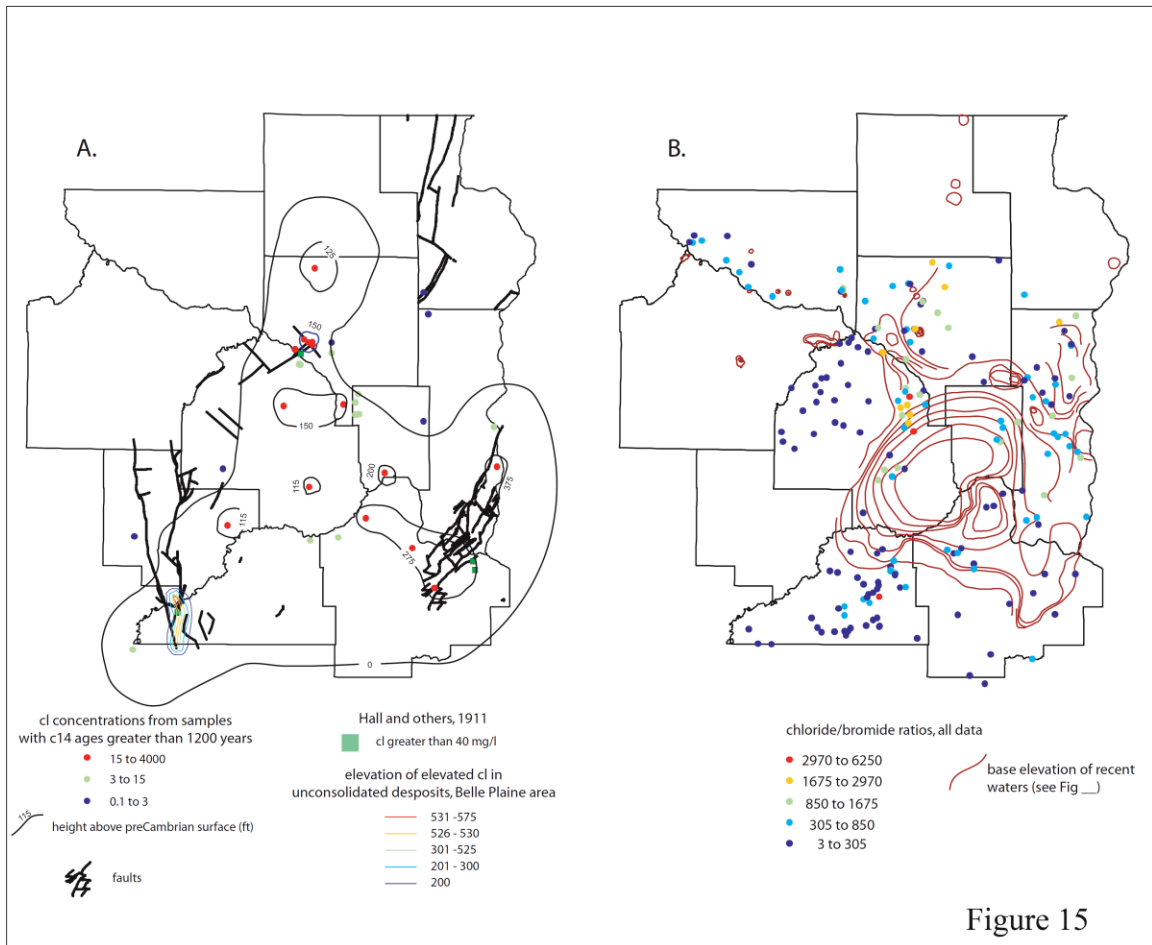
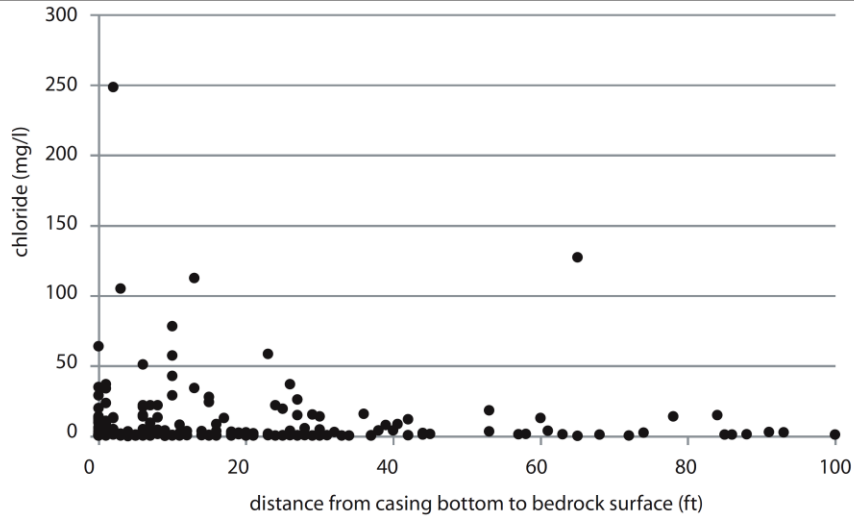


Figure 15

Figure 15. Regional maps showing naturally elevated chloride concentrations. **A.)** Chloride concentrations in mg/l for wells with carbon 14 – determined ages of greater than 1200 years. Also shown are chloride outliers from Hall et al., 1911. Blue contours show height of open hole bottoms above the pre-Cambrian bedrock surface; colored contours show elevation for elevated chloride in unconsolidated deposits in the Belle Plaine area, Scott County. Major metropolitan area bedrock faults are also shown. Old waters with elevated chloride are associated with fault zones, possibly due to upwelling of waters associated with pre-Cambrian bedrock. **B.)** Chloride to bromide ratios, all wells. Chloride to bromide ratios less than 200 considered to be indicator of chloride from bedrock as opposed to anthropogenic sources. Contours of recent water elevations from Figure 13 shown for comparison to chloride bromide ratios. Elevated ratios (greater than 1000) are generally found in shallow wells with recent waters.

This page is blank

Figure 16. Scatterplot and summary statistics for chloride concentrations compared to distance from casing bottom to the bedrock surface, domestic wells only. Location map shows distribution of points. Box plots show median, upper and lower quartile and outlier values for distance from well open-hole to the bedrock surface. Median concentrations for datasets with distances greater than or less than 10 feet are not significantly different from one another at $\alpha = 0.05$. The spread of chloride values from samples with a distance less than or equal to 10 feet is greater and reflected in a higher mean value for this data group.



	chloride (ppm)	
	> 10 feet	<= 10 feet
min	0.3	0.1
max	127.4	248.5
median	1.6	1.8
mean	6.9	11.3
upper quartile	3.9	12.5
lower quartile	0.7	0.8
std dev	17.13	27.61
	n = 120	n = 116

median values not different at 0.05 significance level ($p = 0.113$)

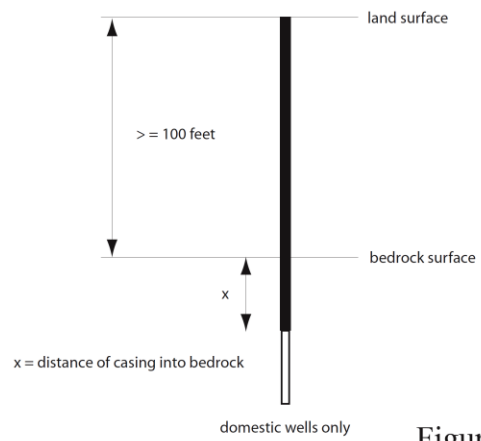
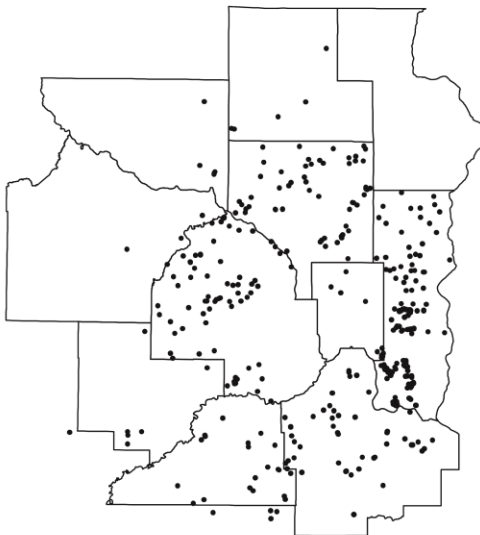
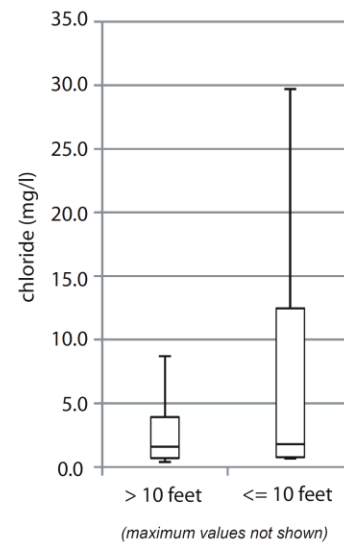
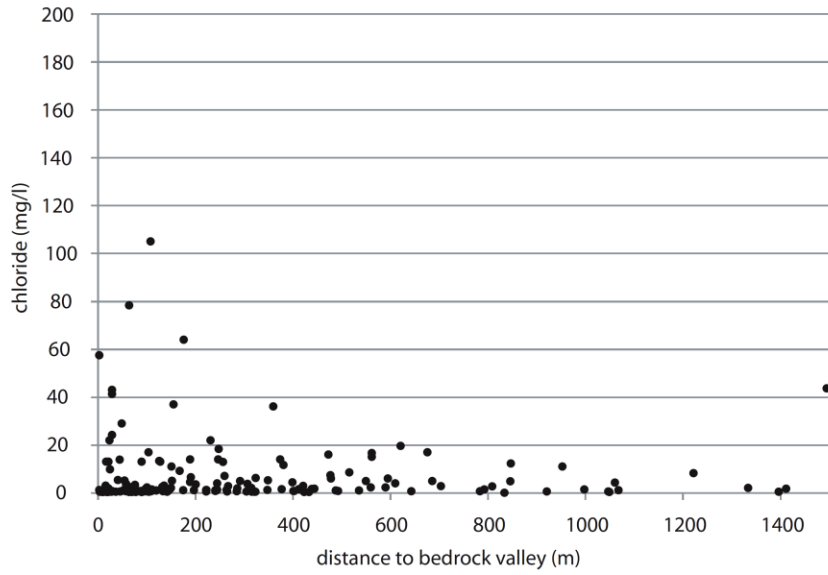
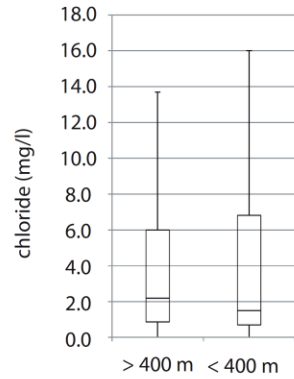


Figure 16

Figure 17. Scatterplot and summary statistics for chloride concentrations compared to distance from a bedrock valley, domestic wells only, threshold distance of 400 meters. Location map shows distribution of points. Box plots show median, upper and lower quartile and outlier values for distance from well to the bedrock valley. Median concentrations for datasets with distances greater than or less than 400 meters are not significantly different from one another at $\alpha = 0.05$. The spread of chloride values from samples with a distance less than or equal to 400 meters is greater and reflected in a higher mean value for this data group.

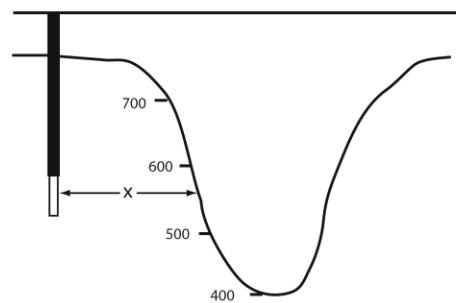
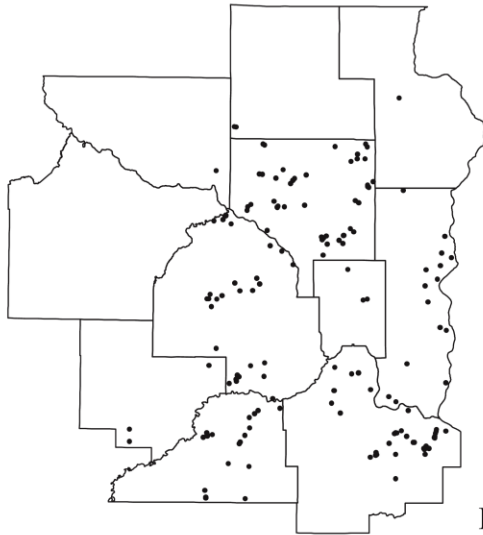


chloride (ppm)		
distance to bedrock valley		
	> 400 m	< 400 m
min	0.1	0.4
max	43.6	105.0
median	2.2	1.5
mean	5.4	8.0
upper quartile	6.0	6.8
lower quartile	0.9	0.7
std dev	7.78	15.99
	n = 46	n = 115



median values not different at 0.05 significance level ($p = 0.681$, one sided test)

(maximum values not shown)

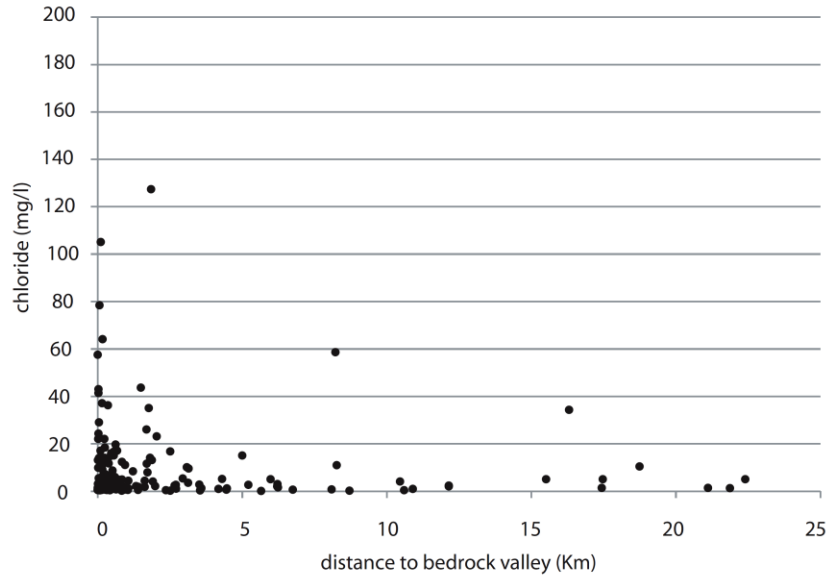


x = distance to bedrock valley (m)
 500 — elevation above mean sea level (ft)

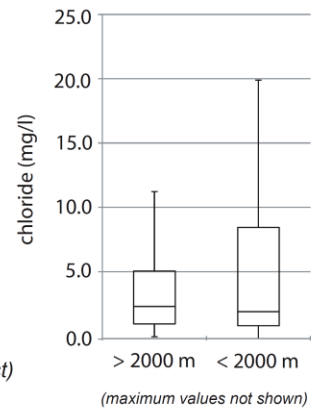
domestic wells only

Figure 17

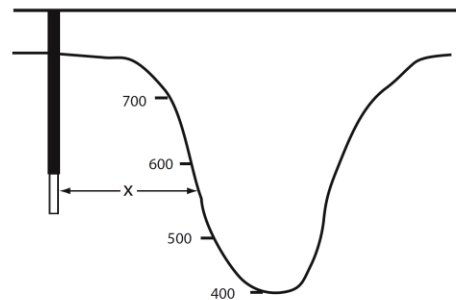
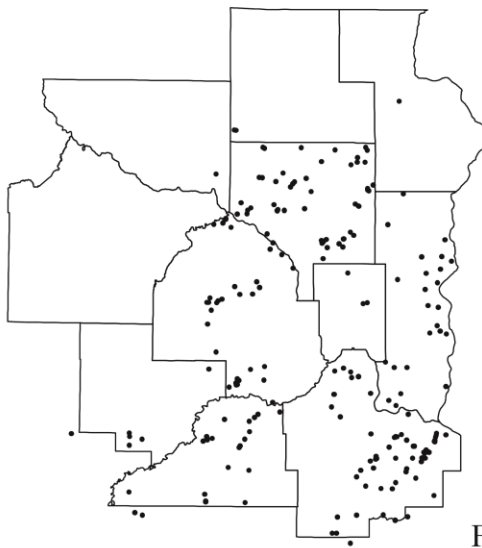
Figure 18. Scatterplot and summary statistics for chloride concentrations compared to distance from a bedrock valley, domestic wells only, threshold distance of 2000 meters. Location map shows distribution of points. Box plots show median, upper and lower quartile and outlier values for distance from well to the bedrock valley. Median concentrations for datasets with distances greater than or less than 2000 meters are not significantly different from one another at $\alpha = 0.05$. The spread of chloride values from samples with a distance less than or equal to 2000 meters is greater and reflected in a higher mean value for this data group.



	chloride (ppm)	
	distance to bedrock valley	
	> 2000 m	< 2000m
min	0.15	0.1
max	58.6	127.4
median	2.5	1.9
mean	6.2	8.2
upper quartile	5.1	8.4
lower quartile	1.0	0.8
std dev	10.71	16.74
	n = 42	n = 171



median values not different at 0.05 significance level ($p = 0.502$, one sided test)

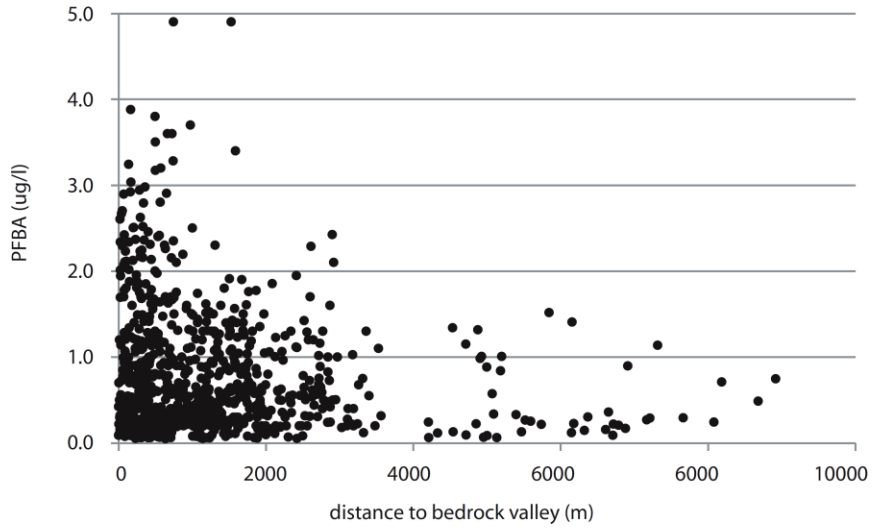


x = distance to bedrock valley (km)
 500 — elevation above mean sea level (ft)

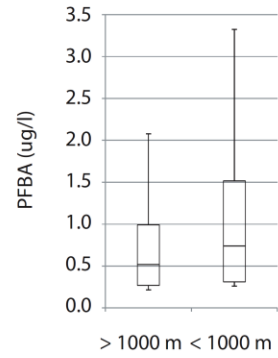
domestic wells only

Figure 18

Figure 19. Scatterplot and summary statistics for PFBA concentrations greater than 1 microgram per liter, compared to distance from a bedrock valley, threshold distance of 1000 meters. Location map shows distribution of points. Box plots show median, upper and lower quartile and outlier values for distance from well to the bedrock valley. Median concentrations for datasets with distances greater than or less than 1000 meters are significantly different from one another at $\alpha = 0.05$. The spread of PFBA values from samples with a distance less than or equal to 1000 meters is greater and reflected in a higher mean value for this data group.

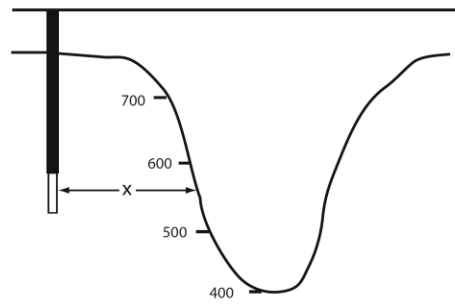


	PFBA (ppb)	
	distance to bedrock valley	
	> 1000 m	< 1000 m
min	0.1	0.1
max	8.0	242.6
median	0.5	0.7
mean	0.7	2.1
upper quartile	1.0	1.5
lower quartile	0.3	0.3
std dev	0.74	12.76
	n = 397	n = 412



median values different at 0.05 significance level ($p = <0.001$, one sided test)

(maximum values not shown)



x = distance to bedrock valley (m)
 500 — elevation above mean sea level (ft)

Figure 19

Figure 20. Lithostratigraphic column showing distribution of residence time by open hole interval. Recent waters found most often in bedrock stratigraphically higher than the St. Lawrence Formation

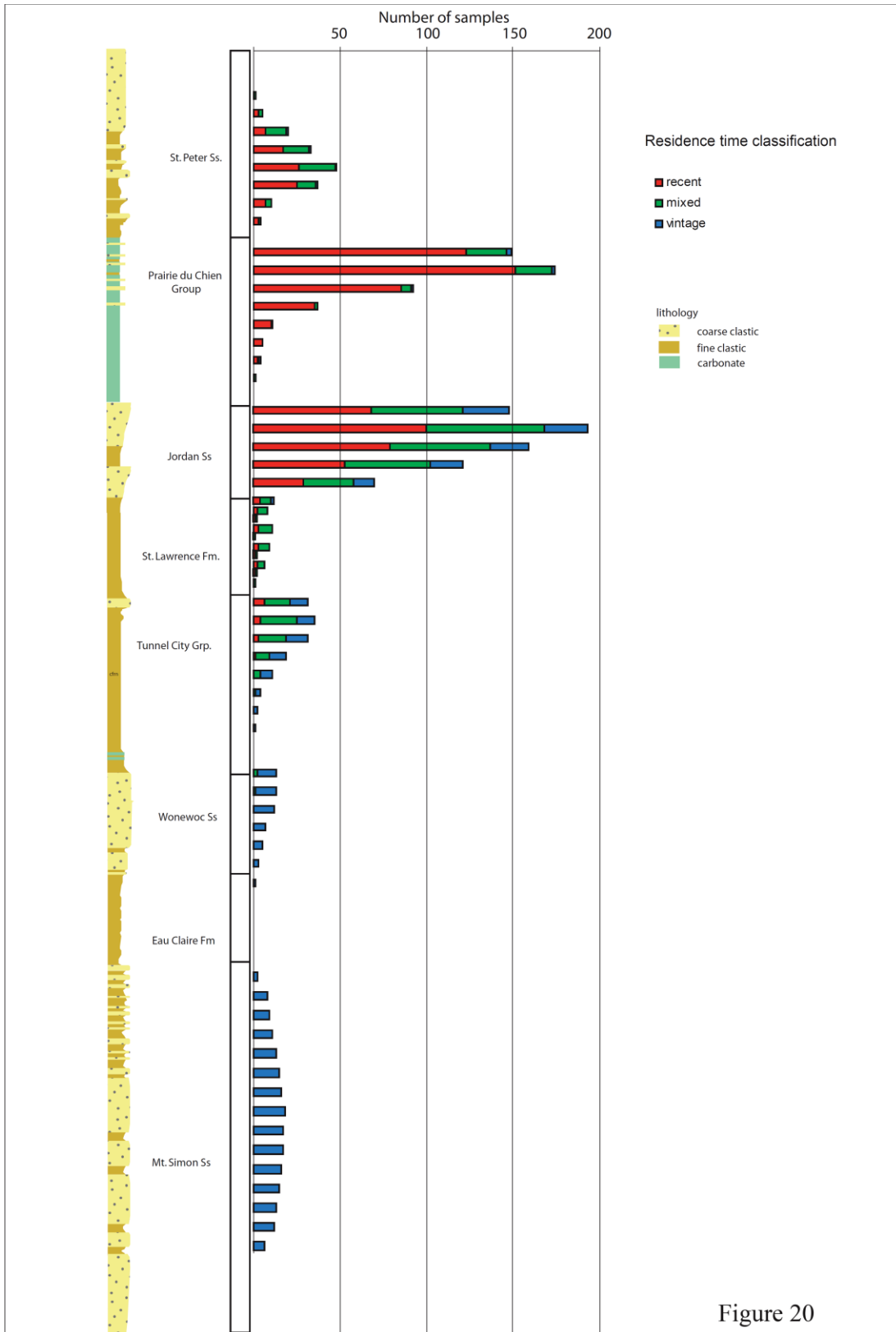


Figure 20

Figure 21. Boxplots of chloride concentrations in Prairie du Chien and Jordan samples, grouped by western, central and eastern regions. In the west region, concentrations are low in both Prairie du Chien and Jordan samples, with a greater spread and higher median value in the Prairie du Chien; Greater spread and higher median values in the Prairie du Chien are also found in the east region, with overall median values for both Prairie du Chien and Jordan sets greater than respective units in the other two regions; In the central region, there are lower median values but a greater spread in the Jordan compared to the Prairie du Chien.

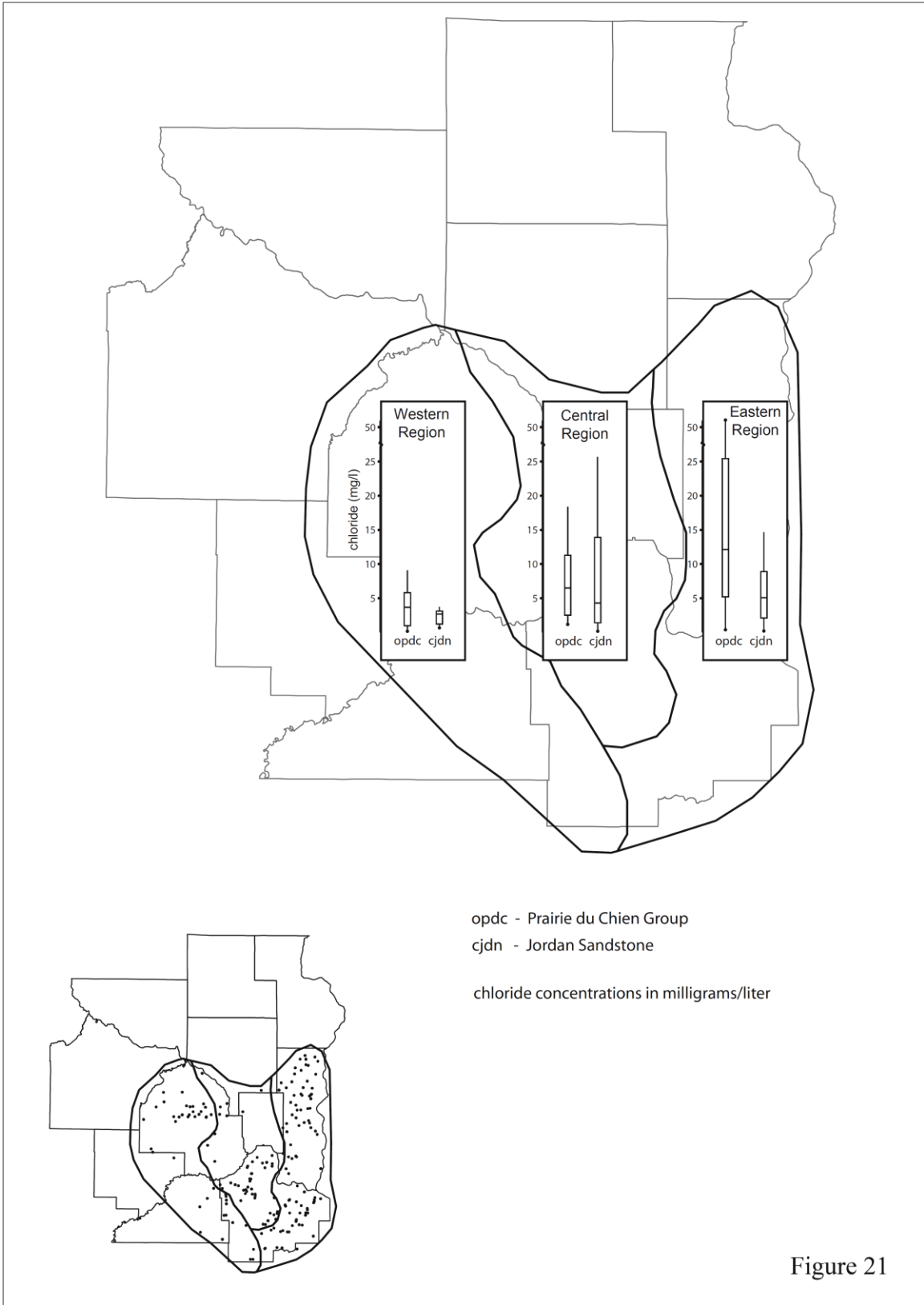


Figure 21

Figure 22. Series of stacked columns, showing the number of detect verses non-detects of PFBA for both the Prairie du Chien and Jordan wells, in regularly spaced sectors across southern Washington County. Location of cross section H-H' (Figure 36) is shown.

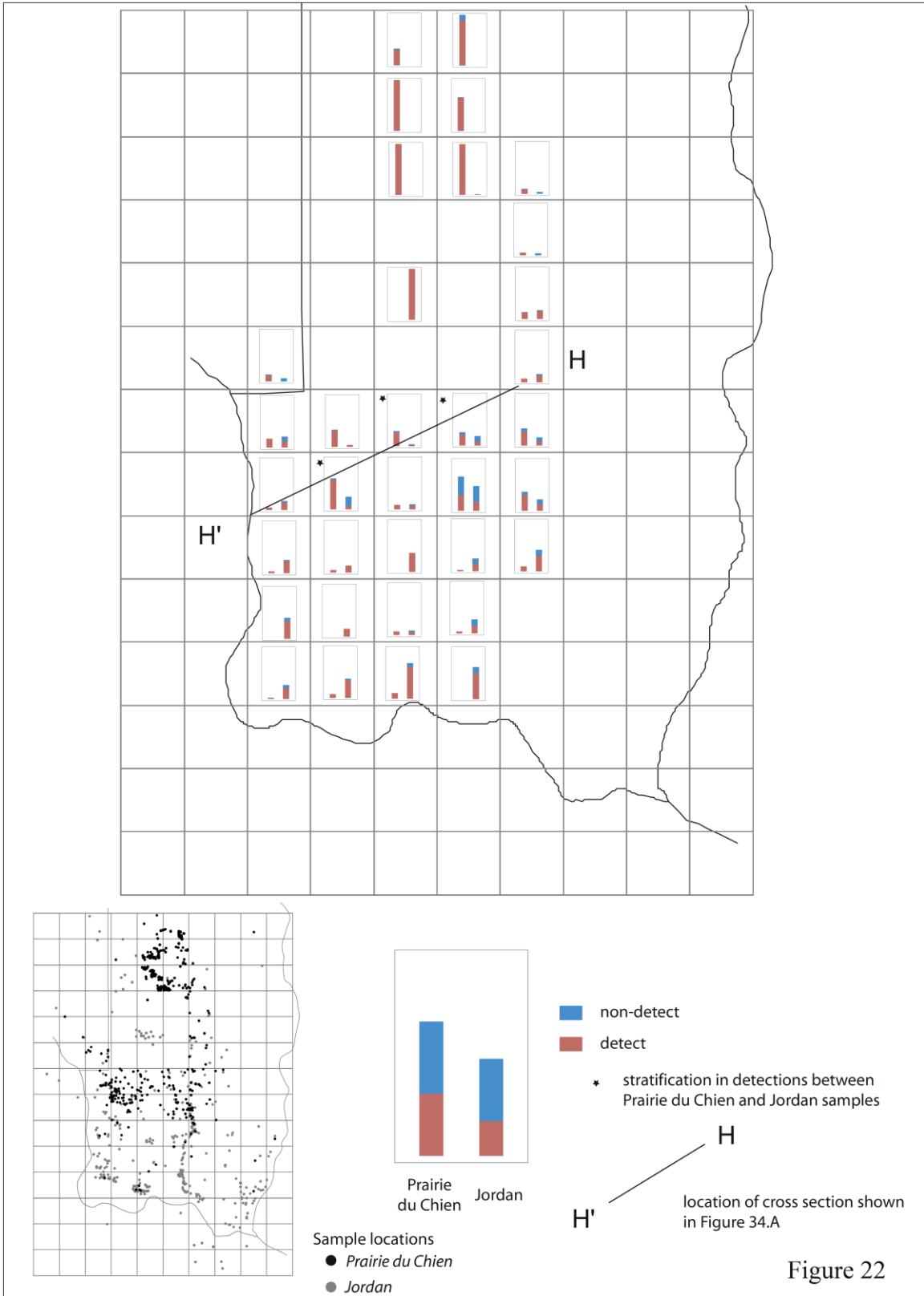


Figure 22

Figure 23. Estimated composite vertical hydraulic conductivity in feet per day from the land surface to the bedrock surface. Estimate based on harmonic mean of texture-based hydraulic conductivities of unconsolidated subsurface materials, calculated at regularly spaced 250 meter by 250 meter intervals in the horizontal direction. Details on subsurface texture database construction included in Appendix A.

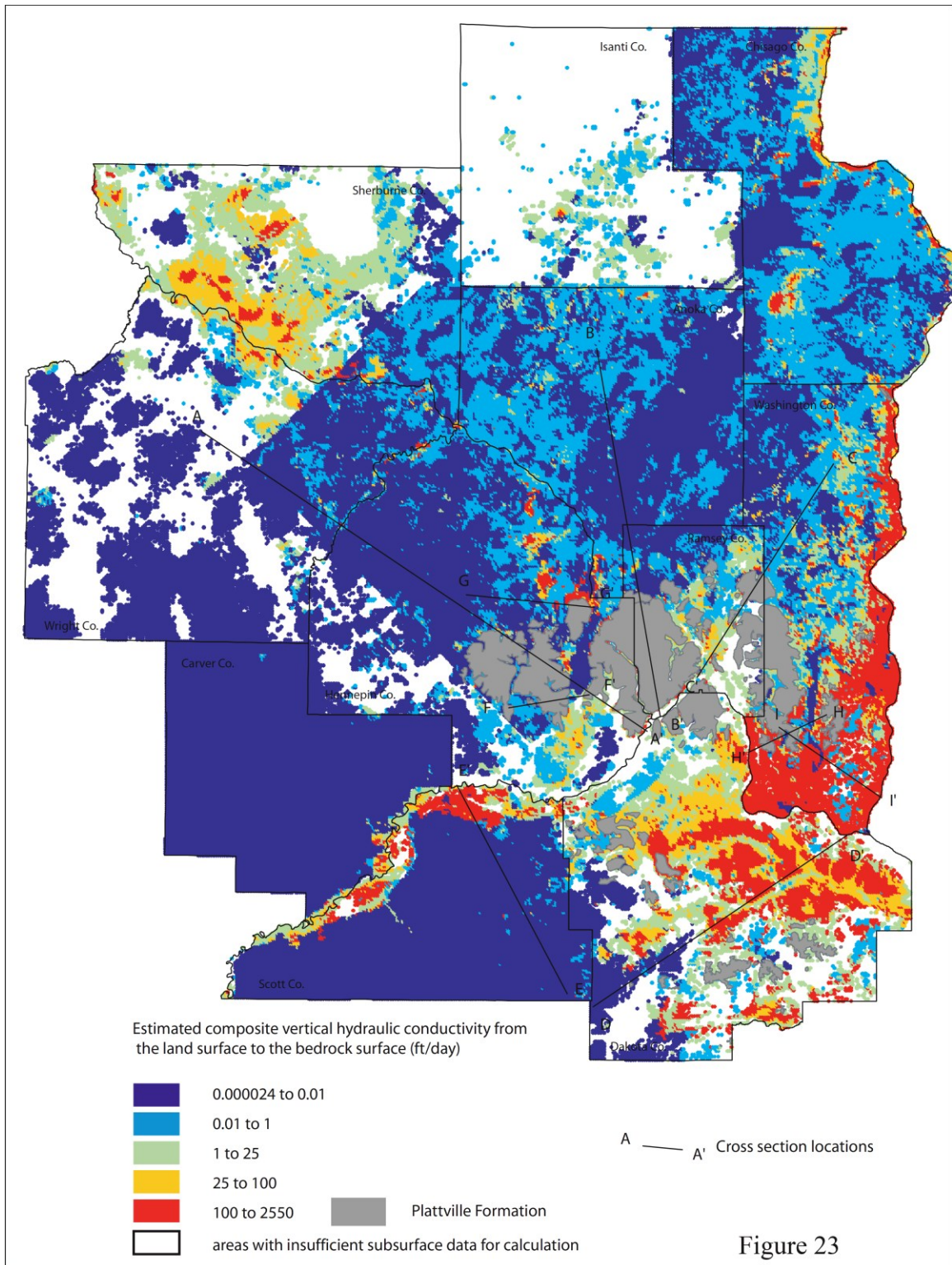


Figure 23

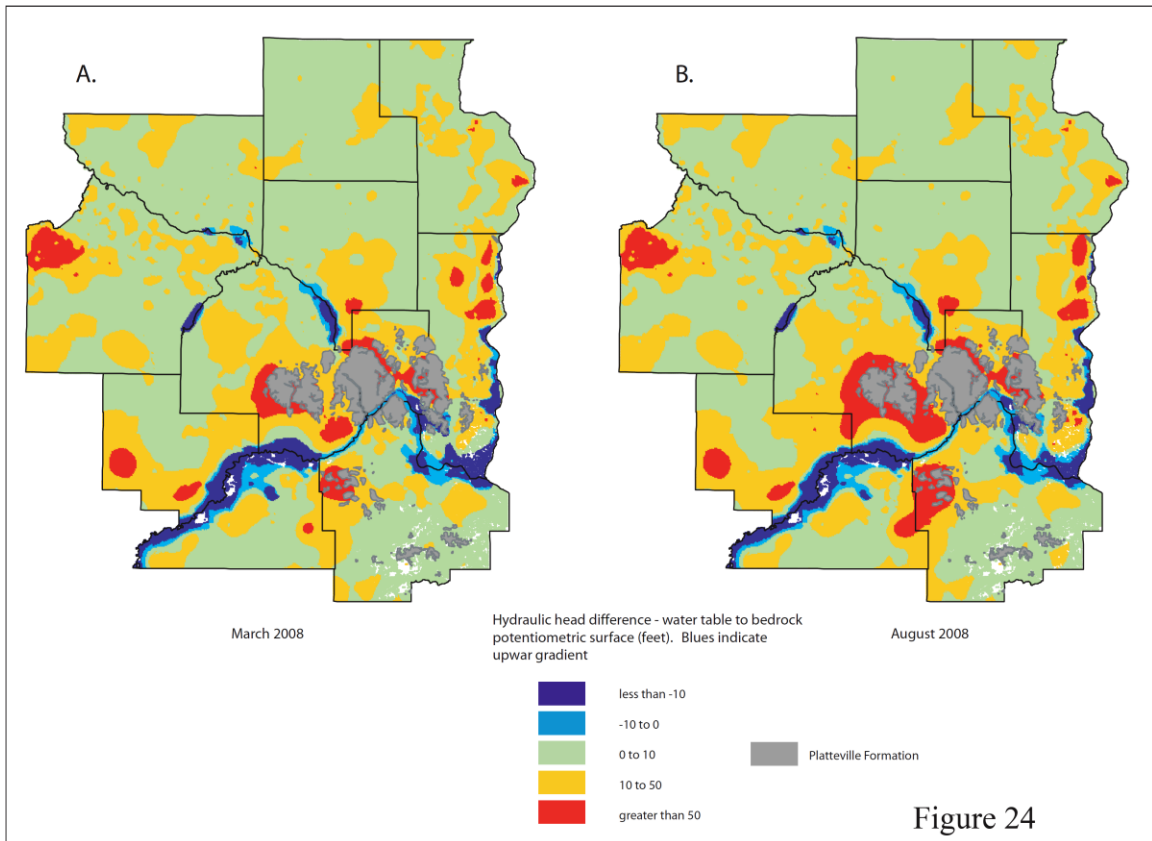


Figure 24. Regional maps showing adjusted vertical change in hydraulic head for March (A.) and August (B.) 2008. Bedrock surfaces were adjusted to be one half foot below the water table surface except in areas of groundwater discharge (Mississippi, Minnesota, St. Croix, and portions of the Crow River). Constructed by subtracting the bedrock potentiometric surface from the water table surface, summer increases in hydraulic gradient are most visible in the central metropolitan area. These changes reflect increased drawdown in the bedrock potentiometric surface due to higher summer pumping rates from the Prairie du Chien Group and Jordan Sandstone.

This page is blank

Figure 25. Calculated vertical travel time from regional water table the bedrock surface (saturated conditions) travel times greater than 500 years calculated for much of the western metropolitan area, where a thick sequence of clay loam NW provenance till and sandy loam NE provenance tills overlie bedrock. Shorter residence times are present where relatively coarse sediment overlies bedrock and in areas of large hydraulic gradient.

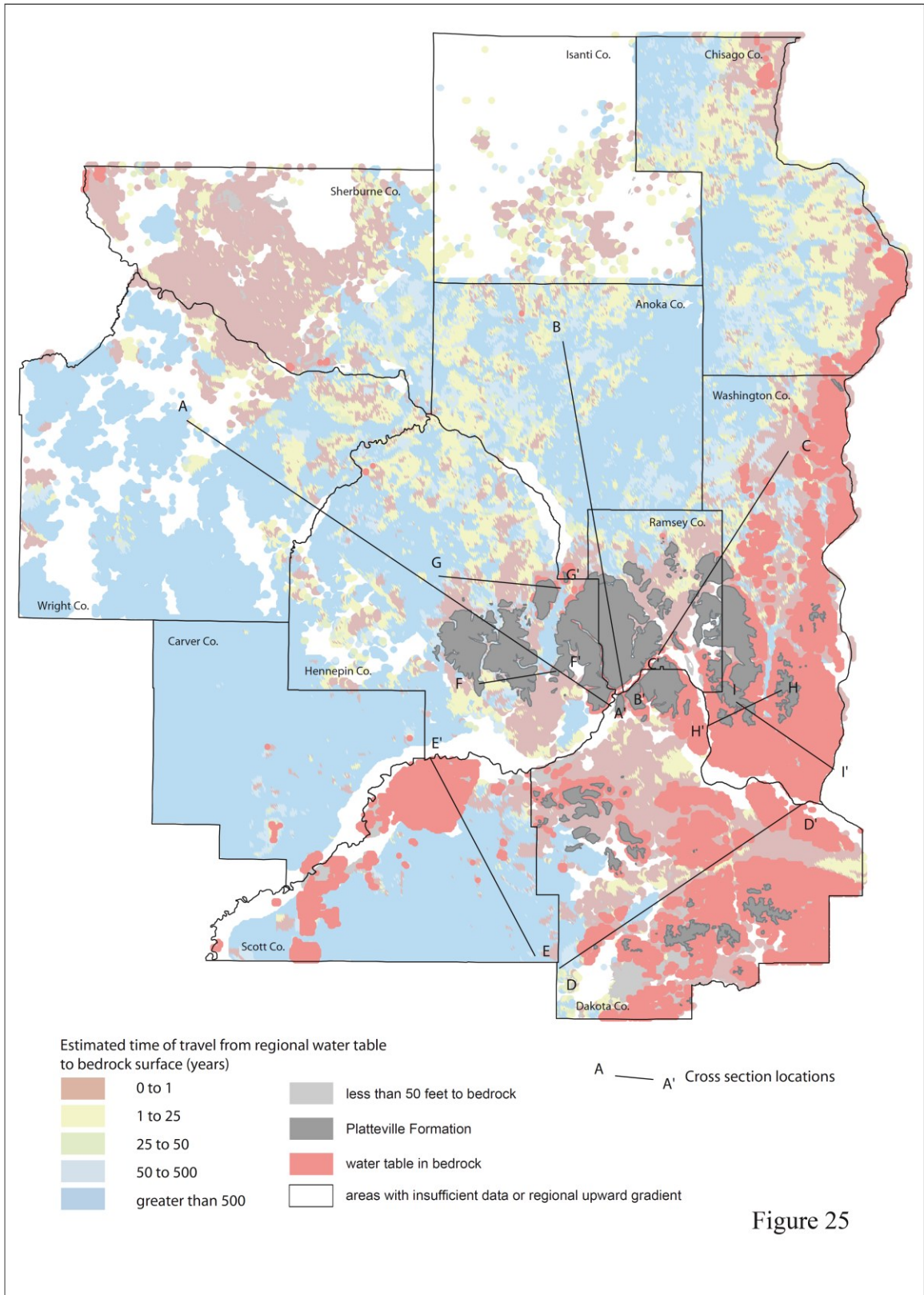
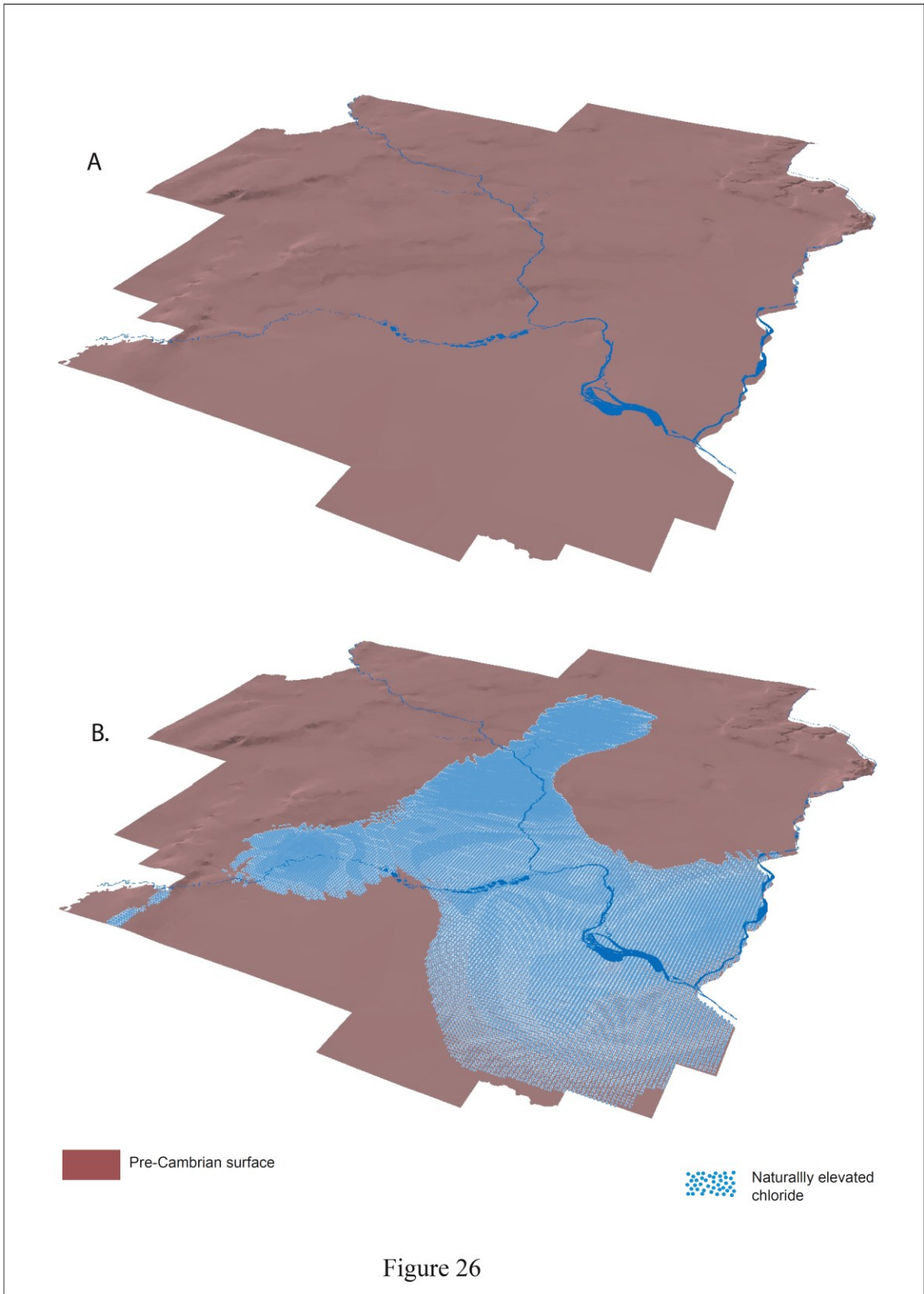
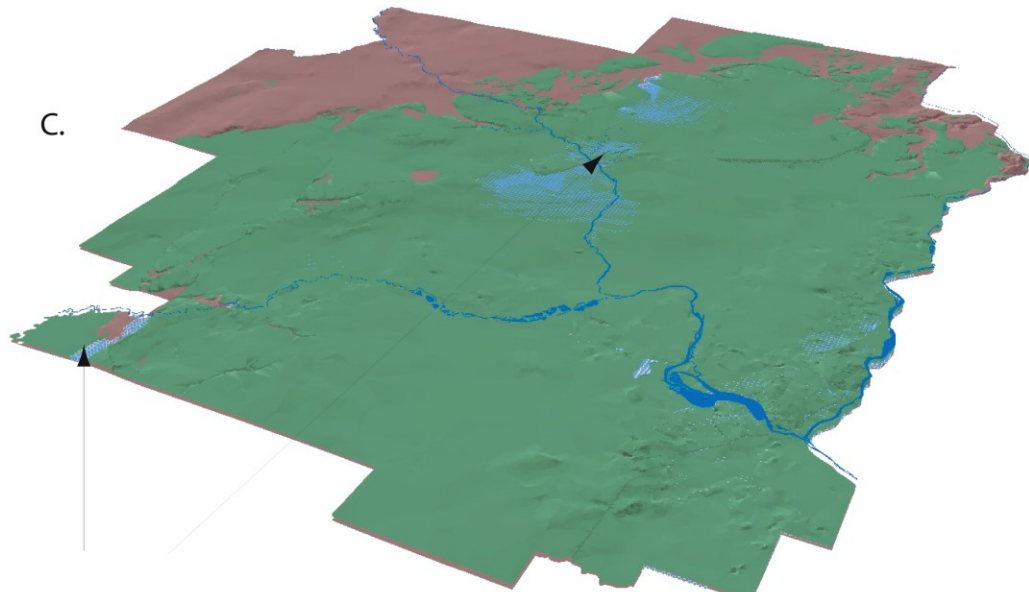
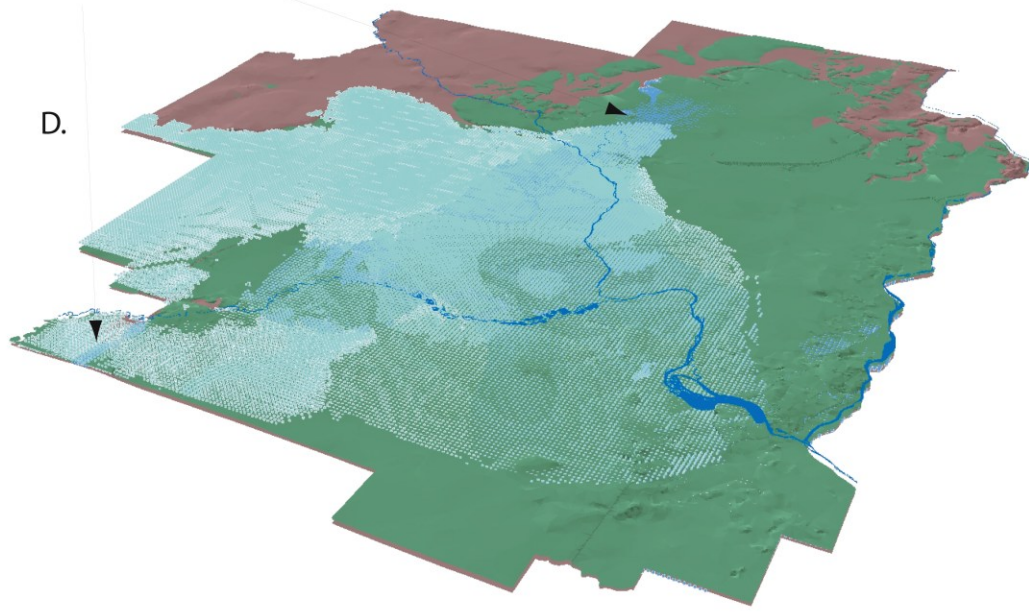


Figure 26. Oblique views of the TCMAX from the southeast, showing the three dimensional distribution of regional hydrochemical facies in bedrock and surficial deposits. Selected bedrock units included for vertical reference. **A.** Pre-Cambrian surface and major rivers; **B.** Naturally elevated chloride are present above the Pre-Cambrian in the lower St. Mt. Simon; **C.** Naturally elevated chloride present above the Eau Claire Formation, shown in green, in fault zones; **D, E and F.** Elevated Sr/(Ca+Mg) waters present in the western TCMAX in Quaternary, Jordan, Prairie du Chien and Mt. Simon (not shown); **G, H, I.** Recent waters found at elevations below 700 feet in the central TCMAX, broadening out at elevations closer to the land surface.





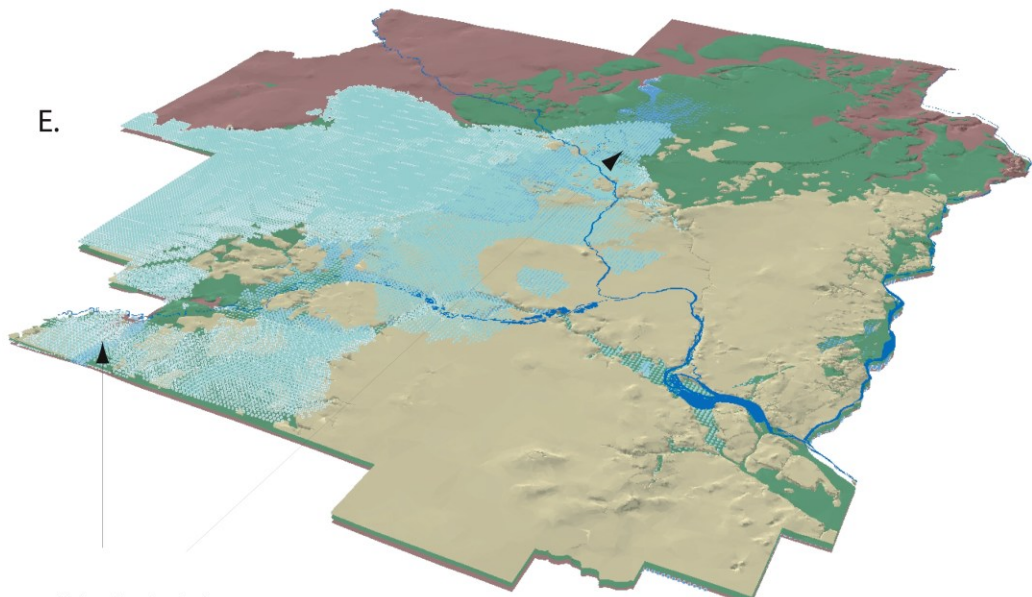
Naturally elevated chloride



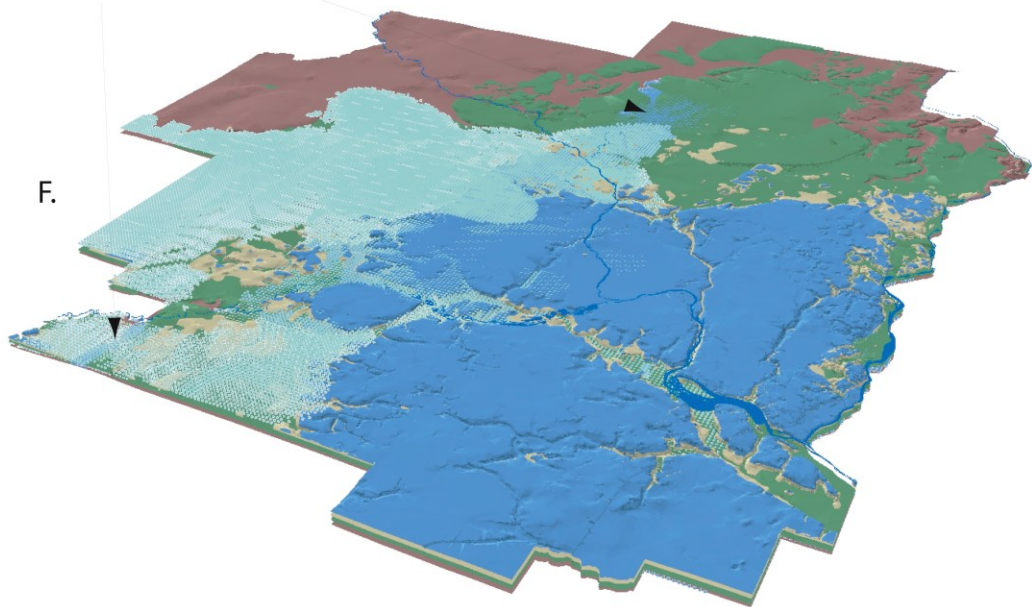
Eau Claire Formation
 Pre-Cambrian surface

Elevated strontium
 Naturally elevated chloride

Figure 26 (continued)



Naturally elevated chloride



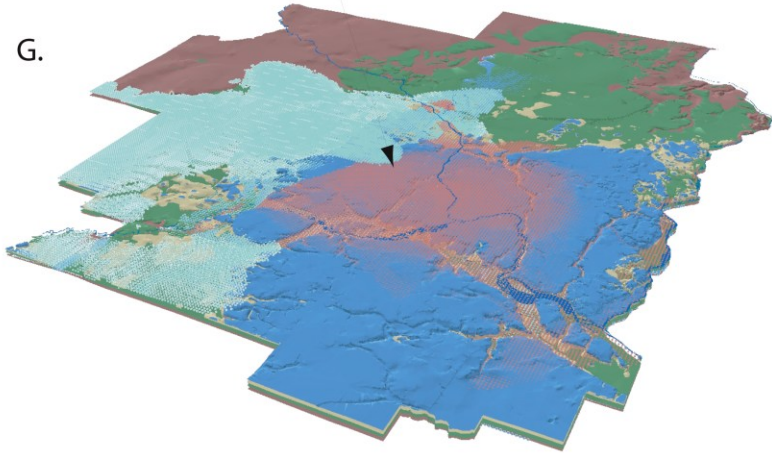
- Prairie du Chien Group
- Jordan Sandstone
- Eau Claire Formation
- Pre-Cambrian surface

- Elevated strontium
- Naturally elevated chloride

Figure 26 (continued)

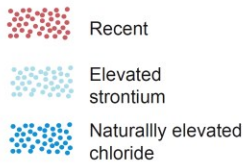
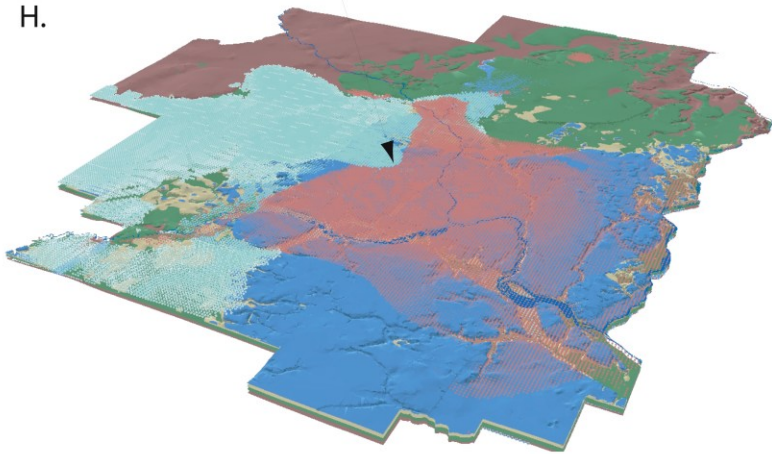
extent of recent waters at elevation 700 ft above msl

G.



extent of recent waters at elevation 800 ft. above msl

H.



recent waters at the land surface

I.

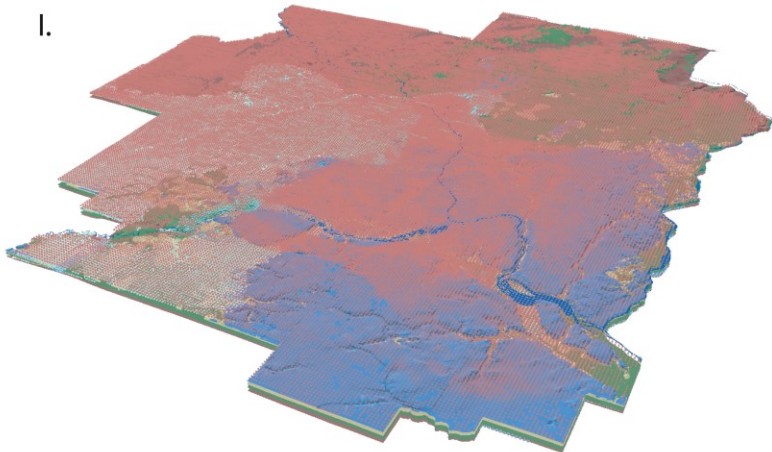


Figure 26 (continued)

This page is blank

Figure 27. Cross section key for Figures 26 through 33.

hydrochemical facies

Recent/anthropogenic waters:

waters distinguished primarily by the presence of detectable tritium. Other indicators of recent water such as elevated chloride, nitrate, or anthropogenic compounds generally also present.



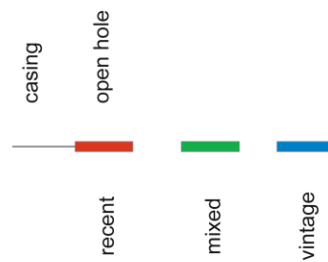
Elevated strontium to calcium plus magnesium ratios:

waters distinguished by having strontium to calcium plus magnesium molar ratios greater than 0.001. Elevated strontium to calcium plus magnesium ratios may be associated with recharge through NW provenance tills, and are also considered to an indicator of longer residence time



Naturally elevated chloride:

waters distinguished by having chloride levels greater than 15 ppm and carbon 14 age dates greater than 1,000 years. Where data is available, these waters should also have chloride to bromide ratios less than 300.



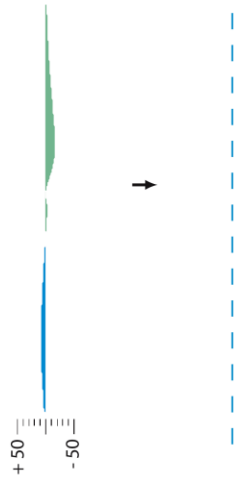
Selected wells from the water chemistry database. Colors of open-hole intervals correspond to assigned qualitative age classes. Recent waters are dominated by waters having entered the ground since the late 1950s; Vintage water are dominated by waters having entered the ground prior to the late 1950's; Mixed waters are considered a combination of recent vintage waters. See text for discussion

Mt. Simon Aquifer age determined from carbon-14 analysis; well name (Lively, et al., 1992) for wells not shown, location projected to cross section line.

Figure 27






hydraulic gradient

Head difference between regional water table and bedrock potentiometric surface, in feet. Blue indicates upward gradient; green indicates downward gradient flowmeter measurement. arrow indicates direction of ambient flow in an open borehole



700 feet above msl line, marks regional discharge elevation as approximate elevation of the Mississippi, Minnesota and St. Croix Rivers

mapped Quaternary stratigraphy

-  sand and gravel
-  loam to clay loam - generally NW provenance till
-  loam to sandy loam - generally NE provenance till
-  loam, silt rich; silt and clay - generally N provenance till; lacustrine deposits
-  undifferentiated



interpolated model




-  likelihood of coarse-grained deposits > 40%
-  likelihood of coarse- to fine-grained deposits > 40%
-  likelihood of fine-grained material > 40%



Figure 27 (continued)

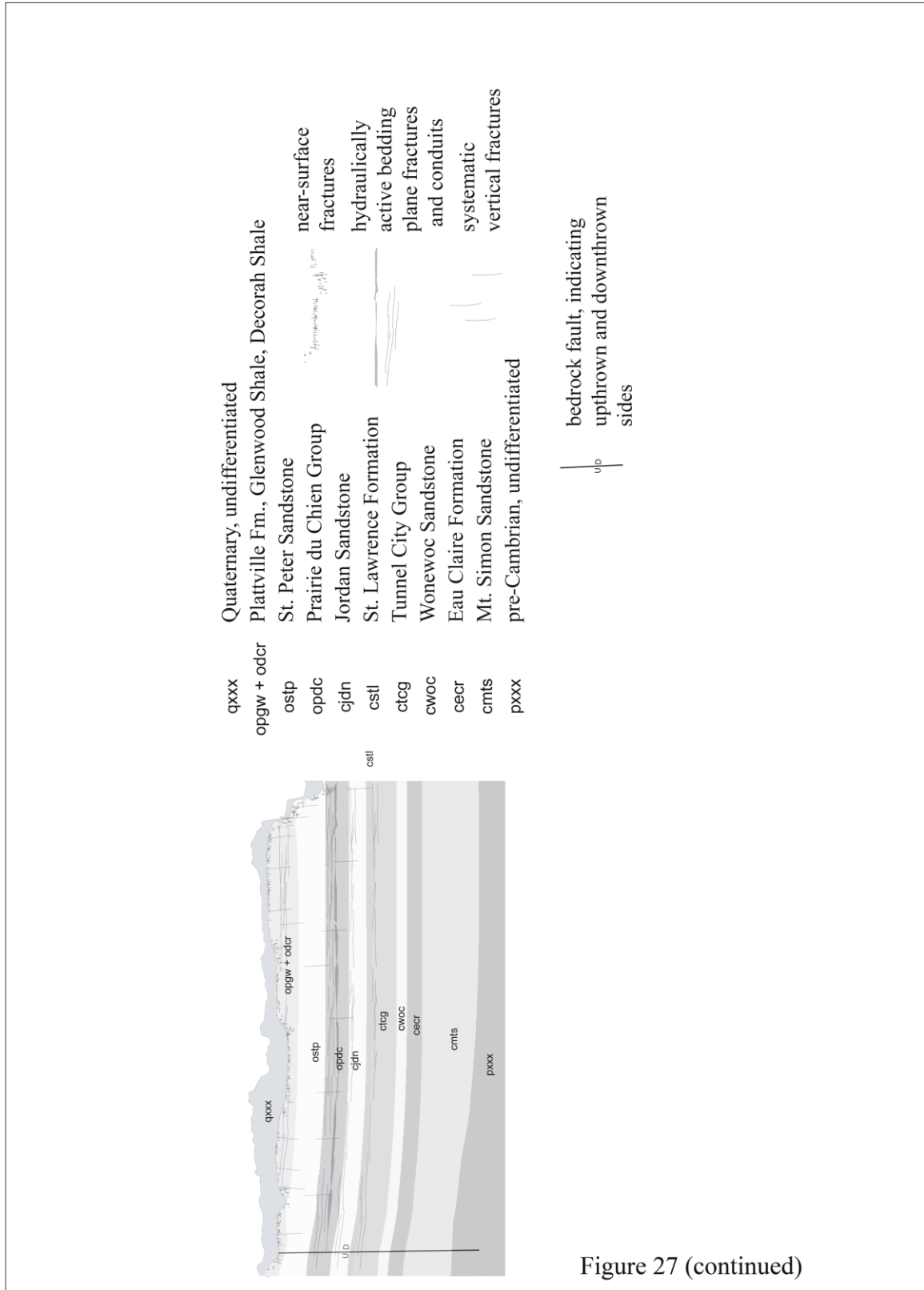


Figure 27 (continued)

Figure 28 and 29. Left and right sides of regional cross section A-A', Sherburne County to Mississippi River. Recent waters interpreted as present in the upper 50 feet of unconsolidated deposits, increasing with depth in the central part of the basin. Lowest elevation of recent waters occurs in the Jordan Sandstone. Carbon 14 dates for Mt. Simon are shown, indicating a sharp contrast in recharge rates for the upper and lower aquifer systems.

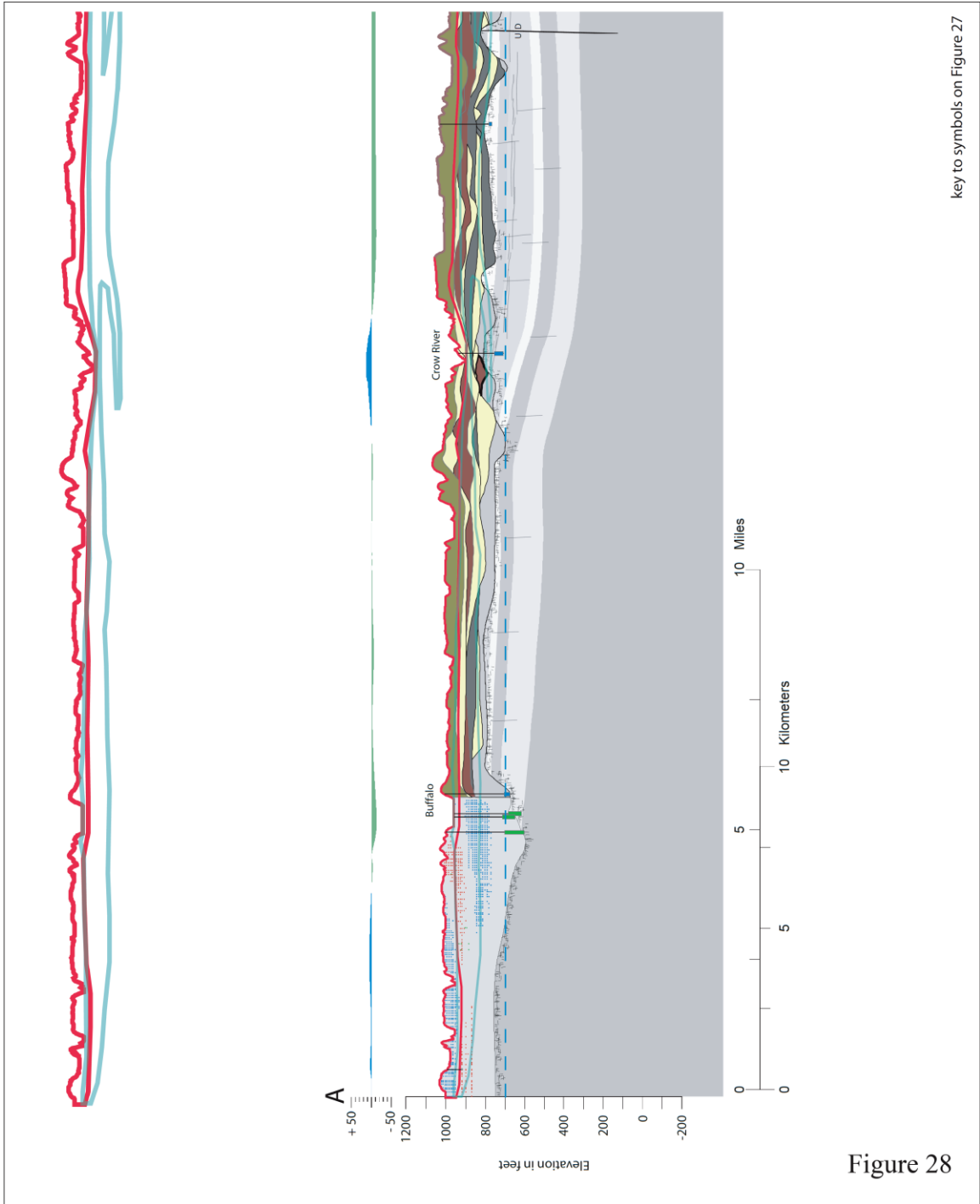
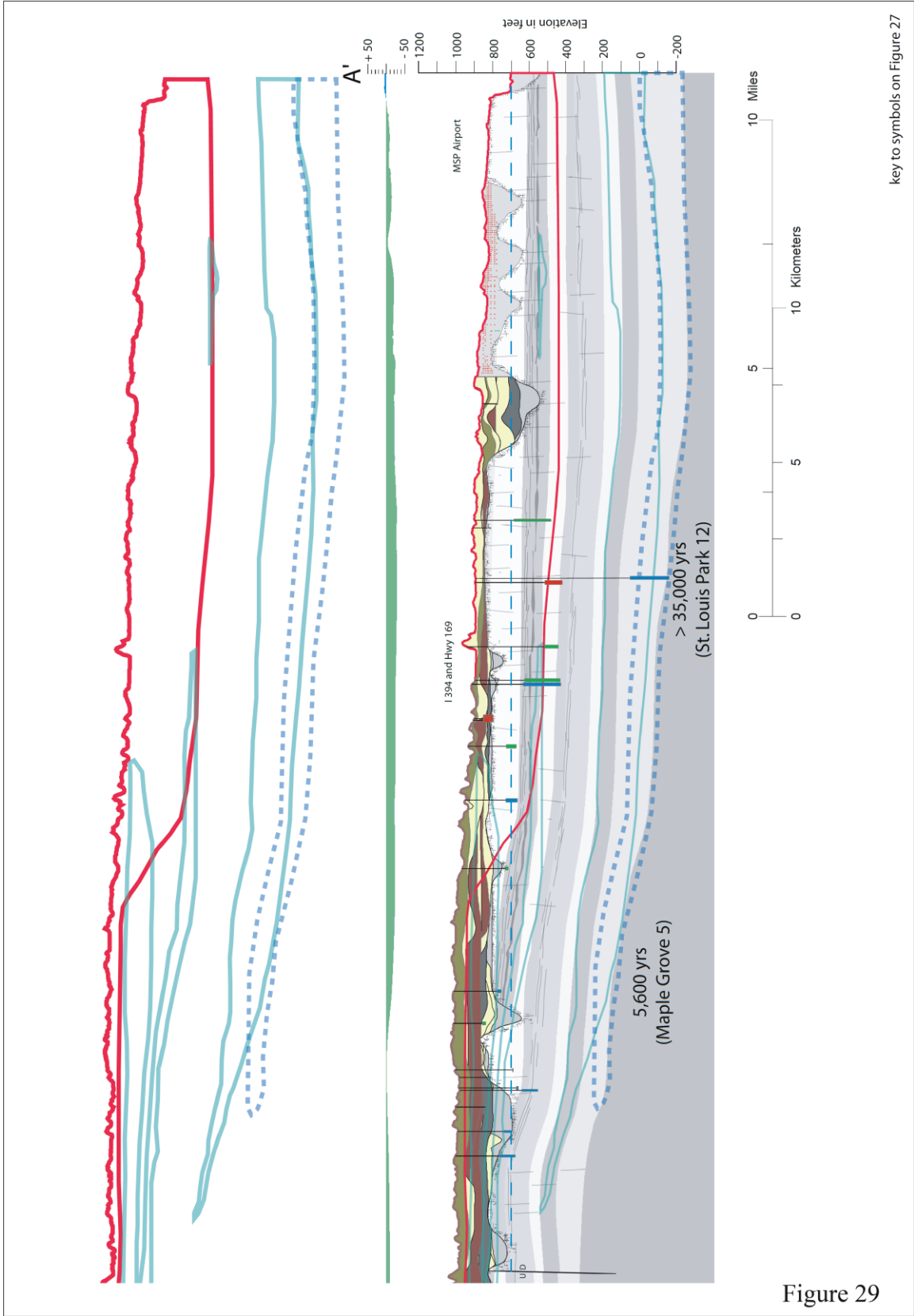


Figure 28

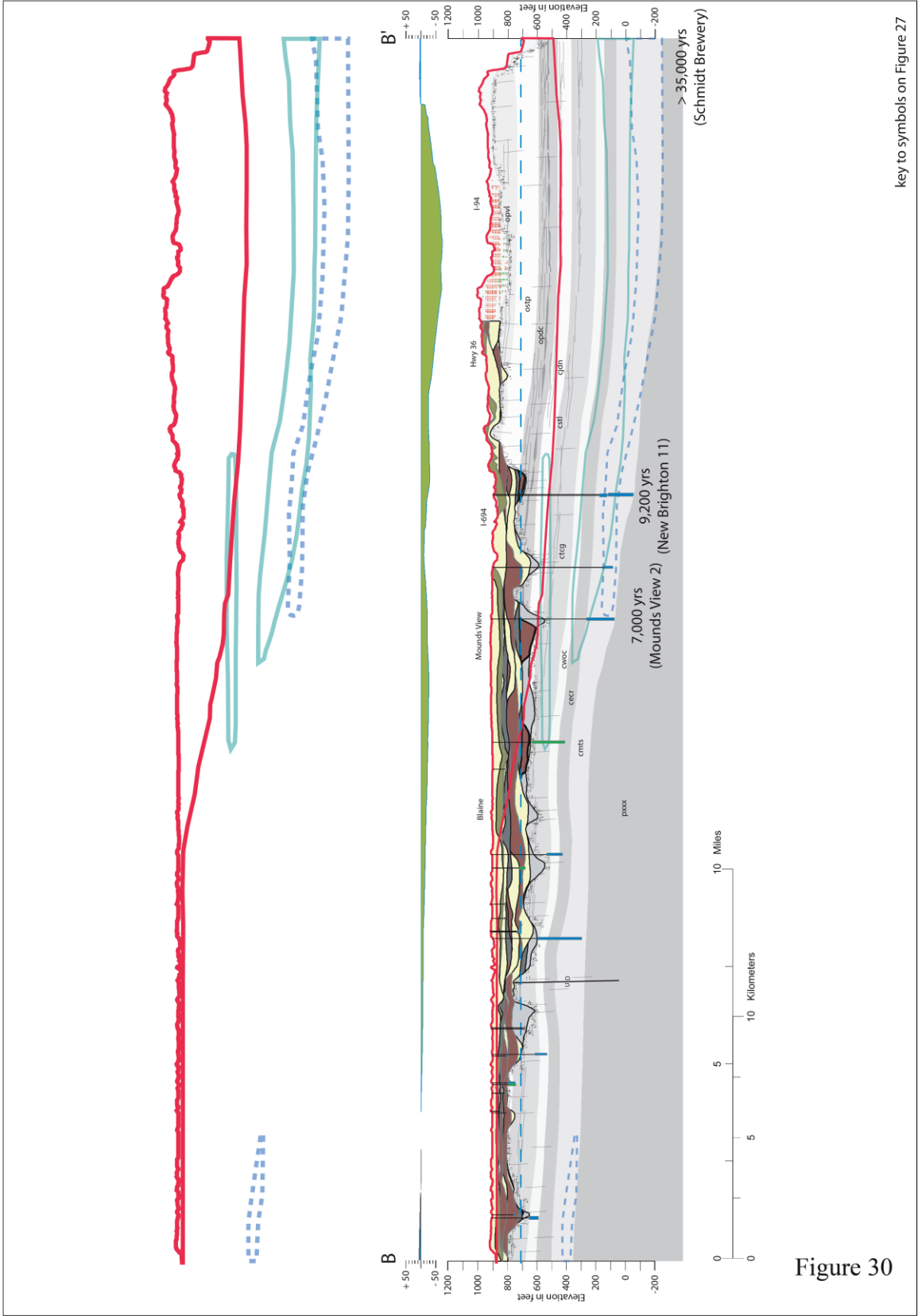


key to symbols on Figure 27

Figure 29

This page is blank

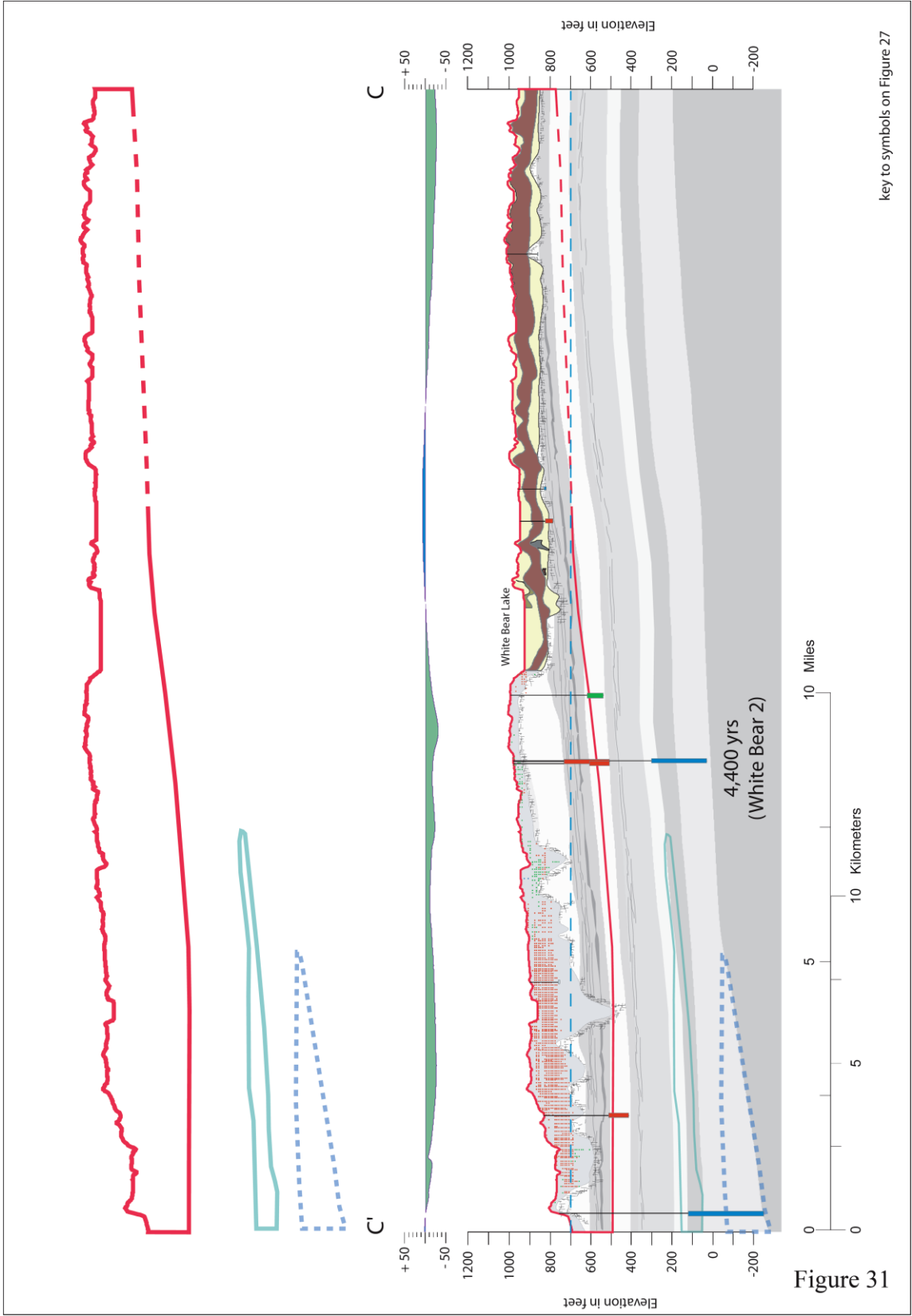
Figure 30. Regional cross section B-B', St. Francis, Anoka County to Mississippi River. Recent waters interpreted as present in the upper 50 feet of unconsolidated deposits, increasing with depth in the central part of the basin. Lowest elevation of recent waters occurs in the Jordan Sandstone. Complexity of unconsolidated deposits over bedrock, below surficial sands is shown.



key to symbols on Figure 27

Figure 30

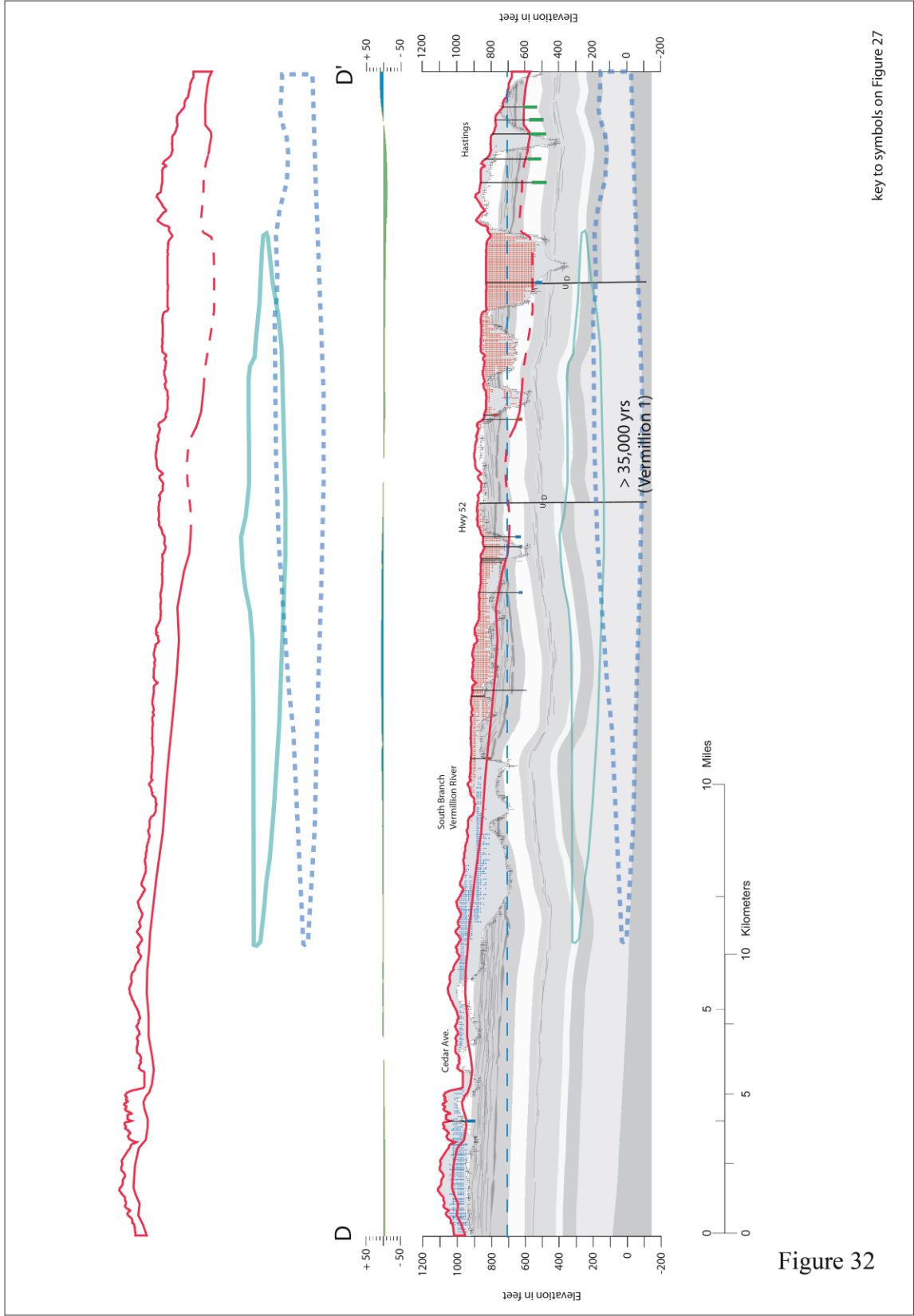
Figure 31. Regional cross section C-C', Big Marine Lake, Washington County to Mississippi River near downtown St. Paul. Recent waters between Big Marine and White Bear Lake in the Prairie du Chien Group largely based on tritium measurements from samples west and east of the cross section line interpreted as mixed waters (TU between 1 and 10). Recent water is found at depth toward downtown St. Paul, coincident with a downward gradient and coarse unconsolidated deposits over bedrock. Slight upward gradient at White Bear Lake; downward gradient near Big Marine possibly marking groundwater divide, with regional discharge west toward the St. Croix River. Vintage waters in the Mt. Simon aquifer.



key to symbols on Figure 27

Figure 31

Figure 32. Regional cross section D-D', western Dakota County to Mississippi River near Hastings. Limited data show presence of clay, based on the interpolated model, restrict the downward movement of water west of the South Branch of the Vermillion River. Remainder of the cross section is largely sand and gravel over Prairie du Chien Group. A large buried valley filled with sand and gravel is present west of Hastings. Recent waters within this valley based on sampled wells within and on the edges of the valley to the southeast.



key to symbols on Figure 27

Figure 33. Regional cross section E-E', southeastern Scott County to Minnesota River near Shakopee. Anthropogenic waters absent below cover of alternating NW and NE provenance tills. Elevated Sr/(Ca+Mg) ratios limited to bedrock valley in upper aquifers and to the Mt. Simon in the lower aquifer. Naturally elevated chloride present in the Mt. Simon at the northeast end of the cross section. Presence of recent water in the Jordan in this area based on sampled wells to the east and west of the cross section line. A strong upward gradient from the Jordan is present near the Minnesota River.

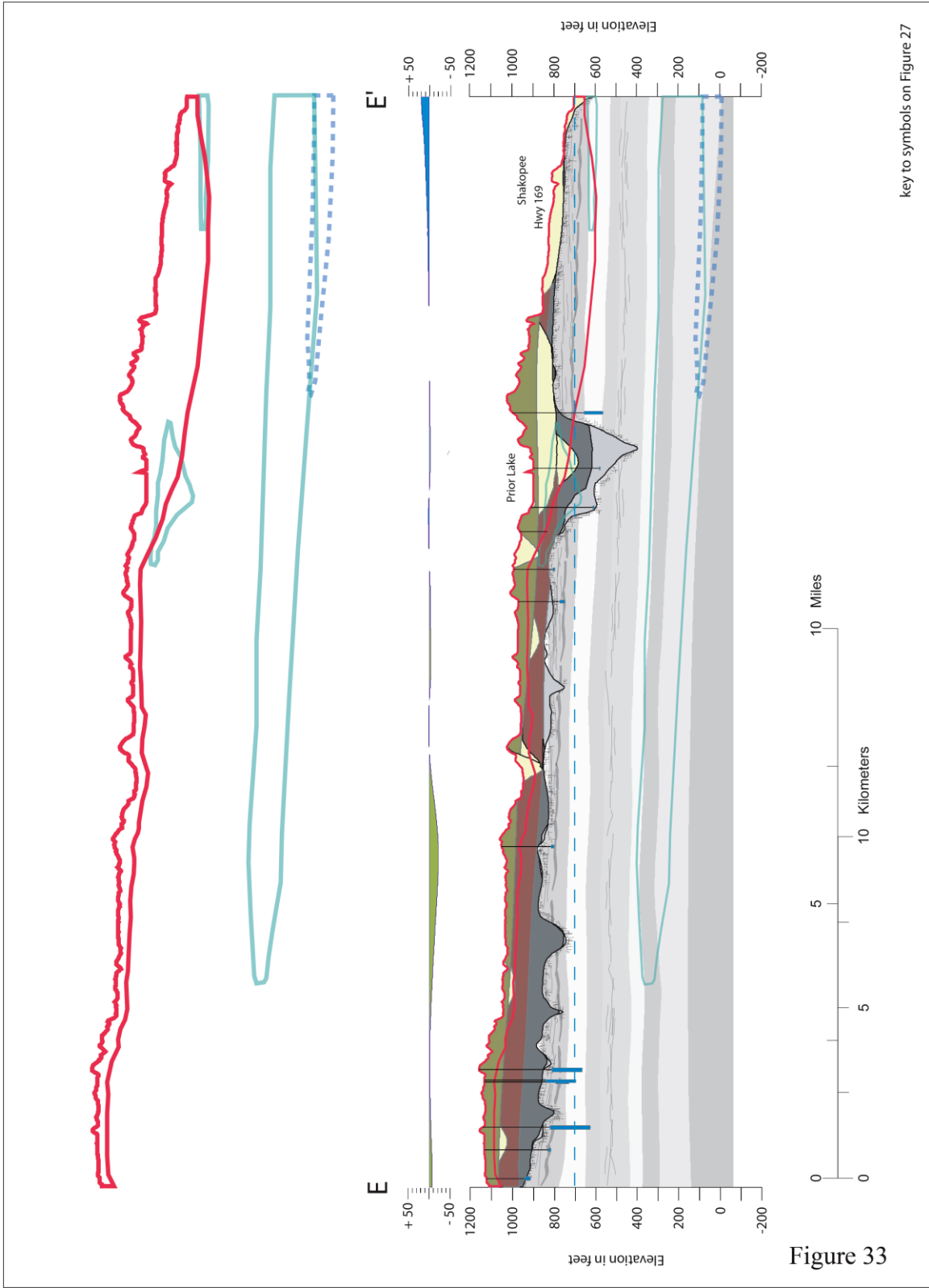
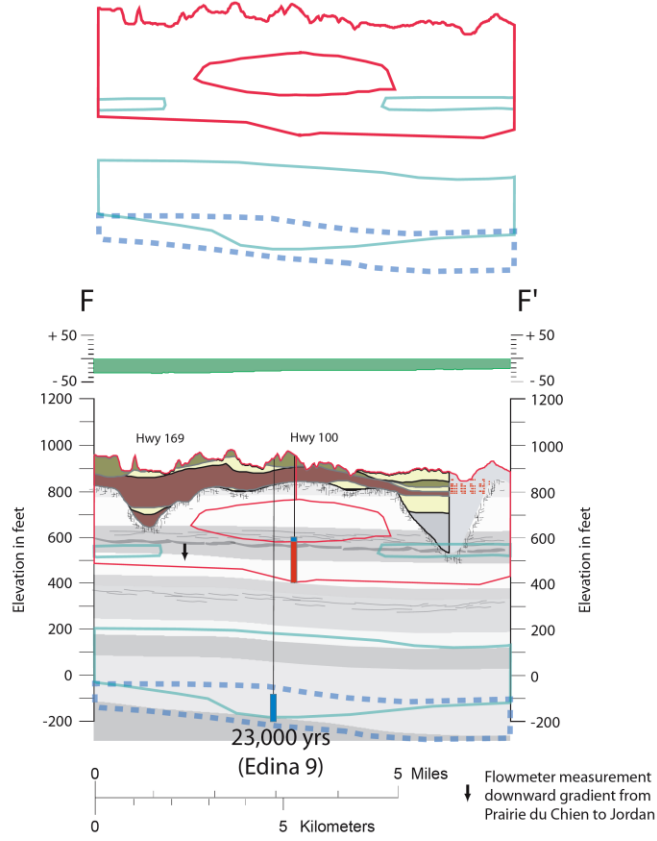


Figure 34.A. Local cross section F-F' Edina area. Age inversion within the open hole of a single well is shown. Grab samples from the lower portion of the open hole had detectible tritium, while the uppermost sample, located within the Shakopee Formation – Prairie du Chien Group, did not (MDH, 2010b). Flow logging from a nearby test well (MN unique well no. 748656) showed strong downflow from the lower Shakopee to the Jordan Sandstone, corresponding to stratigraphic position of detectible tritium in this well. Interpreted stagnation zone of older water illustrated as present underneath the central portion of the Platteville/Glenwood cap.

Figure 34.B. Local cross section G-G' Eastern Hennepin County. Recent water occurs at depth east of till cover. Flow logging east of Highway 169 showed strong upflow from fractures in the upper Jordan Sandstone to the upper Oneota Formation - Prairie du Chien Group (MN unique well no. 676445).

A.



B.

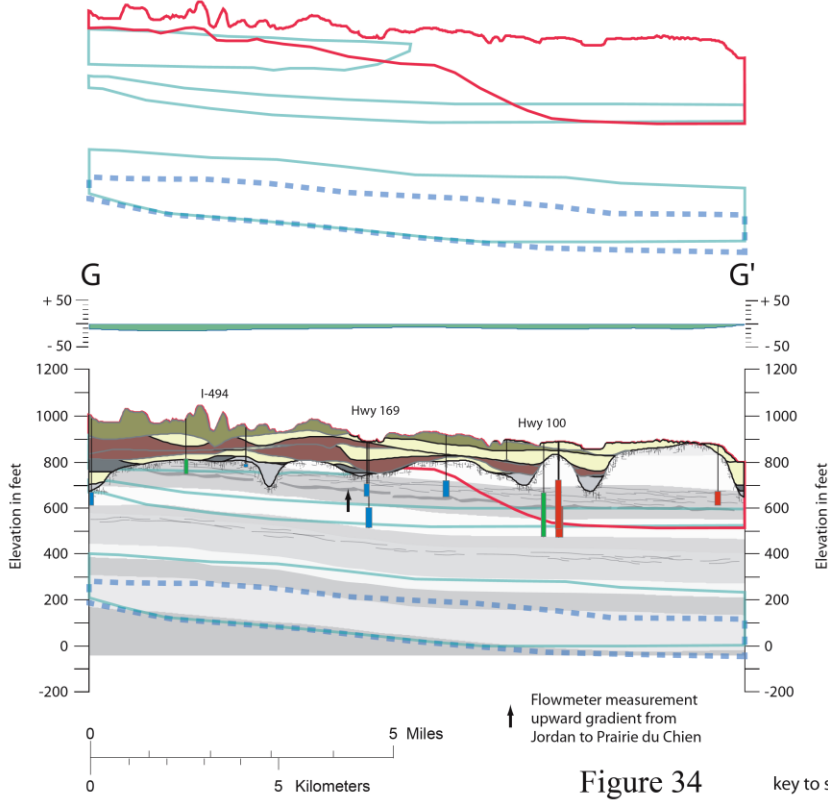


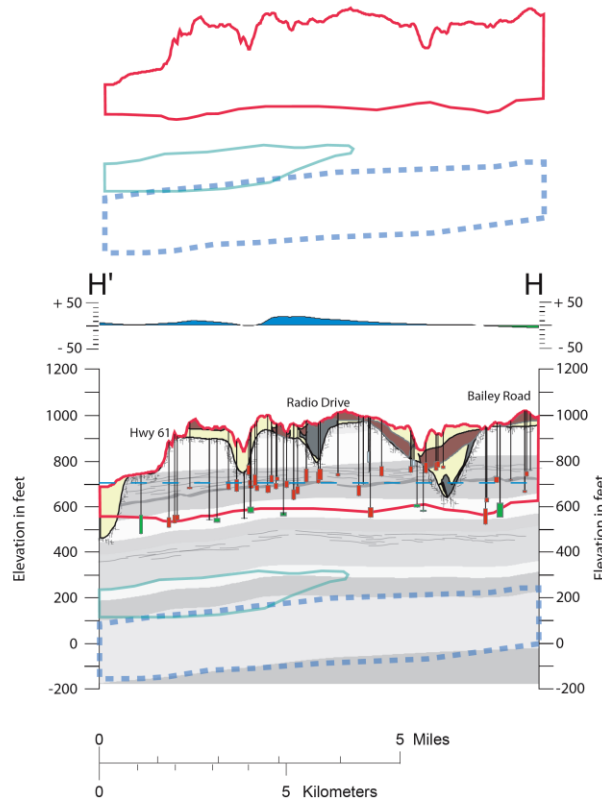
Figure 34

key to symbols on Figure 27

Figure 35.A. Local cross section H-H', south central Washington County to Mississippi River. Stratification of perfluorochemical (PFC) detections between Shakopee (upper Prairie du Chien Group) and Jordan samples is shown. Results infer separate flow systems, with possibly greater flux through the Shakopee Formation compared to the Jordan Sandstone.

Figure 35.B. Local cross section I-I', southeastern Washington County to St. Croix River. Downward gradient over a north-south trending bedrock valley in the center of the cross section, west of Manning Avenue. The valley, filled with primarily coarse-grained material, shows cluster of PFC detections. Occurrence of PFC's near the St. Croix River indicates movement of groundwater through fractures and fault blocks, crossing stratigraphic units with wide ranging permeability.

A



B.

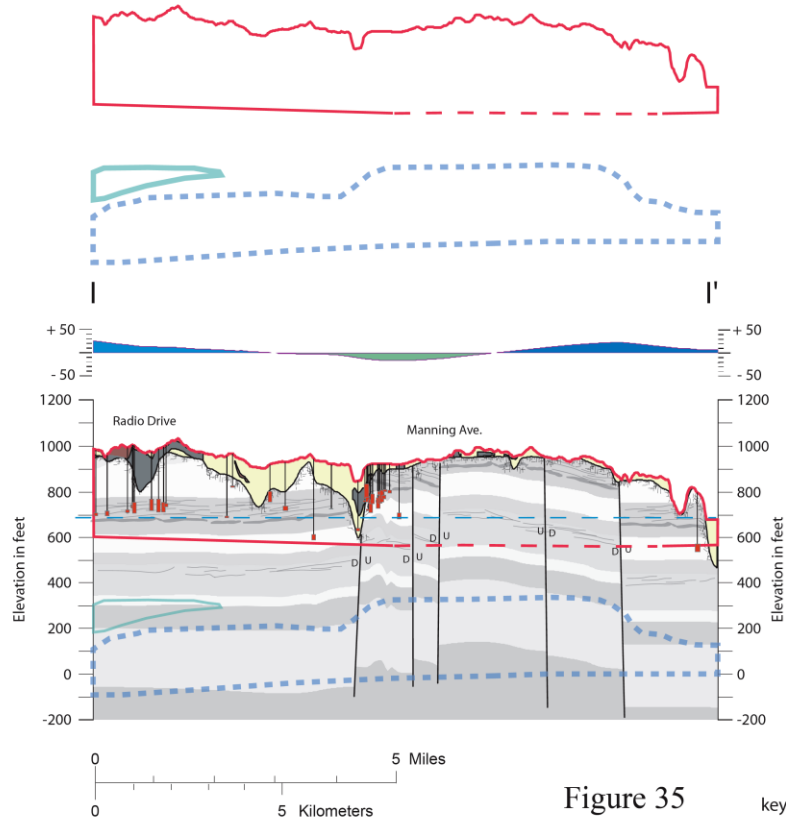


Figure 35

key to symbols on Figure 27

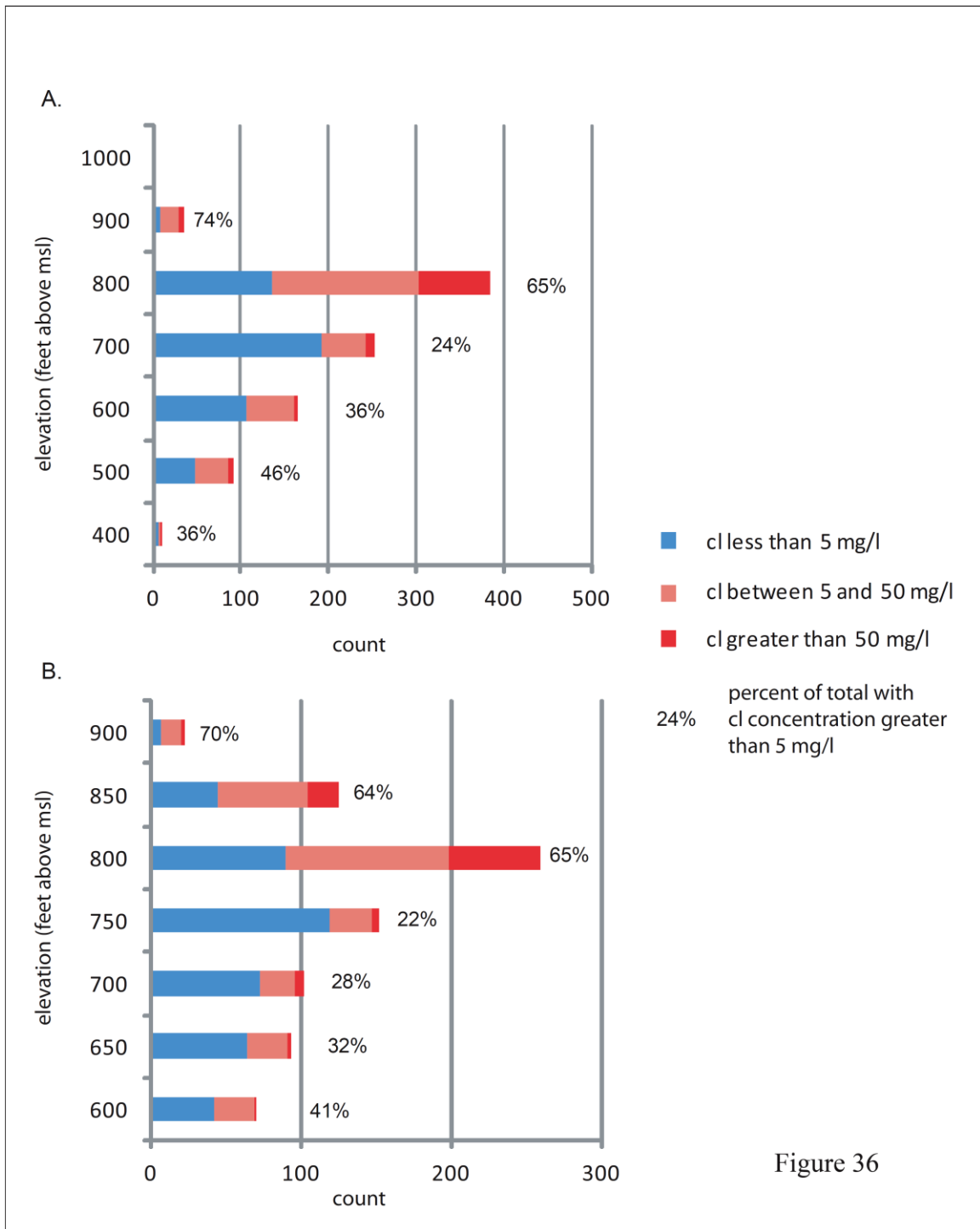


Figure 36. Histogram comparing chloride concentrations to top-of-open-hole elevation in sampled wells. Elevated chloride in metropolitan area water well samples, indicative of recent waters, is typically found at elevations above 700 feet above mean sea level, approximate elevation of the Minnesota, Mississippi and St. Croix Rivers. **A.)** Y axis from 400 to 1000 feet. **B.)** Expanded Y axis from 600 to 900 feet.

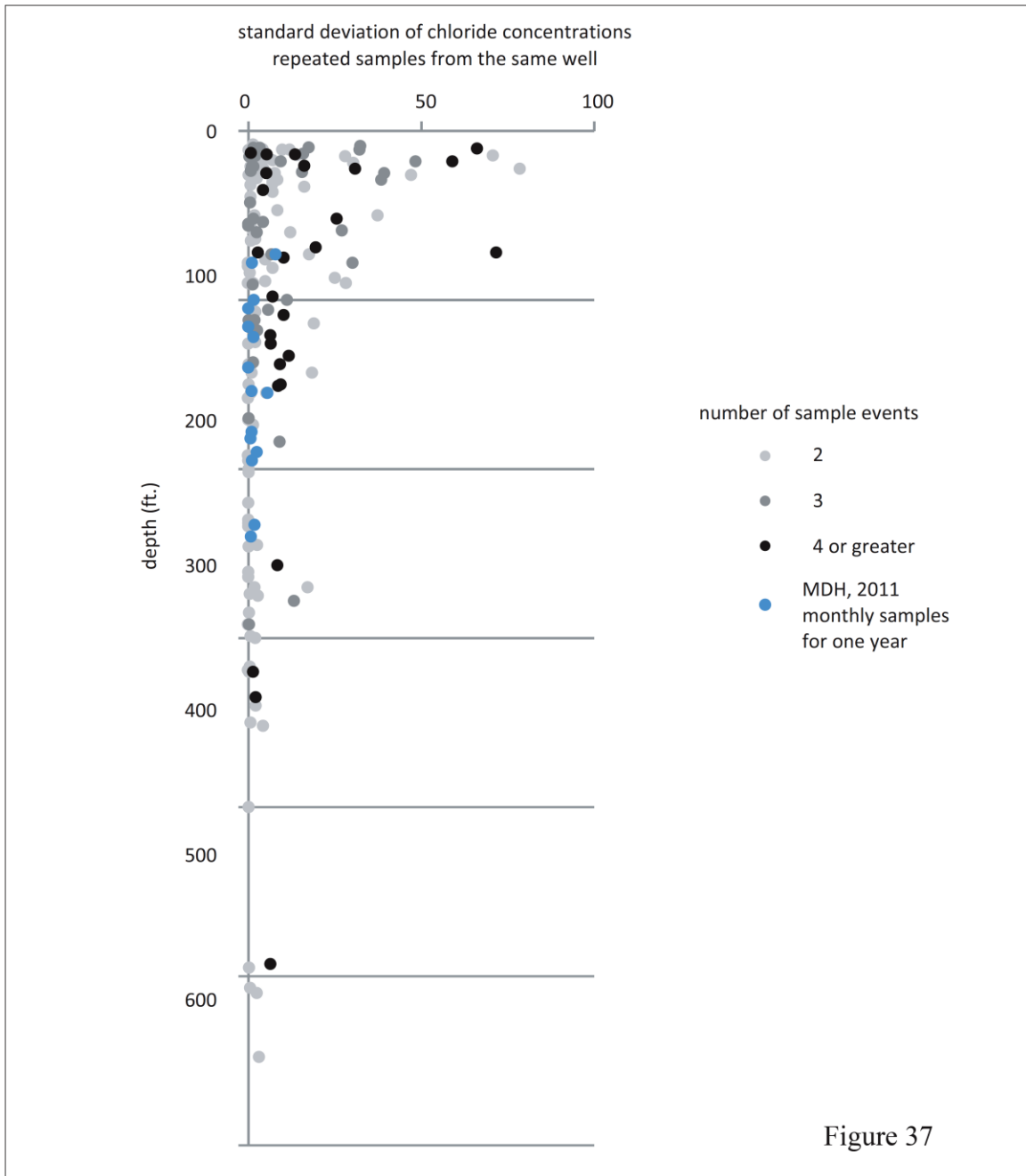


Figure 37. Temporal variability of chloride concentrations compared with depth. Greater variability in chloride concentrations are found at depths less than 150 feet below the land surface.

REFERENCES CITED

- Agrawala, G.K., 2007, Regional ground water interpretation using multivariate statistical methods: Thesis (Ph.D.), The University of Texas at El Paso, 147p.
- Alexander, S.C., 2005, Non-contaminant chemistry of natural waters: Minnesota Groundwater Association Fall Conference, Earle Brown Center, University of Minnesota, St. Paul Campus. November 17, 2005.
http://www.mgwa.org/membersonly/2005_fall/alexander_scott.pdf (accessed September 23, 2011)
- Alexander, S.C., Alexander, E.C. Jr., Pfankuch, H.O., et classica, 2005, Hydrogeology of the St. Paul Campus, January, 2005: Department of Geology and Geophysics, University of Minnesota. 77p.
- Alexander, S.C., and Alexander, E.C., Jr., 2010, Field and Laboratory Methods: Department of Earth Sciences, University of Minnesota, 18p.
- Alexander, S.C. and Ross, M., 2003, Sources and Residence Times of Ground Water Recharge in the St. Croix River Basin: Experience from Northern Washington County: *in* abstracts: St. Croix River Research Rendezvous, Science Museum of Minnesota, <http://www.smm.org/SCWRS/rendezvous/abstracts03.php>
- Andrews, W.J., Fong, A.L., Harrod, Leigh, and Dittes, M.E., 1998, Water-quality assessment of part of the Upper Mississippi River Basin, Minnesota and Wisconsin—Groundwater quality in an urban part of the Twin Cities metropolitan area, Minnesota, 1996: U.S.Geological Survey Water-Resources Investigations Report 97-4248, 54p.
- Andrews, W.J., Fong, A.L., and Stark, J.R., 1999, Ground-water quality along a flowpath in the Twin Cities metropolitan area, 1997-1998 [abs.]: 44th Annual Midwest Ground Water Conference, October 13-15, 1999, St. Paul, Minn., p.34.
- Appelo, C.A.J., and Postma, D., 1994, Groundwater Chemistry and Pollution: A.A. Balkema, Rotterdam, Netherlands; Brookfield, Vermont. 536p.
- Appleyard S.J., 1995, The impact of urban development on recharge and groundwater quality in a coastal aquifer near Perth, Western Australia: *Hydrogeology Journal*, v.3, no. 2, p.65–75.
- Artimo, A., 2003, Three-dimensional geologic modeling and numerical groundwater modeling of Finnish aquifers: A new approach for characterization and visualization: Thesis (Ph. D.), University of Turku, Turun Ylioipisto, Turku, Finland. 15p.

- Back, W., 1960, Origin of hydrochemical facies of ground water in the Atlantic Coastal Plain: *in* Proceedings of 21st International Geological Congress, Copenhagen 1960, part 1. p.87-95.
- Back, W., 1966, Hydrochemical facies and ground-water flow in the Atlantic Coastal Plain: United States Geological Survey Professional Paper 498-A, 47p.
- Barr Engineering, 2005, Intercommunity groundwater protection: sustaining growth and natural resources in the Woodbury/Afton area: Report on development of a groundwater flow model for southern Washington County, Minnesota: Report to the Legislative Commission on Minnesota Resources, 66p.
- Barr Engineering, 2010, Evaluation of groundwater and surface-water interaction: guidance for resource assessment, Twin Cities Metropolitan Area, Minnesota: Prepared for Metropolitan Council, June 2010. 27p. plus GIS files.
<http://www.metrocouncil.org/environment/WaterSupply/gwswinteractionevaluation.htm> (Accessed August 17, 2011).
- Benischke, R., Goldschneider, N., and Smart, C., 2007, Tracer techniques: *in* N. Goldscheider, N., and Drew, D., eds., Karst Hydrogeology: International Association of Hydrogeologists, Taylor and Francis, London., 263p.
- Barrett, M.H., Hiscock, K.M., Pedley, S., Lerner, D.N., Tellam, J.H., and French, M.J., 1999, Marker species for identifying urban groundwater recharge sources; a review and case study in Nottingham UK: *Water Research* v.33, no. 14, p.3083–3097.
- Bradbury, K.R., Gotkowitz, M.B., Hart, D.J., Eaton, T.T., Cherry, J.A., Parker, B.L., and Borchardt, M.A., 2006, Contaminant transport through aquitards: technical guidance for aquitard assessment: American Water Works Research Foundation, IWA Publishing, 144p.
- Bradbury, K.R. and Runkel, A.C., 2011, Recent advances in the hydrostratigraphy of Paleozoic bedrock in the Midwestern United States: *GSA Today*, v. 21, no. 9, p.10-12.
- Burman, S., R., 1995, Pilot study for testing and refining an empirical groundwater sensitivity assessment methodology: Unpublished M.S. Thesis, University of Minnesota, 256p
- Camp, M.V. and Walraevens, K., 2008, Identifying and interpreting baseline trends, *in* Edmunds, W.M., and Shand. P., eds., *Natural Groundwater Quality*: Blackwell Publishing, Oxford England, p.441-462.

- Clark, J.F., Hudson, G.B., Davisson, M.L., Woodside, G. and Herndon, R., 2004, Geochemical Imaging of flow near an artificial recharge facility, Orange County, California: *Ground Water*, v. 42, no. 2, p.167-174.
- County Well Index – State water well database – Minnesota Department of Health, Minnesota Geological Survey. <http://www.health.state.mn.us/divs/eh/cwi/>.
- Dakota County, 2006, Dakota County Ambient Groundwater Quality Study, 1999-2003 Report, 108p.
<http://www.co.dakota.mn.us/NR/rdonlyres/00000697/voufacfgaabyefpolhbqfulqbvwywace/AmbientGroundwaterQualityStudy.pdf> (accessed May 5, 2012)
- Davis, S.N., Whittemore, D.O., and Fabryka-Martin, J., 1998, Uses of chloride/bromide ratios in studies of potable water: *Ground Water* v. 36, no. 2, p.338-350.
- Delin, G. and Woodward, D.G., 1984, Hydrogeologic setting and the potentiometric surfaces of regional aquifers in the Hollandale embayment, southeastern Minnesota, 1970-80: United States Geological Survey Water Supply Paper 2219, 56p.
- Dragon, K., and Gorski, J., 2009, Identification of hydrogeochemical zones in postglacial buried valley aquifer (Wielkopolska Buried Valley Aquifer, Poland): *Environmental Geology*, v. 58, p.859-866.
- Eckman, J., and Alexander, S.C., 2002, Ground-water chemistry and residence time, Regional Hydrogeologic Assessment Ottertail Area, West-Central Minnesota: Minnesota Department of Natural Resources Regional Hydrologic Assessment Series RHA-5, technical appendix to part B, 15 p.
- Edmunds, W.M., Fellman, E., Goni, I.B., and Prudhomme, C., 2002, Spatial and temporal distribution of groundwater recharge in northern Nigeria: *Hydrogeology Journal*, 2002, v. 10, p.205-215.
- Edmunds, W.M., and Shand, P., 2008, Natural ground-water quality – summary and significance for resources management: in Edmunds, W.M., and Shand, P., eds., *Natural Groundwater Quality*: Blackwell Publishing, Oxford England, p. 441-462.
- ESRI, 2012, Geodatabase storage: <http://www.esri.com/software/arcgis/geodatabase/data-storage.html> (accessed 5/31/2012).
- Fallon, J., and Chaplin, B. 2001, Chloride-related studies in streams and ground water of the Twin Cities metropolitan area, Minnesota, 1996-1998 – A summary of published and new results: United States Geological Survey, extended abstract, 3 p.
http://mn.water.usgs.gov/pubs/Chloride_abstract.pdf

- Fong, A.L., Andrews, W.J., and Stark, J.R., 1998, Water-quality assessment of part of the Upper Mississippi River Basin, Minnesota and Wisconsin -- Ground-water quality in the Prairie du Chien-Jordan aquifer, 1996: U.S. Geological Survey Water- Resources Investigations Report 98-4248, 45p.
- Freeman, J.T., 2007, The use of bromide and chloride mass ratios to differentiate salt-dissolution and formation brines in shallow groundwater of the western Canadian Sedimentary Basin: *Hydrogeology Journal*, v.15, no. 7, p.1377-1385.
- Glynn, P.D., and Plummer, L.N., 2005, Geochemistry and the understanding of groundwater systems: *Hydrogeology Journal*, v.13, p.263-287.
- Guler, C. and Thyne, G.D., 2006, Statistical clustering of major solutes: Use as a tracer for evaluating interbasin groundwater flow into Indian Wells Valley, California: *Environmental and Engineering Geoscience*, v.12, no. 1, p.53-65.
- Hall, C.W., Meinzer, O.E., and Fuller, M.L., 1911, Geology and underground waters of southern Minnesota: United States Geological Survey Water-Supply Paper 256, 406p.
- Hart, D.J., Bradbury, K.R., and Feinstein, D.T., 2006, The vertical hydraulic conductivity of an aquitard at two spatial scales: *Ground Water*, v.44, no.2, p.201-211.
- Held, I., Klinger, J., Wolf, L., and Hotzl, H., 2007, Direct measurements of exfiltration in a sewer test site in a medium-sized city in southwest Germany: *in* Ken W.F. Howard, ed., *Urban groundwater – meeting the challenge: Selected papers from the 32nd International Geological Congress (IGC), Florence, Italy, August 2004*, p.65-77.
- Helsel, D.R. and Hirsch, R.M., 2002, Statistical methods in water resources, chapter A3 in United States Geological Survey, Book 4, *Hydrologic Analysis and Interpretation*, <http://pubs.usgs.gov/twri/twri4a3/> (accessed 4/30/2012).
- Howard, K.W.F., and Maier, H., 2007, Road de-icing salt as a potential constraint on urban growth in the Greater Toronto Area, Canada: *Journal of Contaminant Hydrology*, v.91, nos.1-2, p.146-170.
- Huang, T. and Pang, Z., 2011, Estimating groundwater recharge following land-use change using chloride mass balance of soil profiles: a case study at Guyuan and Xifeng in the Loess Plateau of China: *Hydrogeology Journal*, v.19, p.177-186.
- Jirsa, M.A., Boerboom, T.J., Chandler, V.W., Mossler, J.H., Runkel, A.C. and Setterholm, D.R., 2011, *Geologic Map of Minnesota – Bedrock Geology: Minnesota Geological Survey State Map Series S-21. Scale 1:500,000.* <http://purl.umn.edu/101466>.

- Jurgens, B.C., McMahon, P.B., Chapelle, F.H., and Eberts, S.M., 2009, An Excel workbook for identifying redox processes in ground water, United States Geological Survey Open File Report 2009-1004, 15 p.
- Kanivetsky, R., 1986, Major-constituent chemistry of selected Phanerozoic aquifers in Minnesota: Minnesota Geological Survey Miscellaneous Map Series M-61.
- Kelly, W.R., 2008, Long-term trends in chloride concentrations in shallow aquifers near Chicago: *Ground Water*, v.46, no.5, p.772-781.
- Kendall, C., 2005, Isotope hydrology workshop: Minnesota Ground Water Association Fall Conference, November 18, 2005, Continuing Education and Conference Center, St. Paul, Minnesota, copy on file at Minnesota Geological Survey.
- Larson-Hidgem, D., Larson, S.P., Norvitch, R.F., 1975, Configuration of the water table and distribution of downward leakage to the Prairie du Chien-Jordan aquifer in the Minneapolis-St. Paul metropolitan area, Minnesota: U.S. Geological Survey Open-File Report 75-342, 33p.
- Lee, K.E., Yaeger, C.S., Jahns, N.D., and Schoenfuss, H.L., 2008, Occurrence of endocrine active compounds and biological responses in the Mississippi River—study design and data, June through August 2006: U.S. Geological Survey Data Series 368, 27 p. with Appendix.
- Lerner, D.N., 2002, Identifying and quantifying urban recharge: a review: *Hydrogeology Journal*, v.10, p.143-152.
- Lively, R.S., Jameson, R., Alexander, E.C. Jr., and Morey, G.B., 1992, Radium in the Mt. Simon-Hinckley aquifer, east-central and southeastern Minnesota: Minnesota Geological Survey Information Circular IC-36, 58p.
- Lusardi, B.A. and Tipping, R.G., 2006, Quaternary Stratigraphy, pl 4 of Setterholm, D.R., project manager, Geologic Atlas of Scott County, Minnesota. Minnesota Geological Survey County Atlas C-17.
- Lusardi, B. and Tipping, R.G., 2009, Quaternary Stratigraphy and Sand Distribution Model, pl.4 of Bauer, E.J., project manager, Geologic Atlas of Carver County, Minnesota. Minnesota Geological Survey County Atlas C-21, Part A.
- Maderak, M.L., 1963, Quality of waters, Minnesota: a compilation, 1955-1962: State of Minnesota, Minnesota Conservation Department, Bulletin 21, St. Paul, MN, 104p.
- Marsh, R., 1996, Groundwater chemistry and recharge estimation using environmental tritium: Anoka County, Minnesota. Anoka County Community Health and

- Environmental Services Department. Prepared under An Agricultural Preservation and Conservation Awareness Grant. 62p.
- Marsh, R., 2001, Hydrogeology of the buried drift aquifers: Anoka County, Minnesota. Anoka County Community Health and Environmental Services Department. Prepared under An Agricultural Preservation and Conservation Awareness Grant. 44p.
- Matter, J.M., Waber, N.H., Loew, S., and Matter, A., 2005, Recharge areas and geochemical evolution of groundwater in an alluvial aquifer system in the Sultanate of Oman: *Hydrogeology Journal*, v. 14, p.203-244.
- Mattle, N., Kinzelback, W., Beyerly, U., Huggenberger, P., Loosli, H.H., 2000, Exploring an aquifer system by integrating hydraulic, hydrogeologic and environmental tracer data in a three dimensional hydrodynamic transport model: *Journal of Hydrology*, v. 242, p.183-196.
- Mazor, E., 2004, *Chemical and Isotopic Groundwater Hydrology*, 3rd ed., Marcel Dekker, Inc., New York, Basel, 453p.
- Mendizabal, I., Stuyhfzand, P.J., and Wiersma, A.P., 2011, Hydrochemical system analysis of public supply well fields, to reveal water-quality patterns and define groundwater bodies: the Netherlands: *Hydrogeology Journal*, v. 19, p.83-100.
- Metropolitan Council, 2010, Summary of 2010 census data, <http://stats.metc.state.mn.us/stats/pdf/Population2010.pdf> (Accessed April 14, 2012).
- Metropolitan Council, 2012. Metro Model 2, <http://www.metrocouncil.org/environment/WaterSupply/metrogroundwatermodel.htm> (Accessed May 31, 2012)
- Meyer, G.N., 2007, Surficial Geology of the Twin Cities metropolitan area, Minnesota: Minnesota Geological Survey Miscellaneous Map M-178, scale 1:125,000.
- Meyer, G.N., 2010, Quaternary Stratigraphy, pl 4 of Runkel, A.C., project manager, Geologic atlas of Chisago County, Minnesota. Minnesota Geological Survey County Atlas C-22, Part A.
- Meyer, G. and Tipping, R.G., 1998, Digital elevation models of tops and bottoms of four tills within Washington County, Minnesota: Minnesota Geological Survey, Unpublished Manuscript Maps, Scale 1:50,000, eight digital files.
- Meyer, G.N. and R.G. Tipping, 2007, Geology in support of ground-water management for the Twin Cities Metropolitan Area, Metropolitan Council Water Supply Master Plan Development – Phase I: Minnesota Geological Survey Open File Report OF07-02, 48p.

- Minnesota Department of Health, 2004, Public health assessment: Baytown Township groundwater contamination site. Prepared by: Minnesota Department of Health Under Cooperative Agreement with the, Agency For Toxic Substances And Disease Registry, <http://www.health.state.mn.us/divs/eh/hazardous/sites/washington/baytown/baytownpha.pdf>, 86 p. (accessed April 11, 2012).
- Minnesota Department of Health, 2008, Public Health Assessment: Perflourochemical contamination in Lake Elmo and Oakdale, Washington County Minnesota, EPA Facility ID: MND980704738 and MND980609515. Prepared by: Minnesota Department of Health Under Cooperative Agreement with the U.S. Department of Health and Human Services, Agency for Toxic Substances and Disease Registry. <http://www.health.state.mn.us/divs/eh/hazardous/sites/washington/lakeelmo/phaelmoaokdale.pdf> (accessed April 11, 2012).
- Minnesota Department of Health, 2010, Perfluorochemical data for portions of Washington and Ramsey and Dakota Counties, Minnesota. (MDH, written communication).
- Minnesota Department of Health, 2011, Assessment monitoring pilot study, December, 2011. 61 p. (MDH, written communication).
- Minnesota Department of Health and Minnesota Geological Survey, 2012, The County Well Index, <http://www.mngeo.state.mn.us/chouse/metadata/cwi.html> (accessed 5/31/2012).
- Minnesota Department of Natural Resources, 1991, Criteria and Guidelines for Assessing Geologic Sensitivity of Ground Water Resources in Minnesota. St. Paul, Minnesota.
- Minnesota Department of Natural Resources, 2011, AVSWUDS.ZIP, Water appropriation installation locations, reported pumping data for 1988-2010, file created August 5, 2011. Water Appropriations Permit Program http://www.dnr.state.mn.us/waters/watermgmt_section/appropriations/wateruse.html (accessed August 10, 2011).
- Minnesota Pollution Control Agency. 1998a. Nitrate in Minnesota Ground Water – A GWMAP Perspective. St. Paul, Minnesota. <http://www.pca.state.mn.us/index.php/view-document.html?gid=6350> (accessed May 25, 2012)
- Minnesota Pollution Control Agency. 1998b. Data Analysis Protocol for the Ground Water Monitoring and Assessment Program. St. Paul, Minnesota. <http://www.pca.state.mn.us/index.php/view-document.html?gid=6384> (accessed May 25, 2012).

- Minnesota Pollution Control Agency. 2000a. Ground Water Quality under Three Unsewered Subdivisions in Minnesota. St. Paul, Minnesota. <http://www.pca.state.mn.us/index.php/view-document.html?gid=6339> (accessed May 25, 2012).
- Minnesota Pollution Control Agency. 2000b. Ground Water Quality in Cottage Grove, Minnesota. St. Paul, Minnesota. <http://www.pca.state.mn.us/index.php/view-document.html?gid=6338> (accessed May 25, 2012).
- Minnesota Pollution Control Agency, 2002, Ground Water Quality beneath Twin Cities Metropolitan Communities Served by Individual Sewage Treatment Systems. Prepared by the Minnesota Pollution Control Agency and Metropolitan Council, <http://www.pca.state.mn.us/index.php/view-document.html?gid=6332> (accessed May 25, 2012).
- Minnesota Pollution Control Agency, 2010. GWMAP data, (MPCA, written communication).
- Moran, J.E., Beller, H.R., Leif, R., and Singleton, M.J., 2006, Fate and Transport of Wastewater Indicators: Results from Ambient Groundwater and from Groundwater Directly Influenced by Wastewater, 2006: Lawrence Livermore National Laboratory, Technical Report UCRL-TR-222531, 66p.
- Morris, B.L., Darling, W.G., Goody, D.C., Litvak, R.G., Neumann, I., Nemaltseva, E.J., Poddubnaia, I., 2005, Assessing the extent of induced leakage to an urban aquifer using environmental tracers: an example from Bishkek, capital of Kyrgyzstan, Central Asia: *Hydrogeology Journal* v.14, p.225-243.
- Mossler, J.H., 2008, Paleozoic stratigraphic nomenclature for Minnesota: Minnesota Geological Survey Report of Investigations 65, 84 p.
- Mossler, J.H. and Tipping, R.G., 2000, Bedrock geology and structure of the seven-county Twin Cities metropolitan area, Minnesota: Minnesota Geological Survey, Miscellaneous Map series M-104.
- Mullaney, J.R., Lorenz, D.L., and Arntson, A.D., 2009, Chloride in groundwater and surface water in areas underlain by the glacial aquifer system, northern United States: United States Geological Survey Scientific Investigations Report 2009-5086, 41p.
- Nemetz, D.A., 1993, The geochemical evolution of ground water along flowpaths in the Prairie du Chien-Jordan aquifer of southeastern Minnesota, Unpublished M.S. Thesis, University of Minnesota, 182p.

- Novotny, E., Murphy, D., and Stefan, H., 2007, Road salt effects on water quality of lakes in the Twin Cities metropolitan Area. Project Report No. 505, St. Anthony Falls Laboratory, University of Minnesota, prepared for the Local Road Research Board (LRRB) Minnesota Department of Transportation, 53p.
- Panno, S.V., Hackley, K.C., Hwang, H.H., Greenburg, S.E., Krapec, I.G., Landsberger, S., and O'Kelly, D.J., 2006, Characterization and identification of Na-Cl sources in ground water, *Ground Water* v.44, no.2, p.176-187.
- Plummer, L.N., Bexfield, L.M., Anderholm, S.K., Sanford, W.E., Busenberg, E., 2004, Hydrochemical tracers in the middle Rio Grande Basin, U.S.A., 1. Conceptualization of groundwater flow: *Hydrogeology Journal* v.12, p.259-388.
- Ross, M., Parent, M., and Lefebvre, R., 2005, 3D geologic framework models for regional hydrogeology and land-use management: a case study from a Quaternary basin of southwestern Quebec, Canada: *Hydrogeology Journal* v.13, p.690-707.
- Ruhl, J.F., Kanivetsky, Roman, and Shmagin, Boris, 2002, Estimates of recharge to unconfined aquifers and leakage to confined aquifers in the seven-county metropolitan area of Minneapolis-St. Paul, Minnesota: U.S. Geological Survey Water-Resources Investigations Report 02-4092, 32p.
- Runkel, A.C., Tipping, R.G., Alexander, E.C., Jr., Green, J.A., Mossler, J.H., and Alexander, S.C., 2003, Hydrogeology of the Paleozoic bedrock in southeastern Minnesota: Minnesota Geological Survey Report of Investigations 61, 105p., 2 plates
- Runkel, A.C., Tipping, R.G., Alexander, E.C. Jr., Alexander, S.C., 2006, Hydrostratigraphic characterization of intergranular and secondary porosity in part of the Cambrian sandstone aquifer system of the cratonic interior of North America: Improving predictability of hydrogeologic properties: *Sedimentary Geology*, v.184, p.281-304.
- Sabel, G., 1985, An appraisal of Minnesota's ground water quality: Minnesota Pollution Control Agency – Ground Water Quality Monitoring Program, 55p. plus appendices.
- Sander, A., Novotny, E., Mohseni, O., and Stefan, H., 2007, Inventory of road salt uses in the Minneapolis/St. Paul metropolitan area: St. Anthony Falls Laboratory, Project Report 503, Prepared for the Minnesota Department of Transportation, 45p.
- Sanocki, C.A., Langer, S.K., and Menard, J.C., 2009, Potentiometric surfaces and changes in groundwater levels in selected bedrock aquifers in the Twin Cities Metropolitan Area, March–August 2008 and 1988–2008: United States Geological Survey Scientific Investigations Report 2009–5226, 76p.

- Sanford, W.E., Plummer, L.N., McAda, P., Bexfield, L.M., and Anderholm, S.K., 2004, Hydrochemical tracers in the middle Rio Grande Basin, USA: 2. Calibration of a groundwater-flow mode: *Hydrogeology Journal*, v.12, p.389-407.
- Sanford, W.E., Aeschbach-Hertig, W., Herczeg, A.L., 2011, Insights from environmental tracers in groundwater systems: *Hydrogeology Journal*, v.19, p.1-3.
- Scanlon, B.R., 2010, Chemical tracer methods, chapter 7 in Healy, R.W., 2010, Estimating groundwater recharge. Cambridge University Press, Cambridge, United Kingdom, 245p.
- Scanlon, B.R., Healy, R.W., and Cook, P.G., 2002, Choosing appropriate techniques for quantifying groundwater recharge: *Hydrogeology Journal* v.10, p.18-39.
- Shapiro, A.M., 2011, The challenge of interpreting environmental tracer concentrations in fractured rock and carbonate aquifer:, *Hydrogeology Journal*, v.19., p.9-12
- Smith, S.E., and Nemetz, D.A., 1996, Water quality along selected flowpaths in the Prairie du Chien-Jordan aquifer, southeastern Minnesot:, U.S. Geological Survey Water-Resources Investigations Report 95-4115, 76p.
- Stark, J.R., Hanson, P.E., Goldstein, R.M., Fallon, J.D., Fong, A.L., Lee, K.E., Kroening, S.E., and Andrews, W.J., 2001, Water quality in the Upper Mississippi River Basin, Minnesota, Wisconsin, South Dakota, Iowa, and North Dakota, 1995-1998: U.S. Geological Survey Circular 1211, 34p.
- Subyani, A.M., 2004, use of chloride-mass balance and environmental isotopes for evaluation of groundwater recharge in the alluvial aquifer, Wadi Tharad, western Saudi Arabia: *Environmental Geology*, v.46, p.741-749.
- Swanson, S.K., Bahr, J.M., Schwarz, M.T., and Potter, K.W., 2001, Two-way cluster analysis of geochemical data to constrain spring source waters: *Chemical Geology*, v.179, p.73-91.
- Swanson, S.K., Bahr, J.M., Bradbury, K.R., and Anderson, K.M., 2006, Evidence for preferential flow through sandstone aquifers in southern Wisconsin: *Sedimentary Geology*, v.184, p.331-342.
- Swanson, S.K., 2007, Lithostratigraphic controls on bedding-plane fractures and the potential for discrete groundwater flow through a siliciclastic sandstone aquifer, southern Wisconsin: *Sedimentary Geology* v.197, pp.65-78.
- Suk, H., and Lee, K.K., 1999, Characterization of a ground water hydrochemical analysis: clustering into ground water zones: *Ground Water*, v.37, no.3, p.358-366.

- Taylor, R.G., Cronin, A.A., Lerner, D.N., Tellam, J.H., Bottrell, S.H., Rueeki, J., and Barrett, M.H., 2006, Hydrochemical evidence of the depth of penetration of anthropogenic recharge in sandstone aquifers underlying two mature cities in the UK: *Applied Geochemistry*, v.2, no.9, p.1570-1592.
- Tipping, R.G., 1992, An isotopic and chemical study of groundwater flow in the Prairie du Chien and Jordan Aquifers, unpublished M.S. Thesis, University of Minnesota, 117p.
- Tipping, R.G., 1994, Southeastern Minnesota regional ground water monitoring study, a report to the Southeast Minnesota Water Resources Board: Minnesota Geological Survey Open File Report 94-1, 117p.
- Tipping, R.G., Runkel, A.C., Alexander, E.C., Jr., Alexancer, S.C., and Green, J.A., 2006, Evidence for hydraulic heterogeneity and anisotropy in the mostly carbonate Prairie du Chien Group, southeastern Minnesota, USA,. *Sedimentary Geology*, v.184, p.305-330.
- Tipping, R.G., Runkel, A.C. and Gonzalez, C.M., 2010, Geologic investigation for portions of the Twin Cities Metropolitan Area: I. Quaternary/bedrock hydraulic conductivity, II. Groundwater chemistry: Informal report delivered to the Metropolitan Council for Metropolitan Council Water Supply Master Plan Development, 62 p.
- U.S. Geological Survey, 2010, National Water Inventory System, <http://waterdata.usgs.gov/nwis> (accessed June 29, 2010).
- Vazquez-Sune, E., Sanchez-Vila, X., and Carrera, J., 2005, Introductory review of specific factors influencing urban groundwater, an emerging branch of hydrogeology, with reference to Barcelona, Spain: *Hydrogeology Journal* v.13, p.522-533
- Walsh, J.F. 1992. Tritium in groundwater as a tool to estimate well vulnerability. Minnesota Department of Health. 128 p.
- Weissmann, G.S., Zhang, Y., LaBolle, E.M., and Fogg, G.E., 2002, Dispersion of groundwater age in an alluvial aquifer system: *Water Resources Research*, v.38, no.10, 1198, doi:10.1029/2001WR00907.
- Wenck and Associates, Inc., 1997, Phase II: Detailed site investigation report and Phase II workplan for the hydrogeologic investigation of the proposed Red Wing ash disposal facility expansion: 36p.
- Wilcoxon, F. 1945, Individual comparisons by ranking methods, *Biometrics Bulletin*, v.1, no.6, p.80-83.

- Wolf, L., and Hotzl, H., 2006, Upscaling of laboratory results on sewer leakage and the associated uncertainty, *in* Ken W.F. Howard, ed. Urban groundwater – Meeting the Challenge. London, Taylor and Francis, p.79-94 (IAH selected paper series).
- Woocay, A., 2008, Groundwater hydrochemical facies, flowpaths and recharge determined by multivariate statistical, isotopic and chloride mass-balance methods, Ph.D., The University of Texas at El Paso, 152 p.
- Woodward, D, 1986, Hydrogeologic framework and properties of regional aquifers in the Hollandale Embayment, southeastern Minnesota: U.S Geological Survey HA -677.
- Zhang, P., Johnson, W., Piana, M.J., Fuller, C.C., and Naftz, D.L., 2001, Potential artifacts in interpretation of differential breakthrough of colloids and dissolved tracers in the context of transport in a zero-valent iron permeable reactive barrier: Ground Water, v.39, no.6, p.831-840.
- Zuber, A. Witczak, S., Roznaski, K., Sliwka, I., Opoka, M., Mochalski, P., Kuc, T., Karlikowska, J., Kania, J., Jackowicz-Korczynski, M., and Dulinski, M., 2005, Groundwater dating with ^3H and SF_6 in relation to mixing patterns, transport modeling and hydrochemistry: Hydrological Processes, v.19, p.2247-2275

APPENDICIES

Appendix A. Methods for determining the distribution and hydraulic characteristics of subsurface unconsolidated materials.

In this investigation, vertical hydraulic conductivity values for unconsolidated materials are based on their textural distribution from the land surface to the bedrock surface. Subsurface mapping of unconsolidated deposits is not continuous across the Twin Cities metropolitan area (Figure 38). As a result, the compilation of subsurface Quaternary textures presented here is a hybrid of detailed subsurface mapping based on cross sections, and interpolation of textures from the state water well database – the County Well Index (CWI).

Although the methods for detailed subsurface mapping have changed with time, the basic approach is the same. Subsurface materials are mapped in three dimensions by evaluating well records and cuttings, rotosonic core and textural analyses, within the context of stratigraphic order and conditions of deposition. To clarify textural descriptions in this report, the term *fine-grained materials* is used to describe clay loam to sandy loam basal tills, but can include lacustrine deposits composed of laminated fine sand, silt and clay; the term *coarse-grained materials* is used to describe sand and gravel glacio-fluvial deposits, including ice contact, valley train, subglacial and outwash deposits; the term *mixed fine and coarse-grained materials* is used to describe textures found in ice stagnation zones and other conditions resulting in a complex mixture of the two. Digital elevation models of the tops and bottoms of stratigraphic units produced by

subsurface mapping were used in this investigation to delineate subsurface textures in these mapped areas shown on Figure 38.

Within the TCMAx, areas with no Quaternary subsurface mapping include Dakota, Ramsey, Isanti and portions of Hennepin County. Subsurface mapping is currently underway as part of the Wright and Sherburne geologic atlases, but are not completed at this time. In order to determine the distribution of subsurface textures in these areas, interpolation methods were used modified from those earlier geologic atlases were used (e.g. Meyer et al., 1995). With this approach, stratigraphic records from water wells are coded based on primary lithology into three generalized textural categories of fine-grained, coarse-grained, or a mixture of fine and coarse-grained. In driller's records, these intervals are typically referred to as clay, sand/gravel, and sandy clay/clayey sand. The stratigraphic record is then resampled into equal 10 foot elevation intervals. Two-dimensional interpolation using ordinary kriging is used to determine the likelihood of each category for a given elevation interval.

Two-dimensional, rather than three-dimensional interpolation is used, based on the premise that glacial deposits have undergone minimal structural deformation since their deposition, and that correlation is optimized by evaluating data at equal elevations. Interpolated results for each elevation interval are merged to into a single dataset to create a three-dimensional model for each of the three textural types.

In order to combine textural datasets from subsurface mapping and the interpolated model, a matrix of points between the land surface and bedrock surface was created, spaced 250 meters apart in the horizontal direction and 20 feet apart in the

vertical direction, herein referred to as gridpoints. The size was chosen to cover the TCMAx at a scale that can be reasonably managed on a desktop computer. A range of vertical hydraulic conductivities (K_v) were assigned each gridpoint, based on its location within mapped Quaternary stratigraphic layers. Where subsurface mapping does not exist, a range of values were assigned based on interpolated model results. If neither of these sources were available for a given gridpoint, a null value was assigned. A final adjustment to assigned K_v values was made based on depth. If the gridpoint is within 20 feet of the land surface (upper-most gridpoint) it texture-derived hydraulic conductivity was assigned based on the current 1:200,000 scale surficial geologic map of the Twin Cities metropolitan region (Meyer, 2007). If the gridpoint is greater than 60 feet in depth from the land surface, its assigned range of hydraulic conductivity is two orders of magnitude less than the values assigned to a similar texture in the upper 60 feet. Textures and assigned ranges of hydraulic conductivities are included in Table 3. These estimates are based on a regional compilation of hydraulic conductivity measurements for glacial deposits, conducted at a wide range of scales (Tipping et al., 2010). Methods for gridpoint assignment are illustrated on Figure 39.

In addition to hydraulic conductivities, gridpoints contain attributes on texture, texture source (subsurface mapping or interpolated model), Quaternary stratigraphic unit if mapped, surficial map unit, and unique identifiers for the six neighboring points. The latter is included to facilitate finite difference modeling.

For travel time calculations, a single “composite” K_v was assigned to each gridpoint based on the following hierarchy. If no other texture estimate was available,

K_v was assigned based on texture from interpolated model. These K_v's were replaced by texture-based K_v's from subsurface mapping, which in turn were replaced by texture-based K_v's from the surficial map (upper 20 feet only). After these assignments were made, if a single column of gridpoints from the land surface to the bedrock surface had texture-derived K_v's for more than 40 percent of its points, the remaining blanks were assigned an intermediate value 10.05 ft/day; if less than 40 percent had texture-derived K_v's, the remaining blanks had no value assigned.

A second dataset was created to summarize subsurface conditions for each XY location within gridpoints, herein referred to as XY locations. This dataset contains information on: what percent of the subsurface is represented, either by subsurface and surface mapping or interpolation, by a texture attribute and associated K value; regional water table surface elevation; bedrock potentiometric surface elevation; and top of bedrock elevation.

For each XY location with greater than 40 percent of its subsurface gridpoint textures represented by mapping or interpolation, arithmetic, geometric and harmonic mean K_v values were calculated. This calculation was done both for points from water table elevation to the bedrock surface and from the water table elevation to the land surface, and are referred to as "K_{v_sat}" and "K_{v_unsat}" respectively in dataset XY locations. K_{v_sat} values based on harmonic mean of each composite K_v for a given XY location are shown on Figure 6. Field descriptions for datasets gridpoints and XY locations are included in Appendix D.

Hydraulic Gradient

Hydraulic head differences used to establish a hydraulic gradient between the water in upper, unconsolidated deposits and water in bedrock aquifers were determined using raster calculations. The regional water table raster surface was constructed to help evaluate the impact of pumping on surface water bodies at a regional scale (Barr, 2010). By design, it is well suited for this investigation, by providing generalized regional elevations of saturated conditions, without including zones of perched groundwater systems. Main sources of data sources for the regional water table surface are Minnesota Department of Natural Resources observation well network for water table wells, the County Well Index (CWI), and data from site specific studies. Results from regional groundwater flow models and surface-water elevations for reaches of some streams known to be gaining were also used as a control, particularly where data from other sources were sparse (Barr, 2010).

The regional bedrock potentiometric raster surface is a combination elevations from contoured synoptic water level measurements in the Prairie du Chien Group and Jordan Sandstone (Sanocki et al., 2009) and contoured water levels from the County Well Index for upper-most bedrock aquifers where the Prairie du Chien and Jordan are not present. The resultant bedrock potentiometric surface is meant to provide generalized bedrock hydraulic head data for flow systems most directly connected to activities at the land surface.

The regional water table and bedrock potentiometric surfaces are generalized surfaces both spatially and temporally. Both surfaces are based, in part, on measurements

from CWI, taken most often at the date of installation, spanning all seasons over many decades. Filtering and data processing and final cross-validation of the water table CWI dataset resulted in values dropped with absolute residuals 20 feet or greater (Barr, 2010). Error for both regional water table surface and the bedrock potentiometric surface elevations are estimated to be at a minimum +/- 20 feet in areas based solely on data from CWI. Water table data from the DNR's observation well network are based on reliable measurements, but are subject to seasonal variations not included in this model. Bedrock water level data from 2008 synoptic water level measurements provide data that is temporally consistent across the metro area. Measurements were taken in March and August of 2008, and provide information on seasonal changes in hydraulic head within bedrock aquifers.

Subtracting the bedrock potentiometric surface from the regional water table surface produced negative values over much of the TCMAX. Many of these areas were focused on the major rivers, where upward discharge of bedrock aquifers is reflected in expected negative values. In other areas, it is less clear whether actual artesian conditions exist, or where uncertainty in the surface values produces overlap. For the purposes of travel time calculations, areas with negative values near major discharge areas, or areas where CWI records indicate flowing (artesian) bedrock wells were identified and are shown on the vertical recharge map. Outside of these areas, bedrock potentiometric surface elevations greater than the regional water table were lowered to one-half foot below the regional water table.

Subtraction of the adjusted bedrock potentiometric surface from the regional water table surface reveals seasonal changes in bedrock hydraulic head (Figure 24). Synoptic measurements taken in August 2008 show a broadening and deepening of hydraulic head in the central metropolitan area when compared to March 2008 measurements. The cause of this change is likely increased high capacity pumping in response to increased summer demand.

The hydraulic gradient between the regional water table and bedrock aquifers was determined by dividing the difference in hydraulic head by the vertical distance from the water table to the bedrock surface (Figure 8). Perched conditions in the central metropolitan area are present within and above the Plattville Formation; in places, the St. Peter Sandstone is partially unsaturated below it. These conditions invalidate the use of a Darcy flux- based calculation to estimate travel time from the water table to the Prairie du Chien Group and Jordan Sandstones. Although unsaturated conditions within glacial sediment are known to occur under the regional water table surface, the unconsolidated deposits below the regional water table were considered to be fully saturated for the travel-time calculation.

Calculation of vertical travel times

Vertical travel times were calculated as follows:

$$T = L / ((K_v * 365_{\text{days}} * (\Delta h / L)) / n)$$

$$= L^2 n / (365_{\text{days}} * K_v * \Delta h)$$

T = vertical time of travel in years

L = distance from regional water table to bedrock surface, in feet

K_v = bulk vertical hydraulic conductivity in feet/day

for saturated conditions: mean value of gridpoints from water table to bedrock surface

Δh = difference in elevation between regional water table and bedrock potentiometric surfaces in feet. (vertical hydraulic head gradient = $\Delta h / L$)

n = effective porosity, set equal to 0.20

Time of travel estimates were calculated for arithmetic, geometric and harmonic means for saturated conditions, and are included in the XY location dataset.

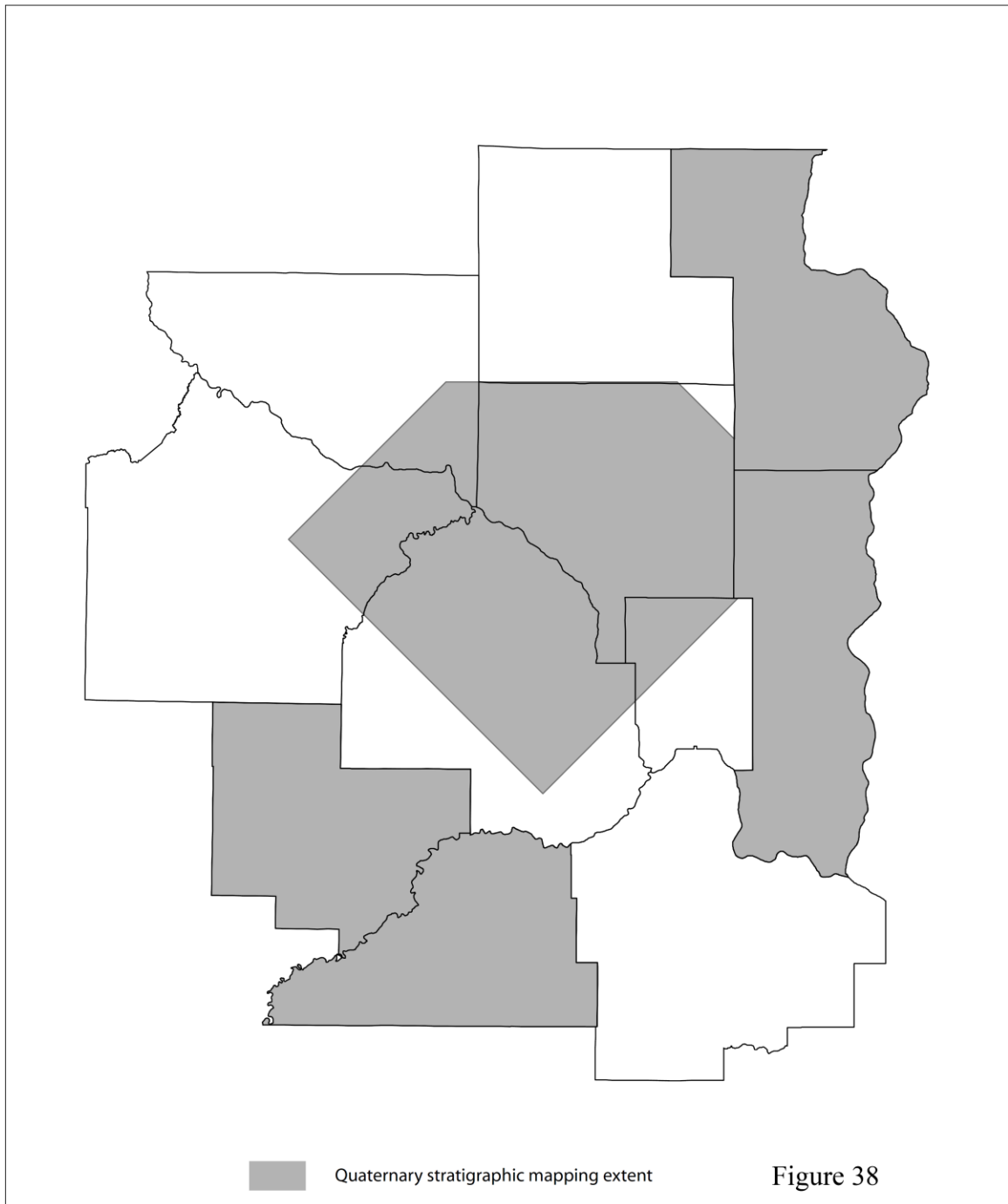


Figure 38. Eleven county extended TCMAx showing areas where subsurface Quaternary stratigraphy has been mapped. (Meyer and Tipping, 1998; Lusardi and Tipping, 2006; Meyer and Tipping, 2007; Lusardi and Tipping, 2009; Meyer, 2010)

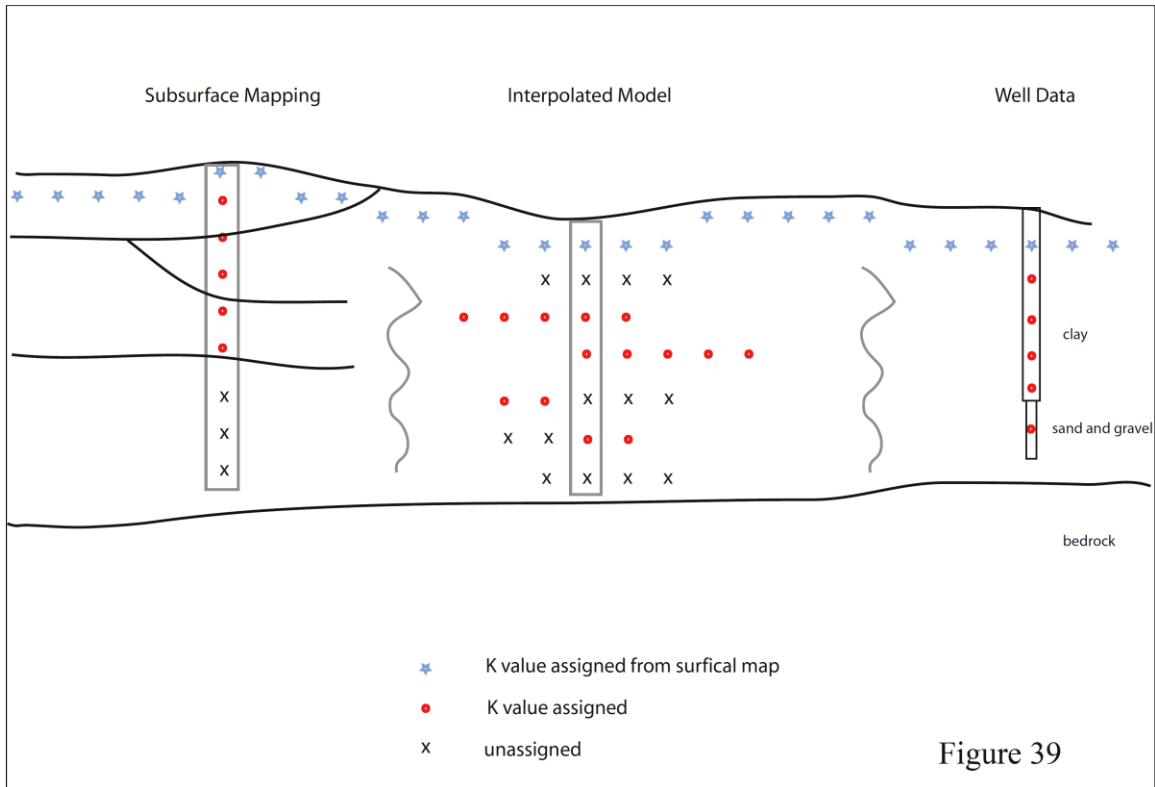


Figure 39. Schematic drawing of Quaternary points model. Columns of points where less than 40 percent of the column can be assigned texture- and depth-based range of hydraulic conductivities were left out of the final time of travel calculation.

Appendices B-D. GIS and supporting data included in supplemental files.

Appendix B. Point data geodatabase structure.

Geodatabase Name: PointData.mdb (personal geodatabase)

Spatially enabled data tables

Name	Description
C_complete	Water chemistry, complete dataset. 1 row for each sample event
C_indx	Water chemistry, index summary data, linked to subsets of C_complete (tables with name beginning 'Csub') by field "relate_date"

Subset data tables

Name	Description
Csub_age	Subset of water chemistry containing interpreted age and supporting data
Csub_agency_program	Subset of water chemistry containing agency and program information associated with water sample
Csub_field_parameters	Subset of water chemistry containing field parameter data
Csub_goodchargebalance	Subset of water chemistry containing samples with charge balance error less than 5%
Csub_isotopes	Subset of water chemistry containing samples with stable or radiogenic isotope data
Csub_majorcations_anions	Subset of water chemistry containing major cation and anion data. Strontium, barium, and choride concentrations included here because of their use for data interpretation.
Csub_PFCs	Subset of water chemistry containing PFC data from Washington County and portions of Ramsey and Dakota County, assembled by the Minnesota Department of Health

Lookup tables

Name	Description
xAGENCY	Corresponds to field "agency," code specifies agency or organization that administers program under which data was collected or managed: C02 Anoka County C19 Dakota County C82 Washington County DNR MN Department of Natural Resources

	<p>DOT MN Department of Transportation</p> <p>MDA MN Department of Agriculture</p> <p>MDH MN Department of Health</p> <p>METC Metropolitan Council</p> <p>MWCC Metropolitan Waste Control Commission</p> <p>PCA Mn Pollution Control Agency</p> <p>UMN University of Minnesota</p> <p>USEPA U.S. Environmental Protection Agency</p> <p>USGS United States Geological Survey</p>
xDATA_REFERENCE	Corresponds to field "agency_prg," which is a concatenation of fields "agency" and "program." For water chemistry data, this field uniquely identifies source of agency/program that collected or managed the data:
xDEPTH_MC	<p>Corresponds to field "depth_mc," code specifies method used to establish depth of borehole or well:</p> <p>EST Estimated from cross section or other</p>
xELEV_MC	<p>Corresponds to field "elev_mc," code specifies method used to establish land surface elevation of sample/test location:</p> <p>A Altimeter (+/- 1 foot)</p> <p>G GPS (Global Positioning System / satellite)</p> <p>H GPS >12M (> +- 40')</p> <p>I GPS 3-12M (+- 10-40')</p> <p>J GPS 1-3M</p> <p>K GPS <= 1M</p> <p>RV report value</p> <p>S Surveyed</p> <p>T 7.5 minute topographic map (+/- 5 feet)</p> <p>T2 Calc from DEM (USGS 7.5 min or equiv.)</p>

	T3 Calc from County 2 ft. DEM																				
<p>xGCMCODE</p> <p>Corresponds to field "gcm_code," code specifies method used to establish sample/test location:</p> <p>A Digitized - scale 1:24,000 or larger</p> <p>A** Digitized from Washington Co. 1/2 section maps, verified by County Survey GPS</p> <p>B Digitized - scale 1:100,000 to 1:24,000</p> <p>DS1 Digitization (Screen) - Map (1:24,000)</p> <p>DS2 Digitization (Screen) - Map (1:12,000)</p> <p>G3 GPS Differentially Corrected</p> <p>G6A GPS SA On (averaged)</p> <p>G6O GPS SA Off (averaged)</p> <p>I GPS; accuracy 3 to 12 meters (+ 6 to 40 feet)</p> <p>PQ6 Public Land Survey - QQQQQ Section</p> <p>RD From report description (estimated error +/- 1000 m)</p> <p>SM digitized from georeferenced site map, accuracy unknown</p> <p>SPL</p> <p>UNK Unknown method</p>																					
<p>xPROGRAM</p> <p>Corresponds to field "program," code specifies which program within a given agency collected the data:</p> <table border="1"> <thead> <tr> <th><i>Program</i></th> <th><i>Agency Description</i></th> </tr> </thead> <tbody> <tr> <td>ACHES</td> <td>C02 Anoka County Community Health And Environmental Services</td> </tr> <tr> <td>CGA</td> <td>MGS Minnesota Geological Survey County Geologic Atlas Part A</td> </tr> <tr> <td>CMTS_RA</td> <td>MGS MGS-UMN Mt. Simon Aquifer Radium Study</td> </tr> <tr> <td>DNEM_MS</td> <td>UMN University Of MN - David Nemetz M.S. Thesis (1993)</td> </tr> <tr> <td>DOW</td> <td>DNR Dept. of Natural Resources Division Of Waters</td> </tr> <tr> <td>EM</td> <td>CO19 Dakota County Environmental Management</td> </tr> <tr> <td>ES</td> <td>METC Metropolitan Council Environmental Services</td> </tr> <tr> <td>GWM_04-08</td> <td>MPCA PCA Groundwater Monitoring & Assessment Program, Ambient Data 2004-2008</td> </tr> <tr> <td>GWM_92-96</td> <td>MPCA PCA Groundwater Monitoring & Assessment Program, Baseline Data 1992-1996</td> </tr> </tbody> </table>	<i>Program</i>	<i>Agency Description</i>	ACHES	C02 Anoka County Community Health And Environmental Services	CGA	MGS Minnesota Geological Survey County Geologic Atlas Part A	CMTS_RA	MGS MGS-UMN Mt. Simon Aquifer Radium Study	DNEM_MS	UMN University Of MN - David Nemetz M.S. Thesis (1993)	DOW	DNR Dept. of Natural Resources Division Of Waters	EM	CO19 Dakota County Environmental Management	ES	METC Metropolitan Council Environmental Services	GWM_04-08	MPCA PCA Groundwater Monitoring & Assessment Program, Ambient Data 2004-2008	GWM_92-96	MPCA PCA Groundwater Monitoring & Assessment Program, Baseline Data 1992-1996	
<i>Program</i>	<i>Agency Description</i>																				
ACHES	C02 Anoka County Community Health And Environmental Services																				
CGA	MGS Minnesota Geological Survey County Geologic Atlas Part A																				
CMTS_RA	MGS MGS-UMN Mt. Simon Aquifer Radium Study																				
DNEM_MS	UMN University Of MN - David Nemetz M.S. Thesis (1993)																				
DOW	DNR Dept. of Natural Resources Division Of Waters																				
EM	CO19 Dakota County Environmental Management																				
ES	METC Metropolitan Council Environmental Services																				
GWM_04-08	MPCA PCA Groundwater Monitoring & Assessment Program, Ambient Data 2004-2008																				
GWM_92-96	MPCA PCA Groundwater Monitoring & Assessment Program, Baseline Data 1992-1996																				

	<p>LCMROPDC MGS Sampling For LCMR Prairie Du Chien Hydrogeology Project</p> <p>METC_NW1 MGS Sampling For Metropolitan Council Phase I Study</p> <p>NAWQA USGS USGS National Water Quality Assessment Program</p> <p>PFC MDH Dept. of Health PFC Investigation</p> <p>PWS MDH Dept. of Health Public Water Supply</p> <p>RTIP_MS UMN University Of MN - Robert Tipping M.S. Thesis (1992)</p> <p>SBUR_MS UMN University Of MN - Sandeep Burman M.S. Thesis (1995)</p> <p>SCA_1 UMN University Of MN - Scott Alexander, MN Groundwater Age Data (MNGWAGE.XLS)</p> <p>SCA_2 UMN University Of MN - Scott Alexander, Washington County Data (WASHCODATA.XLS)</p> <p>SCA_3 UMN University Of MN - Scott Alexander, Dakota County Data (DAKOTA3D.XLS)</p>
xREPORT_REFERENCES	<p>Corresponds to field "report_ref," contents specify author and year associated with data:</p> <p>Alexander, S.C., 2010a, Minnesota groundwater age data, University of Minnesota Hydrogeochemistry Laboratory, written communication</p> <p>Alexander, S.C., 2010b, Washington County groundwater data, University of Minnesota Hydrogeochemistry Laboratory, written communication</p> <p>Alexander, S.C., 2010c, Dakota County groundwater data, University of Minnesota Hydrogeochemistry Laboratory, written communication</p> <p>Andrews et al., 2005 Andrews, W.J., Stark, J.R., Fong, A.L., and Fallon, J.D., 2005, Water-quality assessment of part of the Upper Mississippi River Basin, Minnesota and Wisconsin – Ground-water quality along a flow system in the Twin Cities metropolitan area, 1997-1998. 44 p</p> <p>Burman, 1995 Burman, S.R., 1995, Pilot study for testing and refining an empirical groundwater sensitivity assessment methodology, Unpublished M.S. Thesis, University of Minnesota, 256 p.</p> <p>Dakota County, 2006 Dakota County Environmental Management, 2006, Jill Trescott, written communication.</p>

DNR, 2001	Minnesota Department of Natural Resources, 2001 tritium sample of American Linen Mt. Simon well, data from Scott Alexander, file wtr13h98.xls
EOR, 2003	Emmons and Olivier Resources, 2003, Integrating Groundwater and Surface Water Management – Northern Washington County, a Report to Washington County. Data CD.
Hall et al., 1911	Hall, C.W., Meinzer, O.E., and Fuller, M.L., 1911, Geology and underground waters of southern Minnesota: USGS Water-Supply Paper 256, 406 p.
Lively et al., 1992	Lively, R.S., Jameson, R., Alexander, E.C. Jr., and Morey, G.B., 1992, Radium in the Mt. Simon-Hinckley aquifer, east-central and southeastern Minnesota, Minnesota Geological Survey Information Circular IC-36. 58 p.
Maderak, 1963	Maderak, M.L., 1963, Quality of waters, Minnesota: a compilation, 1955-1962: State of Minnesota, Minnesota Conservation Department, Bulletin 21, St. Paul, MN, 104 p.
Marsh, 1996	Marsh, R., 1996, Groundwater chemistry and recharge estimation using environmental tritium. : Anoka County, Minnesota. Anoka County Community Health and Environmental Services Department. 62 p.
Marsh, 2001	Marsh, R., 2001, Hydrogeology of the buried drift aquifers: Anoka County, Minnesota. Anoka County Community Health and Environmental Services Department.
MDH, 2010a	Minnesota Department of Health, 2010a, Perfluorochemical data for portions of Washington and Ramsey and Dakota Counties, Minnesota. Written communication.
MDH, 2010b	Minnesota Department of Health, 2010b, Sourcewater protection tritium data, Justin Blum, written communication
MDH, 2010c	Minnesota Department of Health, 2010c, Radium study, written communication
MGS, 2001	Minnesota Geological Survey, 2001, chemistry collected as part of a LCMR sponsored investigation into hydrogeology of the Prairie Du Chien Group, CUFS No. 1542-6114,

	<p>unpublished data, on-file at MGS.</p> <p>Minnesota Geological Survey, 2010a, data from county atlas and regional hydrogeologic assessments, 1990-1991. Data from CWI version 3 datasets, on-file at MGS.</p> <p>Minnesota Pollution Control Agency, 1998, Baseline water quality of Minnesota's principal aquifers. Ground Water Monitoring and Assessment Program (GWMAP) 1992-1996</p> <p>Minnesota Pollution Control Agency, 2010, Ground water monitoring and assessment program , ambient data 2004-2008, Sherri Kroening, written communication</p> <p>Nemetz, D.A., 1993, The geochemical evolution of ground water along flow paths in the Prairie du Chien-Jordan aquifer of southeastern Minnesota, Unpublished M.S. Thesis, University of Minnesota, 182 p.</p> <p>Tipping, R.G., and Meyer, G.N., 2007, Geology in support of ground-water management for the Twin Cities Metropolitan Area, Metropolitan Council Water Supply Master Plan Development - Phase I. Minnesota Geological Survey Open-File Report OF07-02</p> <p>Tipping, R.G., 1992, An isotopic and chemical study of groundwater flow in the Prairie du Chien and Jordan Aquifers, unpublished M.S. Thesis, University of Minnesota, 117 p.</p> <p>United States Geological Survey, 2010, National Water Information System, United States Geological Survey, http://waterdata.usgs.gov/nwis, Accessed November 10, 2010.</p>
xTDS_MC	<p>Corresponds to field "tds_mc," contents specify method used to determine total dissolved solids: EV residue on evaporation</p>
xVALUE_MINMAX	<p>Corresponds to field "minmax," contents specify if K value is a minimum or maximum value < indicates K value is a maximum value > indicates K value is a minimum value</p>

Appendix C. Water Chemistry field names and descriptions

Geodatabase Name: PointData.mdb (personal geodatabase)

Water chemistry table: C_complete (note: detection and uncertainty fields are not listed. Blank in fieldname_det - reported concentration is the measured value; "<" - reported concentration is the detection limit; Blank in fieldname_unc - uncertainty unknown. Unless otherwise noted, fieldname_unc reported in same units as fieldname, error estimate - larger of 1. Predicted standard deviation, 2. Measured standard deviation).

Field Name	Description
relateid	CWI unique identifier
unique_no	Minnesota unique well number
wellname	Well name. Info from CWI if available
alt_id	Alternate identifier, e.g. field sample number
mpca_ambient_id	MPCA Ambient Groundwater Monitoring Identifier
mpca_EDA_id	MPCA Environmental Data Access Identifier
mdh_PWSID	MDH Public Water Supply Identifier
agency	Agency
program_id	Agency program associated with sample event
sample_date	date of sample collection as text in format yyyyymmdd where equivalent sample_date2 available
sample_date2	date of sample collection as date/time field
cond_TC25	specific conductance of sample corrected to 25 degrees Celsius and reported as microsiemens per centimeter
cond	specific conductance of sample reported as microsiemens per centimeter - may or may not be corrected for temperature.
temp_c	temperature in degrees Celsius, assumed to be at time of sampling unless noted otherwise in remarks
pH	Negative log of hydrogen concentration
ORP	Eh: oxidation-reduction potential referenced to standard hydrogen electrode, in millivolts
ORP2	oxidation-reduction potential relative to the silver:silver

	chloride reference electrode, in millivolts
DO	dissolved oxygen concentration in milligrams per liter
DO_units	A few DO analyses reported as percent atmospheric, indicated by "%" in this column
TOC	total organic carbon in milligrams per liter
Ca	calcium concentration in milligrams per liter
Mg	magnesium concentration in milligrams per liter
Na	sodium concentration in milligrams per liter
K	potassium concentration in milligrams per liter
Na_K	sodium plus potassium concentration in milligrams per liter - (used in Hall and others, 1911)
Fe	iron concentration in milligrams per liter
Mn	manganese concentration in milligrams per liter
Sr	strontium concentration in milligrams per liter
Ba	barium concentration in milligrams per liter
P	phosphorous concentration in milligrams per liter
Al	aluminum concentration in milligrams per liter
Si	silicon concentration in milligrams per liter as SiO2 - assumed
TOTS	Total sulfur concentration in milligrams per liter as sulfur
TOTP	total phosphorous concentration in milligrams per liter as phosphorous
Alk_CaCO3	total alkalinity of the solution reported as calcium carbonate in milligrams per liter
Cl	chloride concentration in milligrams per liter
SO4	sulfate concentration in milligrams per liter
S2O3	thiosulfate concentration in milligrams per liter
Br	bromide concentration in milligrams per liter
F	fluoride concentration in milligrams per liter
NO3_N	nitrate concentration in milligrams per liter reported as nitrogen
NO2_NO2_asN	nitrite concentration in milligrams per liter reported as nitrogen

TOTN	Total nitrogen (nitrate + nitrite + ammonia + organic-N) in milligrams per liter
NH3_N	Ammonia concentration in milligrams per liter as nitrogen
NH3_OrgN_N	Ammonia plus organic nitrogen concentration in milligrams per liter reported as nitrogen
NH4	Ammonium concentration in milligrams per liter
ORTHO_PO4_P	orthophosphate concentration in milligrams per liter reported as phosphorus
PO4_P	phosphate concentration in milligrams per liter reported as phosphorus
TOTAL_CATIONS	total cations in milli-equivalents per liter
TOTAL_ANIONS	total anions in milli-equivalents per liter
PERCENT_ERR	charge balance percent error
TDS	total dissolved solids in milligrams per liter
TDC_MC	Total dissolve solids method code, "EV" indicates residue on evaporation
deuterium	deuterium isotope (per mil)
oxygen_18	oxygen 18 isotope (per mil)
sulfur_34	sulfur 34 isotope (per mil)
Gross_Alpha	gross alpha concentration in picocuries per liter
Polonium	polonium concentration in picocuries per liter
Rn_det	
Rn	radon concentration in picocuries per liter
Ra226_det	
Ra226	radium 226 concentration in picocuries per liter
Ra228_det	
Ra228	radium 228 concentration in picocuries per liter
U_det	
U	uranium concentration in micrograms per liter
U234_U238	uranium 234 to uranium 238 activity ratio
U238_U234	uranium 238 to uranium 234 activity ratio

H3_det	
tritium	tritium concentration in tritium units (TU)
H3_err	tritium error (precision)
C14_PMC	carbon-14 reported as percent modern carbon
C14_PMC_unc	reported one sigma counting error
C14_corr	carbon-14 corrected, reported as percent modern carbon
C14_corr_unc	
C13	carbon-13 (per mil)
soil_dC13_C12	
Methane_dC13_C12	
SF6	sulfur hexafluoride concentration in femtograms per kilogram
CFC	Chlorofluorocarbon
Years_modifier	modifier, less than (<) or greater than (>)
Years	Model estimated age in years
Years_unc	Model estimated age uncertainty in years
age_Model	Name of model used to estimate age (C14; H3/He; SF6; CFC; other)
age_class	age class
age_basis	basis for age class
PFOs_det	
PFOS	perfluorochemicals: perfluorooctonate sulfate concentration in micrograms per liter
PFOA_det	
PFOA	perfluorochemicals: perfluorooctanoic Acid concentration in micrograms per liter
PFBA_det	
PFBA	perfluorochemicals: perfluorooctanoic Acid concentration in micrograms per liter
PFBS_det	
PFBA	perfluorochemicals: perfluorobutanoic acid concentration in micrograms per liter

PFBS_det	
PFBS	perfluorochemicals: perfluorobutane sulfonate concentration in micrograms per liter
PFHxA_det	
PFHxA	perfluorochemicals: perfluorohexanoic acid concentration in micrograms per liter
PFHxS_det	
PFHxS	perfluorochemicals: perfluorohexanesulfonate concentration in micrograms per liter
PFPeA_det	
PFPeA	perfluorochemicals: perfluoropentanoic acid concentration in micrograms per liter
Acetate_det	
Acetate	organic acid: acetate concentration in milligrams per liter
Lactate_det	
Lactate	organic acid: lactate concentration in milligrams per liter
Chlorate_det	
Chlorate	organic acid: chlorate concentration in milligrams per liter
Formate_det	
Formate	organic acid: formate concentration in milligrams per liter
Oxalate_det	
Oxalate	organic acid: oxalate concentration in milligrams per liter
utm	Universal Transverse Mercator easting, UTM zone 15 extended, NAD83
utm_n	Universal Transverse Mercator northing, UTM zone 15 extended, NAD83
gcm_code	geographic coordinate method code
geoc_src	geographic coordinate source
elevation	land surface elevation in feet above mean sea level. Info from CWI if available
elev_mc	elevation method code. Info from CWI if available

depth_comp	depth completed in feet. Info from CWI if available
case_depth	casing depth in feet. Info from CWI if available
depth2bdrk	depth to bedrock in feet. info from CWI if available
first_bdrk	upper most bedrock. info from CWI if available
ohtopunit	open hole top unit. info from CWI if available
ohbotunit	open hole bottom unit. info from CWI if available
ohtopelev	top of open hole elevation
ohbotelev	bottom of open hole elevation
depth_top	depth to top of sampled interval if different from casing depth (in feet)
depth_bot	depth to bottom of sampled interval if different from depth _completed (in feet)
grout	well grouted? (Y, N, U). Info from CWI if available
use_c	well use code. Info from CWI if available
file_src	name of source file(s)
agency_prg	unique agency-program ID: concatenation of agency and program_id fields
relate_date	sample event comparison field
duplicate	duplicate from same sample date, 1 = yes
remarks	comments on data in row
report_ref	report reference, if available
redox_cat	Redox category as assigned by Jurgens and others (2009) based on DO, NO3_N, Mn, Fe and SO4 concentrations
redox_process	Redox process as assigned by Jurgens and others (2009) based on DO, NO3_N, Mn, Fe and SO4 concentrations
sr_ca_mg_ratio	strontium to calcium plus magnesium molar ratio
cl_br_ratio	chloride to bromide ratio, mg/L
fig_goodchargebalance	data flag - good charge balance
fig_fieldparameters	data flag - 1 indicates field parameters/physical characteristics (cond, temp, pH, DO)
fig_stable_radio_isotope	data flag - 1 indicates stable and radiogenic isotopes

flg_nutrients	data flag - 1 indicates nutrient data (phosphorous, nitrogen compounds)
flg_pfc	data flag - 1 indicates PFC data
flg_trace_metals	data flag - 1 indicates trace metals
flg_other	data flag - 1 indicates major cations and anions, physical characteristics - no or poor charge balance
flg_age	data flag - 1 indicates age determination
flg_redox_condition	data flag - 1 indicates redox condition assigned
flg_swuds	data flag - 1 indicates unique number matched DNR SWUD
flg_metro	data flag - 1 indicates sample location within 11-county metro area plus 5000 meters
flg_deliver	data flag - 1 indicates deliver to met council
seqno	Unique row identifier

Appendix D. Regional summary geodatabase structure and field names/descriptions.

Geodatabase Name: RegionalData.gdb (file geodatabase)

Spatially enabled data table

Name	Description
gridpoints_Q	3D collection of regularly spaced grid points with estimated range of K data for unconsolidated deposits. This version differs from gridpoints in Tipping et al., 2010 by having 250 meter horizontal resolution as opposed to 500 meter horizontal resolution
gridpoints_waterchem	3D collection of regularly spaced grid points showing regional hydrochemical facies. Subset of Tipping et al., 2010, containing hydrochemical facies only
XY_locations	2D collection of points regularly spaced points, summarizing subsurface conditions used for vertical travel time calculations, for each XY location in gridpoints_Q.

Field names and definitions: gridpoints_Q

Name	Description
elev	Elevation of point in feet above mean sea level
utm_e, utmn	Universal Transverse Mercator easting and northing for each point. North American Datum 83, zone 15
loc_code	Unique identifier for each point – combination of text string values for utme, utmn and elevation (in feet)
Loc_codeXY	Identifier for XY location of each datapoint – combination of text string values for utme and utmn
nT, nB, nE, nW, nN, nS	Loc_codes of six neighboring points. Used to facilitate groundwater modeling
Kx, Ky, Kz, Ss, pH, R, Q, delta_h, h1, h2, b, sat	Place holder fields for hydraulic parameters. Used to facilitate groundwater modeling
sand_prob	Likelihood that point texture is coarse-grained. Result of subsurface interpolation of water well data
mix_prob	Likelihood that point texture is mixture of fine and coarse-grained. Result of subsurface interpolation of water well data in CWI
clay_prob	Likelihood that point texture is fine-grained. Result of subsurface interpolation of water well data in CWI
grid_code	Quaternary subsurface map code
maplabel	

K_classM	Hydraulic conductivity class code for sub surface points, based on subsurface interpolation of water well data, see lookup table xK_CLASS
K_class	Hydraulic conductivity class code for near-surface points, based on subsurface Quaternary stratigraphy mapping, see lookup table xK_CLASS
K_classSG	Hydraulic conductivity class code for near-surface points, based on surficial geology map units, see lookup table xK_CLASS
K_class_composite	Hierarchy of K class assignments for each point: K_classSG replaces K_class; K_class replaces K_classM – this field can be used to display textures only. Select by value = code as specified in table xK_CLASS
K_classNULL	Value of 1 indicates points with no K class designation due to insufficient data
K_composite	Composite K value based on K_class composite depth. With the exception of sand and gravel, values are taken as arithmetic mean for K_class ranges as specified in table xK_CLASS. Points with K_classNULL = 1 are assigned an intermediate value of 10.05 feet/day. Sand and gravel are assigned a value of 50 ft/day

Field names and definitions: gridpoints_waterchem

Name	Description
POINTID	Unique identifier for each point
GRID_CODE	Quaternary subsurface map code
ELEV	Elevation of point in feet above mean sea level
K_class	Hydraulic conductivity class code, see lookup table xK_CLASS
K_class_sgpg	Hydraulic conductivity class code for near-surface points, based on surficial geology map units, see lookup table xK_CLASS
nat_elev_cl	Data flag – 1 indicates waters likely to have elevated chloride concentrations (greater than 15 ppm) likely due to natural conditions – not anthropogenic inputs.
srcamg	Data flag – 1 indicates waters likely to have strontium to calcium plus magnesium molar ratios likely greater than 0.001
recent	Data flag – 1 indicates water likely to contain some component less than 60 years old

Field names and definitions: XY_locations.

Name	Description
loc_codeXY	Unique identifier for each point
loc_codeMAXe	Gridpoints_Q loc_code for given XY with highest elevation (land surface gridpoint_Q_point)

minimum_elev	Minimum gridpoint_Q elevation for given XY, in feet
maximum_elev	Maximum gridpoint_Q elevation for given XY, in feet
utme, umtn	Universal Transverse Mercator easting and northing for each point. North American Datum 83, zone 15, meters
count_loc_codeXY	Number of gridpoints_Q for given XY
count_KzU	Count of unassigned gridpoint_Q for given XY
count_KzM	Number of gridpoints_Q for given XY with assigned texture class from interpolated model
prnct_vertM	Percent of gridpoints_Q for given XY that have assigned texture texture class from interpolated model
prnct_vert	Percent of gridpoints_Q for given XY with assigned texture class from either interpolated model, subsurface mapping or surficial map
maplabel	Map label from surficial geology map MGS Open-File Report 07-02
K_class_sggg	K_class assignment from surfical geology map
elev_WT	Regional water table elevation in feet
elev_bdrk	Bedrock elevation regional bedrock surface digital elevation model (feet above msl)
elev_opcix_M08	Regional bedrock potentiometric elevation, March 2008, in feet
elev_opcix_A08	Regional bedrock potentiometric elevation, August 2008, in feet
delta_h_M08	Difference in hydraulic head, March 2008, in feet (elev_WT – elev_opcix_M08)
delta_h_A08	Difference in hydraulic head, August 2008, in feet (elev_WT – elev_opcix_A08)
grad_h_M08	Hydraulic gradient, March 2008 (delta_h_M08/distance)
grad_h_A08	Hydraulic gradient, August 2008 (delta_h_A08/distance)
Kz_mean_sat	Arithmetic mean of gridpoint Q_K_composite value for points below regional water table, in ft/day
Kz_gmean_sat	Geometric mean of gridpoint Q_K_composite value for points below regional water table, in ft/day
Kz_hmean_sat	Harmonic mean of gridpoint Q_K_composite value for points below regional water table, in ft/day
Kz_mean_unsat	Arithmetic mean of gridpoint Q_K_composite value for points above regional water table, in ft/day
Kz_gmean_unsat	Geometric mean of gridpoint Q_K_composite value for points above regional water table, in ft/day
Kz_hmean_unsat	Harmonic mean of gridpoint Q_K_composite value for points above regional water table, in ft/day
distance	Vertical distance from regional water table to bedrock surface, in feet
distance_unsat	Vertical distance from land surface to regional water table, in feet
porosity	Porosity, used for time of travel calculations. Set to 0.2 for all records
travel_time_yrs_Kzg	Vertical travel time from regional water table to bedrock surface calculated using geometric mean, in years

travel_time_yrs_Kzh	Vertical travel time from regional water table to bedrock surface calculated using harmonic mean, in years
travel_time_yrs_Kzh_unsat	Vertical travel time from land surface to regional water table calculated using harmonic mean and a vertical gradient of 1, in years
eleven_co_metro	Set to 1 where point is within eleven county extended metropolitan area
qstrat_mapped	Set to 1 for areas where subsurface mapping has taken place
WT_above_bdrk	Set to 1 where water table is above bedrock
opgw_absent	Set to 1 where Plattville Formation is not present

Lookup tables

Name	Description	<i>code</i>	<i>Description</i>	<i>Project</i>	<i>Map Label</i>	<i>K</i>
xGRIDCODE	Corresponds to field "GRID_CODE," code specifies Quaternary subsurface map code, unit description and corresponding mapping project name:					
		1	till - sandy to loamy; high to low relief (diamicton)	Washington County (Meyer and Tipping, 1998)	t1	1
		2	till, generally sandy textured (diamicton)	Washington County (Meyer and Tipping, 1998)	t2	2
		3	loam till, generally silt-rich, loam -textured	Washington County (Meyer and Tipping, 1998)	t3	3
		4	till, generally sandy textured (diamicton)	Washington County (Meyer and Tipping, 1998)	t4	4
		5	silt and clay (bedded)	NW Metro (Meyer and Tipping, 2007)	cl	3
		6	till, generally sandy textured (diamicton)	NW Metro (Meyer and Tipping, 2007)	ct1	2
		7	till, generally sandy textured (diamicton)	NW Metro (Meyer and Tipping, 2007)	ct	2
		8	till, generally loamy textured (diamicton)	NW Metro (Meyer and Tipping, 2007)	xt	3
		9	till, generally sandy textured (diamicton)	NW Metro (Meyer and Tipping, 2007)	rt	4

10	till, generally loamy textured (diamicton)	NW Metro (Meyer and Tipping, 2007)	pt	3
11	till, generally sandy textured (diamicton)	NW Metro (Meyer and Tipping, 2007)	vt	4
12	undifferentiated sediment	NW Metro (Meyer and Tipping, 2007)	unk	-1
13	loam to clay loam (diamicton)	Carver County (Lusardi and Tipping, 2009)	dth	1
14	clay loam to sandy loam (diamicton)	Carver County (Lusardi and Tipping, 2009)	dtv	1
15	sandy loam(diamicton)	Carver County (Lusardi and Tipping, 2009)	rt	2
16	loam (diamicton)	Carver County (Lusardi and Tipping, 2009)	bt	3
17	loam to sandy loam (diamicton)	Carver County (Lusardi and Tipping, 2009)	gt	3
18	loam (diamicton)	Carver County (Lusardi and Tipping, 2009)	xt	3
19	unknown	Carver County (Lusardi and Tipping, 2009)	ups	-1
20	silt and clay	NW Metro (Meyer and Tipping, 2007)	nl	1
21	New Ulm till - sandy to loamy; high to low relief (diamicton)	NW Metro (Meyer and Tipping, 2007)	nt	1
22	sandy loam to clay loam (diamicton) - nw provenance	Scott County (Lusardi and Tipping, 2006)	t1	1
23	loam to sandy loam (diamicton) - mixed provenance	Scott County (Lusardi and Tipping, 2006)	t2	1
24	loam (diamicton) - nw provenance	Scott County (Lusardi and Tipping, 2006)	t3	3
26	silt and clay	Chisago County (Meyer, 2010)	nl	1
27		Chisago County (Meyer, 2010)	nt1	1
28	New Ulm till, includes lacustrine silt and clay at base to the north	Chisago County (Meyer, 2010)	qnu	1
29	lacustrine clay and silt to till	Chisago County (Meyer, 2010)	qlc	3
30	Cromwell, sandy till	Chisago County (Meyer, 2010)	qcr	2
31	sandy till, may be finer-textured towards the base in deep valleys	Chisago County (Meyer, 2010)	qce	2
32	loam till, generally silt-rich, loam -textured	Chisago County (Meyer, 2010)	qxt	3
33	Superior provenance - sandy till	Chisago County (Meyer, 2010)	qrt	4
34	undifferentiated sediment	Chisago County (Meyer, 2010)	qu	-1
50	fine sand to gravel (bedded)	NW Metro (Meyer and Tipping, 2007)	co1	5
51	fine sand to gravel (bedded)	NW Metro (Meyer and Tipping, 2007)	co	5

52	fine sand to gravel (bedded)	NW Metro (Meyer and Tipping, 2007	no2	5
53	fine sand to gravel (bedded)	NW Metro (Meyer and Tipping, 2007	no	5
54	fine sand to gravel (bedded)	NW Metro (Meyer and Tipping, 2007	po	5
55	fine sand to gravel (bedded)	NW Metro (Meyer and Tipping, 2007	Ro	5
56	fine sand to gravel (bedded)	NW Metro (Meyer and Tipping, 2007	terr	5
57	fine sand to gravel (bedded)	NW Metro (Meyer and Tipping, 2007	vo	5
58	fine sand to gravel (bedded)	NW Metro (Meyer and Tipping, 2007	xo	5
60	fine sand to gravel (bedded)	Chisago County (Meyer, 2010)	qsc	5
61	fine sand to gravel (bedded)	Chisago County (Meyer, 2010)	qse	5
62	fine sand to gravel (bedded)	Chisago County (Meyer, 2010)	qsl	5
63	fine sand to gravel (bedded)	Chisago County (Meyer, 2010)	qsr	5
65	fine sand to gravel (bedded)	Chisago County (Meyer, 2010)	qsx	5
65	fine sand to gravel (bedded)	Chisago County (Meyer, 2010)	qu	5
67	fine sand to gravel (bedded)	Chisago County (Meyer, 2010)	sp	5
68	fine sand to gravel (bedded)	Chisago County (Meyer, 2010)	sup	5
70	fine sand to gravel (bedded)	Carver County (Lusardi and Tipping, 2009)	sb	5
71	fine sand to gravel (bedded)	Carver County (Lusardi and Tipping, 2009)	sdo	5
72	fine sand to gravel (bedded)	Carver County (Lusardi and Tipping, 2009)	sdv	5
73	fine sand to gravel (bedded)	Carver County (Lusardi and Tipping, 2009)	sg	5
74	fine sand to gravel (bedded)	Carver County (Lusardi and Tipping, 2009)	sr	5
75	fine sand to gravel (bedded)	Carver County (Lusardi and Tipping, 2009)	su	5
76	fine sand to gravel (bedded)	Carver County (Lusardi and Tipping, 2009)	sx	5
80	fine sand to gravel (bedded)	Scott County (Lusardi and Tipping, 2006)	s1	5
81	fine sand to gravel (bedded)	Scott County (Lusardi and Tipping, 2006)	s2	5
82	fine sand to gravel (bedded)	Scott County (Lusardi and Tipping, 2006)	s3	5
83	fine sand to gravel (bedded)	Scott County (Lusardi and Tipping, 2006)	s4	5
84	fine sand to gravel (bedded)	Scott County (Lusardi and Tipping, 2006)	riv	5
90	fine sand and gravel (areas unmapped by till surfaces)	Washington County (Meyer and Tipping, 1998)		5
xMAPLABEL		Corresponds to field "maplabel," code specifies map label and unit description from metro area surficial		

xK_CLASS	<p>geology map, MGS Open-File Report 07-02 (Meyer and Tipping, 2007). Corresponds to fields "K_class," and "K_class_sgpg," code specifies range of expected hydraulic conductivity in feet/day. Reference to "deep" in codes 8-11 are for point depths greater than 60 feet from land surface, estimated to be 2 orders of magnitude lower hydraulic conductivity than equivalent textures in shallow settings:</p> <table border="1" data-bbox="519 588 941 1575"> <thead> <tr> <th><i>code</i></th> <th><i>Texture Description</i></th> <th><i>Kmax (ft/day)</i></th> <th><i>Kmin (ft/day)</i></th> </tr> </thead> <tbody> <tr> <td>1</td> <td>loam to clay loam</td> <td>3.0E-3</td> <td>1.0E-3</td> </tr> <tr> <td>2</td> <td>loam to sandy loam</td> <td>2.0E+1</td> <td>1.0E-1</td> </tr> <tr> <td>3</td> <td>loam, silt rich; silt and clay</td> <td>2.0E-2</td> <td>3.0E-4</td> </tr> <tr> <td>4</td> <td>loam to sandy clay loam</td> <td>2.0E+1</td> <td>1.0E-1</td> </tr> <tr> <td>5</td> <td>sand and gravel</td> <td>5000</td> <td>100</td> </tr> <tr> <td>6</td> <td>fine sand</td> <td>30</td> <td>0.3</td> </tr> <tr> <td>7</td> <td>sandy silt</td> <td>3</td> <td>0.1</td> </tr> <tr> <td>8</td> <td>loam to clay loam - deep</td> <td>3.0E-5</td> <td>1.0E-5</td> </tr> <tr> <td>9</td> <td>loam to sandy loam - deep</td> <td>2.0E-1</td> <td>1.0E-3</td> </tr> <tr> <td>10</td> <td>loam, silt rich; silt and clay - deep</td> <td>2.0E-4</td> <td>3.0E-6</td> </tr> <tr> <td>11</td> <td>loam to sandy clay loam - deep</td> <td>2.0E-1</td> <td>1.0E-3</td> </tr> </tbody> </table>				<i>code</i>	<i>Texture Description</i>	<i>Kmax (ft/day)</i>	<i>Kmin (ft/day)</i>	1	loam to clay loam	3.0E-3	1.0E-3	2	loam to sandy loam	2.0E+1	1.0E-1	3	loam, silt rich; silt and clay	2.0E-2	3.0E-4	4	loam to sandy clay loam	2.0E+1	1.0E-1	5	sand and gravel	5000	100	6	fine sand	30	0.3	7	sandy silt	3	0.1	8	loam to clay loam - deep	3.0E-5	1.0E-5	9	loam to sandy loam - deep	2.0E-1	1.0E-3	10	loam, silt rich; silt and clay - deep	2.0E-4	3.0E-6	11	loam to sandy clay loam - deep	2.0E-1	1.0E-3
<i>code</i>	<i>Texture Description</i>	<i>Kmax (ft/day)</i>	<i>Kmin (ft/day)</i>																																																	
1	loam to clay loam	3.0E-3	1.0E-3																																																	
2	loam to sandy loam	2.0E+1	1.0E-1																																																	
3	loam, silt rich; silt and clay	2.0E-2	3.0E-4																																																	
4	loam to sandy clay loam	2.0E+1	1.0E-1																																																	
5	sand and gravel	5000	100																																																	
6	fine sand	30	0.3																																																	
7	sandy silt	3	0.1																																																	
8	loam to clay loam - deep	3.0E-5	1.0E-5																																																	
9	loam to sandy loam - deep	2.0E-1	1.0E-3																																																	
10	loam, silt rich; silt and clay - deep	2.0E-4	3.0E-6																																																	
11	loam to sandy clay loam - deep	2.0E-1	1.0E-3																																																	

Appendix E. Guide to database use.

Travel time calculations

Several choices were made that impact the time of travel calculations shown on Figures 12 and 13, and on the accompanying map:

- 1.) Harmonic mean of vertical hydraulic conductivity (K_v) values for set of gridpoints at each XY location was used, as opposed to arithmetic or geometric mean. The harmonic mean is influenced more by lower values than the geometric or arithmetic mean. It was chosen based on the premise that low conductivity layers have the greatest influence on ground water flowpaths.
- 2.) In places other than those identified as regional discharge zones, the bedrock potentiometric surface was lowered one-half foot below the regional water table surface in places where it was greater than the water table surface. (Note: gradients shown on cross sections were not changed). This allowed for travel time calculation over a broader area where adequate subsurface data was available.
- 3.) Effective porosity was set at 20% for all calculations based on literature values. It is expected that actual effective porosity varies substantially over a range of textures and depositional environments.

These choices result in *extremely* long travel times under certain conditions, such as very low gradients and low bulk K_v . Rather than replace these travel time values with a realistic number, they were left in to reflect the limitations of this type of method at depicting actual groundwater flow. The resulting map is a reasonable depiction of the relative rather than absolute differences in vertical travel times across the metropolitan area. It should also be noted that in areas identified as regional discharge zones – bedrock potentiometric surface higher than the regional water table – travel time values were set to null.

Layer files

The following ArcGIS layer files are included to assist with database display. Depending on processing speed of the desktop computer, it may be help to use the “Definition Query” tab under layer properties to display only subsets of the larger database.

XY locations feature class

Name	Description
travel_time_yrs_Kzh_sat.lyr	Use to display vertical travel time in years from the regional water table to the bedrock surface calculated using harmonic mean of composite vertical hydraulic conductivity
travel_time_yrs_Kzh_unsat.lyr	Use to display vertical travel time in years from land surface to regional water table calculated using harmonic mean of composite vertical hydraulic conductivity

gridpoints_Q feature class – represents any occurrence from landsurface to bedrock

Name	Description
gridpoints_Q_K_classM.lyr	Use to display subsurface textures as determined by interpolated model – based on driller’s descriptions
gridpoints_Q_K_class.lyr	Use to display subsurface textures as determined by stratigraphic mapping
gridpoints_Q_K_classSG.lyr	Use to display near surface textures as determined by surficial mapping
gridpoints_Q_K_class_composite.lyr	Use to display near surface and subsurface textures, as determined by hierarchy of K_classM superceded by K_class, superceded by K_classSG.

gridpoints_waterchem

Name	Description
gridpoints_waterchem_nat_elev_cl.lyr	Use to display subsurface distribution of naturally elevated chloride waters
gridpoints_waterchem_srcamg.lyr	Use to display subsurface distribution of elevated strontium to calcium plus magnesium waters
gridpoints_waterchem_recent.lyr	Use to display near subsurface distribution of recent waters